Climate variability and change and its potential impact on maize yield in Northeastern Zimbabwe

By

Joseph N Masanganise

A thesis submitted in partial fulfillment of the requirements for the degree of Master of Science in Agricultural Meteorology

Supervisors: Mr. B. Chipindu

Dr. T. Mhizha



Department of Physics

Faculty of Science

University of Zimbabwe

May 2010

ABSTRACT

The main aim of this study was to investigate climate variability and change and its potential impact on maize yield in Northeastern Zimbabwe. Understanding the impact of climate change on crop production may help optimize schemes to increase or stabilize yields. The research used historic climatic data (precipitation and mean air temperature) as well as downscaled model predictions of the same parameters. The models used in the study were the same as those used by the Intergovernmental Panel on Climate Change (IPCC) in formulating the IPCC Special Report on Emissions Scenarios (SRES). Historic (1971-2000) climate trends for five climatological stations in Northeastern Zimbabwe were derived from observational data provided by the Zimbabwe Meteorological Services Department (ZMSD). Time series plots for temperature showed that the mean temperatures recorded at all the stations have increased by about 0.5 - 0.8 °C during the period 1971 to 2000. Rainfall at Mt Darwin, Wedza and Rusape showed slight decreases, while no major changes were observed at Karoi and Agricultural Research Trust (ART) Farm. At Mutoko, rainfall showed an increase during the period 1971 to 2000. Five coupled global climate models were evaluated for simulating monthly precipitation and monthly minimum and maximum temperature. Model performance was assessed statistically using the following quantitative statistical indicators: coefficient of determination (R²), root mean square error (RMSE) and model efficiency (ME). For rainfall, in addition to R² and RMSE, a frequency analysis test was applied at 50 % probability of exceedance. A t-test was then performed at 5 % level of significance to assess the correlation between observed and simulated data. Across all the three variables, four models performed relatively well but one of the models deviated substantially from the other four. All the models however did not perform well in predicting precipitation. The five models were ranked according to their performances and the highest performing model was applied in the study. Using the Climate Change Explorer tool, the highest performing model was applied to investigate the past and future climates at each station. In the case of temperature, downscaled model simulations from the best model consistently predicted a warming of between 1 and 2 °C at most of the stations in the 2046-2065 regime above the baseline (1971-2000) period. In the case of rainfall, all models showed a wide variation in prediction. A crop growth simulation model, AquaCrop, was validated for simulating maize yields. Three quantitative statistical measures were used to assess its performance. These were R², RMSE and the slope. A t-test was performed at 5 % level of significance to assess the usefulness of the model. Statistical analysis showed that AquaCrop is a usable and reliable tool in predicting maize yields. The potential impact of climate change on maize yield by 2046-2065 was investigated. Downscaled model simulations predicted that climate change will shift planting dates towards delayed planting in the 2046-2065 period. AquaCrop was used to simulate the impact on yield. Results of the simulations showed that if current planting dates are maintained in the period 2046-2065, maize yield will decrease but delayed planting will result in

increased yields. AquaCrop also demonstrated that if planting is delayed, yields will be highest for short season varieties as compared to medium and long season ones.

ACKNOWLEDGEMENTS

Thanks be unto Almighty God who has given me life and energy to sail through. It has been a wonderful experience.

My heartfelt gratitude goes to my supervisors, Mr. B. Chipindu and Dr. T. Mhizha, for their assistance and guidance throughout the work. My special thanks to Mr. E. Mashonjowa for his sacrificial spirit in assisting me in using the Climate Change Explorer tool that particularly made this research a success. Many thanks to Mr. A. Ncube for his constructive hand during the course of the project. I am also grateful to the University of Zimbabwe for partially funding the project through graduate teaching assistantship.

To all my classmates with whom I shared ideas, I wish them the best in their intended carriers. I will always cherish the good days we have been together.

Finally I would like to extend my gratitude to cousin and friend Mr. T. Marufu and all my family members for their moral support.

LIST OF ABBREVIATIONS AND SYMBOLS

AGRITEX Department of Agricultural, Technical and Extension

ART Agricultural Research Trust

CARA Consortium for Atlantic Regional Assessment

CCCM Canadian Climate Change Model

CCE Climate Change Explorer

CEC Cation exchange capacity

CERES Crop-Environmental Resource Synthesis

CIMMYT Centro Internacional de Mejoramiento de Maiz y Trigo

CSAG Climatic Systems Analysis Group

CSO Central Statistical Office

ET_a Actual Evapotranspiration

ET_o Reference Evapotranspiration

FAO Food and Agricultural Organization

GCM Global Climate Model

GFDL Geophysical Fluid Dynamics Laboratory

HI Harvest Index

IPCC Intergovernmental Panel on Climate Change

ITCZ Intertropical Convergence Zone

K_c Crop coefficient

K_{sat} Saturated hydraulic conductivity

K_v Yield response factor

ME Model efficiency

RMSE Root mean square error

SRES Special Report on Emissions Scenarios

TAR Third Assessment Report

TAW Total available water

T_r Crop transpiration

WMO World Meteorological Organization

ZMSD Zimbabwe Meteorological Services Department

 θ_{FC} Volumetric soil water content at field capacity

 θ_{pwp} Volumetric soil water content at permanent wilting point

 θ_{sat} Volumetric soil water content at saturation

TABLE OF CONTENTS

ABSTRACT	i
ACKNOWLEDGEMENTS	iii
LIST OF ABBREVIATIONS AND SYMBOLS	iv
LIST OF TABLES	xii
LIST OF FIGURES	xiv
APPENDICES	xxi
CHAPTER 1	1
BACKGROUND AND JUSTIFICATION	1
1.1 Introduction	1
1.2 Problem statement	3
1.3 Objectives of study	5
1.4 Limitations	5
1.5 Expected benefits	5
1.6 Thesis layout	6
CHAPTER 2	7
LITERATURE REVIEW	7
2.1 Introduction	7
2.2 Measuring Climate	7
2.3 Climate of Zimbabwe	8
2.4 Soils of Zimbabwe	8
2.5 Impact of climate variability and change on crop production	8
2.5.1 Factors influencing crop production	9
2.5.1.1 Average temperature increase	9
2.5.1.2 Changes in rainfall	10
2.5.1.3 Carbon dioxide concentration	10
2.5.1.4 Effects of pollution.	11
2.6 The maize gron requirements	11

2.6.1 Soils	11
2.6.2 Soil moisture	12
2.6.3 Temperature	12
2.6.3.1 Germination	
2.6.3.2 Development of stem and leaves	
2.6.3.3 Effects of rise in mean temperature during the reproductive phase	
2.7 Climate change scenarios	14
2.7.1 The A2 scenario	
2.7.2 The B2 scenario	
2.7.3 Scenario predictions	
2.8 Global climate models	17
2.9 Downscaling of climatic data	18
2.10 The Climate Change Explorer Tool	18
2.11 Crop modelling	19
2.11.1 Crop growth simulation models and their uses	19
2.11.1.1 Uses of models	
2.11.1.2 Limitations of crop growth models	20
2.11.2 Types of models	20
2.11.2.1 Empirical and Mechanistic models	20
2.11.2.2 Deterministic and Stochastic models	21
2.11.2.3 Static and Dynamic Models	21
2.11.3 Calibration and validation of models.	21
2.11.3.1 Model Calibration	21
2.11.3.2 Model Validation	22
2.12 The AquaCrop model	22
2.12.1 The evolution of AquaCrop	23
2.12.2 Components of the AquaCrop model	25
2.12.3 Model requirements	26
2.12.3.1 Climatic data	26
2.12.3.2 Crop characteristics	27
2.12.3.3 Soil input parameters	27

2.12.4 Biomass production and partitioning	27
2.12.5 Advantages of the AquaCrop model	28
CHAPTER 3	29
MATERIALS AND METHODS	29
3.1 Introduction	29
3.2 The study area	29
3.3 Types and sources of data	31
3.3.1 Climatic data	31
3.3.1.1 Rainfall	31
3.3.1.2 Temperature	
3.3.1.3 Reference evapotranspiration (ET _o)	
3.3.1.4 Homogeneity test of rainfall data	32
3.3.1.5 Frequency analysis test of rainfall data	
3.3.2 Nonclimatic data	36
3.3.2.1 Soil data	37
3.3.2.2 Crop data	37
3.3.2.3 Carbon dioxide data	39
3.3.2.4 Historical maize yield data	39
3.4 Time series analysis of rainfall and temperature	41
3.5 Model data acquisition	41
3.6 Model selection	41
3.7 Comparison of global climate model performance	42
3.7.1 Regression analysis	43
3.7.2 Model efficiency (ME)	43
3.7.3 Root mean square error (RMSE)	43
3.7.4 Frequency analysis	44
3.7.5 Significance testing	44
3.7.6 Ranking of the models	44
3.8 Application of the Climate Change Explorer tool	44
3.8.1 Baseline climates	48
3.8.2 Projected changes in temperature and rainfall	48

3.8.3 Dry spell analysis	48
3.9 Validation of the AquaCrop model	48
3.9.1 The validation procedure	48
3.9.2 Environment panel	50
3.9.3 Simulation panel	50
3.9.4 Project panel	50
3.9.5 Significance testing	50
3.10 Modelling to simulate historic and future maize yields	50
3.10.1 Simulations under baseline conditions and current planting dates	51
3.10.2 Simulations under future conditions maintaining current planting dates	51
3.10.3 Simulations under future conditions using generated planting dates	51
CHAPTER 4	53
RESULTS AND DISCUSSION	53
4.1 Introduction	53
4.2 Homogeneity testing	53
4.3 Climate characterization	54
4.3.1 Rainfall	54
4.3.2 Temperature.	61
4.4 Evaluation of global climate models	65
4.4.1 Minimum air temperature	65
4.4.2 Maximum air temperature	67
4.4.3 Rainfall	71
4.4.3.1 Frequency analysis	72
4.5 Baseline climate for the stations	76
4.5.1 Mean monthly temperatures	76
4.5.1.1 Baseline temperatures for Mt Darwin.	76
4.5.1.2 Baseline temperatures for Karoi.	77
4.5.1.3 Baseline temperatures for Wedza	78
4.5.1.4 Baseline temperatures for Rusape	78
4.5.1.5 Baseline temperatures for Mutoko	79
4.5.2 Mean monthly rainfall	81

4.5.2.1 Baseline rainfall for Mt Darwin	81
4.5.2.2 Baseline rainfall for Karoi	82
4.5.2.3 Baseline rainfall for Mutoko	82
4.5.2.4 Baseline rainfall for Wedza	83
4.5.2.5 Baseline rainfall for Rusape	84
4.6 Projected changes in temperature and rainfall	84
4.6.1 Changes in temperature	84
4.6.1.1 Minimum temperature anomalies	84
4.6.1.2 Maximum temperature anomalies	85
4.6.2 Changes in rainfall	87
4.6.2.1 Future rainfall change for Mt Darwin	87
4.6.2.2 Future rainfall change for Wedza	88
4.6.2.3 Future rainfall change for Rusape	89
4.6.2.4 Future rainfall change for Karoi	89
4.6.2.5 Future rainfall change for Mutoko	90
4.7 Dry spell analysis	91
4.8 AquaCrop model validation	92
4.8.1 Model performance for the SC513 cultivar	93
4.8.2 Model performance for the SC715 cultivar	94
4.8.3 Model performance for the SC633 cultivar	95
4.9 Modelling the impact of climate change on yield	96
4.9.1 Historical and expected future yields with current planting dates maintained	96
4.9.2 Expected future yields with generated planting dates	99
CHAPTER 5	104
CONCLUSIONS AND RECOMMENDATIONS	104
5.1 Introduction	104
5.2 Summary and conclusions	104
5.2.1 Time series analysis	104
5.2.2 Evaluation of global climate models and the use of CCE tool	104
5.2.3 Validation and use of the AquaCrop model	105
5.3 Adaptation strategies	105

5.4 Recommendations for further studies	107
REFERENCES	108

LIST OF TABLES

Table 2.1 Global climate models used in the study.	. 17
Table 3.1 Characteristics of the stations used in the study.	. 31
Table 3.2 General physical properties of the sandy loam soil predominant in Natural Region 2	2 of
Zimbabwe	. 37
Table 3.3 Cultivar specific crop characteristics used to validate the AquaCrop model	. 37
Table 3.4 Growth stages and crop coefficient (K _c) factors for a 140-day maize	. 38
Table 3.5 Growth stages and yield response factors (Ky) for a 140-day maize	. 38
Table 3.6 Conservative crop characteristics considered for the SC513 cultivar	. 38
Table 3.7 Conservative crop characteristics considered for the SC633 cultivar	. 39
Table 3.8 Conservative crop characteristics considered for the SC715 cultivar	. 39
Table 3.9 Observed yield and planting dates for the SC513 maize variety at ART Farm	. 40
Table 3.10 Observed yield and planting dates for the SC633 maize variety at ART Farm	. 40
Table 3.11 Observed yield and planting dates for the SC715 maize variety at ART Farm	. 40
Table 3.12 Characteristics of the global climate models used in the study	. 42
Table 3.13 Planting dates generated for the period 2046-2065	. 52
Table 4.1(a) Quantitative measures of the performance of the five global climate models for	
simulating minimum temperature at Karoi	. 65
Table 4.1(b) Quantitative measures of the performance of the five global climate models for	
simulating minimum temperature at Wedza.	. 66

Table 4.1(c) Quantitative measures of the performance of the five global climate models for	
simulating minimum temperature at Rusape.	66
Table 4.2(a) Quantitative measures of the performance of the five global climate models for	
simulating maximum temperature at Mt Darwin.	67
Table 4.2(b) Quantitative measures of the performance of the five global climate models for	
simulating maximum temperature at Karoi.	68
Table 4.2(c) Quantitative measures of the performance of the five global climate models for	
simulating maximum temperature at Wedza.	68
Table 4.2(d) Quantitative measures of the performance of the five global climate models for	
simulating maximum temperature at Rusape.	69
Table 4.2(e) Quantitative measures of the performance of the five global climate models for	
simulating maximum temperature at Mutoko	69
Table 4.3(a) Quantitative measures of the performance of the five global climate models for	
simulating rainfall at Mt Darwin.	71
Table 4.3(b) Quantitative measures of the performance of the five global climate models for	
simulating rainfall at Wedza.	71
Table 4.3(c) Quantitative measures of the performance of the five global climate models for	
simulating rainfall at Rusape.	72
Table 4.3(d) Quantitative measures of the performance of the five global climate models for	
simulating rainfall at Mutoko	72
Table 4.4(a) Simulated and observed yield for the SC513 maize variety at ART Farm	93
Table 4.4(b) Simulated and observed yield for the SC715 maize variety at ART Farm	94
Table 4.4(c) Simulated and observed yield for the SC633 maize variety at ART Farm	95

Table 4.4(d)	The statistics used to assess	AquaCrop model performance	90
---------------------	-------------------------------	----------------------------	----

LIST OF FIGURES

Figure 2.1 Future changes in global mean temperature from different emission scenarios using	ng
several different climate models. The bars show the range of simple model results in 2100	16
Figure 2.2 Evolution of AquaCrop from equation (2.1), based on the introduction of two	
intermediary steps: the separation of soil evaporation (E) from crop transpiration (Tr) and the	•
attainment of yield (Ya) from Biomass (B) and harvest index (HI)	24
Figure 2.3 Flowchart of AquaCrop indicating the main components of the soil-plant-atmosph	here
continuum.	26
Figure 3.1 The study area.	30
Figure 3.2 The main menu of RAINBOW.	33
Figure 3.3 The frequency analysis menu of RAINBOW	35
Figure 3.4 Another RAINBOW frequency analysis menu	36
Figure 3.5 The main menu of CCE	45
Figure 3.6 The Summary Statistics panel	46
Figure 3.7 The Seasonal Curves panel	47
Figure 3.8 The main menu of AquaCrop	49
Figure 4.1 Cumulative deviations from mean total annual rainfall for Rusape for the period 1971-2006.	54
Figure 4.2(a) Time series for annual rainfall at Mt Darwin for the period 1970-1999	55
Figure 4.2(h) Rainfall anomalies at Mt Darwin for the period 1970-1999	55

Figure 4.3(a) Time series for annual rainfall at Karoi for the period 1970-2000	56
Figure 4.3(b) Rainfall anomalies at Karoi for the period 1970-2000	56
Figure 4.4(a) Time series for annual rainfall at Wedza for the period 1970-2007	57
Figure 4.4(b) Rainfall anomalies at Wedza for the period 1970-2006	57
Figure 4.5(a) Time series for annual rainfall at Rusape for the period 1970-2007	58
Figure 4.5(b) Rainfall anomalies at Rusape for the period 1970-2007	59
Figure 4.6(a) Time series for annual rainfall at ART Farm for the period 1970-2009	59
Figure 4.6(b) Rainfall anomalies at ART Farm for the period 1970-2009	60
Figure 4.7(a) Time series for annual rainfall at Mutoko for the period 1970-2003	60
Figure 4.7(b) Rainfall anomalies at Mutoko for the period 1970-2003	61
Figure 4.8 Time series of mean annual temperature at Karoi for the period 1971-2000	62
Figure 4.9 Time series of mean annual temperature at Wedza for the period 1971-2000	62
Figure 4.10 Time series of mean annual temperature at Rusape for the period 1971-2000	63
Figure 4.11 Time series of mean annual temperature at ART Farm for the period 1971-2000	64
Figure 4.12 Ranking the perfomance of models for simulating temperature	70
Figure 4.13(a) Model performances at 50% probability of exceedance for Mt Darwin	73
Figure 4.13(b) Model performances at 50% probability of exceedance for Wedza	74
Figure 4.13(c) Model performances at 50% probability of exceedance for Rusape	75
Figure 4.14(a) Baseline temperatures for Mt Darwin for the period 1971 to 2000	76
Figure 4.14(b) Baseline temperatures for Karoi for the period 1971 to 2000	77
Figure 4.14(c) Baseline temperatures for Wedza for the period 1971 to 2000	78
Figure 4.14(d) Baseline temperatures for Rusape for the period 1971 to 2000	79
Figure 4.14(e) Baseline temperatures for Mutoko for the period 1971 to 2000	80

Figure 4.15(a) Baseline monthly rainfall for Mt Darwin for the period 1971 to 2000
Figure 4.15(b) Baseline monthly rainfall for Karoi for the period 1971 to 2000
Figure 4.15(c) Baseline monthly rainfall for Mutoko for the period 1971 to 200082
Figure 4.15(d) Baseline monthly rainfall for Wedza for the period 1971 to 2000
Figure 4.15(e) Baseline monthly rainfall for Rusape for the period 1971 to 2000
Figure 4.16(a) Predicted mean monthly minimum temperature anomalies for the five stations in
the period 2046 – 2065
Figure 4.16(b) Predicted mean monthly maximum temperature anomalies for the five stations in
the period 2046 – 2065
Figure 4.17 (a) Predicted mean monthly rainfall anomalies for Mt Darwin in the period 2046 –
2065
Figure 4.17(b) Predicted mean monthly rainfall anomalies for Wedza in the period 2046 – 2065
Figure 4.17 (c) Predicted mean monthly rainfall anomalies for Rusape in the period 2046 – 2065
Figure 4.17 (d) Predicted mean monthly rainfall anomalies for Karoi in the period 2046 – 2065
Figure 4.17 (e) Predicted mean monthly rainfall anomalies for Mutoko in the period 2046 –
2065
Figure 4.18 Mean monthly dry spells in the periods 1971-2000 and 2046-2065 for Karoi 92
Figure 4.19(a) Comparison of simulated with observed yield at ART Farm for the SC513 maize
variety93

Figure 4.19(b) Comparison of simulated with observed yield at ART Farm for the SC71	5 maize
variety	94
Figure 4.19(c) Comparison of simulated with observed yield at ART Farm for the SC63	3 maize
variety	95
Figure 4.20(a) Changes in yields at Mt Darwin when current planting dates are used	97
Figure 4.20(b) Changes in yields at Karoi when current planting dates are used	97
Figure 4.20(c) Changes in yields at Mutoko when current planting dates are used	98
Figure 4.20(d) Changes in yields at Wedza when current planting dates are used	98
Figure 4.20(e) Changes in yields at Rusape when current planting dates are used	99
Figure 4.21(a) Expected future yields at Mt Darwin with generated planting dates	100
Figure 4.21(b) Expected future yields at Karoi with generated planting dates	100
Figure 4.21(c) Expected future yields at Mutoko with generated planting dates	101
Figure 4.21(d) Expected future yields at Wedza with generated planting dates	101
Figure 4.21(e) Expected future yields at Rusape with generated planting dates	102
Figure A1 CCCMA_CGCM3_1 performance.	115
Figure A2 CSIRO_MK3_5 performance.	115
Figure A3 GFDL_CM2_0 performance.	115
Figure A4 GISS_MODEL_E_R performance.	115
Figure A5 MPI_ECHAM5 performance	115
Figure A6 CCCMA_CGCM3_1 performance	116
Figure A7 CSIRO_MK3_5 performance.	116
Figure A8 GFDL_CM2_0 performance	116

Figure A9 GISS_MODEL_E_R performance	116
Figure A10 MPI_ECHAM5 performance	116
Figure A11 CCCMA_CGCM3_1 performance	117
Figure A12 CSIRO_MK3_5 performance	117
Figure A13 GFDL_CM2_0 performance	117
Figure A14 GISS_MODEL_E_R performance	117
Figure A15 MPI_ECHAM5 performance	117
Figure B1 CCCMA_CGCM3_1performance	118
Figure B2 CSIRO_MK3_5 performance	118
Figure B3 GFDL_CM2_0 performance.	118
Figure B4 GISS_MODEL_E_R performance	118
Figure B5 MPI_ECHAM5 performance	118
Figure B6 CCCMA_CGCM3_1performance	119
Figure B7 GFDL_CM2_0 performance	119
Figure B8 GISS_MODEL_E_R performance	119
Figure B9 MPI_ECHAM5 performance	119
Figure B10 CSIRO_MK3_5 performance	119
Figure B11 CCCMA_CGCM3_1 performance	120
Figure B12 CSIRO_MK3_5 performance	120
Figure B13 GFDL_CM2_0 performance	120
Figure B14 GISS MODEL E R performance	120

Figure B15 MPI_ECHAM5 performance	120
Figure B16 CCCMA_CGCM3_1 performance	121
Figure B17 CSIRO_MK3_5 performance	121
Figure B18 GFDL_CM2_0 performance	121
Figure B19 GISS_MODEL_E_R performance	121
Figure B20 MPI_ECHAM5 performance.	121
Figure B21 CCCMA_CGCM3_1 performance	122
Figure B22 CSIRO_MK3_5 performance	122
Figure B23 GFDL_CM2_0 performance	122
Figure B24 GISS_MODEL_E_R performance	122
Figure B25 MPI_ECHAM5 performance.	122
Figure C1 CCCMA_CGCM3_1 performance	123
Figure C2 CSIRO_MK3_5 performance	123
Figure C3 GFDL_CM2_0 performance	123
Figure C4 GISS_MODEL_E_R performance	123
Figure C5 MPI_ECHAM5 performance.	123
Figure C6 CCCMA_CGCM3_1 performance	124
Figure C7 CSIRO_MK3_5 performance	124
Figure C8 GFDL_CM2_0 performance	124
Figure C9 GISS_MODEL_E_R performance	124
Figure C10 MPI ECHAM5 performance	124

Figure C11 CCCMA_CGCM3_1 performance	125
Figure C12 CSIRO_MK3_5 performance	125
Figure C13 GFDL_CM2_0 performance.	125
Figure C14 GISS_MODEL_E_R performance	125
Figure C15 MPI_ECHAM5 performance	125
Figure C16 CCCMA_CGCM3_1 performance	126
Figure C17 CSIRO_MK3_5 performance	126
Figure C18 GFDL_CM2_0 performance.	126
Figure C19 GISS_MODEL_E_R performance	126
Figure C20 MPI ECHAM5 performance	126

APPENDICES

APPENDIX A: Regression lines for simulating minimum temperature	115
APPENDIX B: Regression lines for simulating maximum temperature	120
APPENDIX C: Regression lines for simulating rainfall	126

CHAPTER 1

BACKGROUND AND JUSTIFICATION

1.1 Introduction

Climate is the average conditions of the weather over long periods, usually years, decades up to centuries. The Intergovernmental Panel on Climate Change (IPCC) defines climate as 'average weather' usually described in terms of the mean and variability of temperature, precipitation and wind over a period of time, ranging from months to millions of years (IPCC, 2007). Ausubel and Biswas (1980) define climate as either the expected or the observed statistical character of weather over some specified period and it varies on all time scales. The World Meteorological Organization (WMO) uses a period of 30 years to define the climate of a region. A longer time period would be most suitable up to even 100 years, however in many countries, this is limited by data availability. The climate system is a complex, interactive system consisting of the atmosphere, land surface, cryosphere (snow, frozen ground, ice, ice sheets and glaciers), hydrosphere (oceans and other water bodies) and the biosphere (living organisms). This system evolves in time under the influence of its own internal dynamics and due to changes in external factors. External factors include natural phenomena such as volcanic eruptions and solar variations as well as anthropogenically-induced changes in atmospheric composition. The climate system is powered by solar radiation (IPCC, 2007).

Climate is important because it creates the long-term conditions that allow ecosystems to evolve and survive. For human societies, climate is important for basic activities such as agriculture and settlement. Climate variability refers to deviations of climate statistics over a given period of time such as month, season or year from the long term climate statistics (Ruddiman, 2003). According to Hosier (1985), climatic variability are variations (ups and downs) in climatic conditions on time scales of months, years, decades, up to millennia. By contrast, climate change is a shift in the state of the climate that can be identified by changes in its average properties, for example, using statistical tests.

These changes can either be natural or a result of anthropogenic drivers and they persist for an extended period, typically decades or longer (IPCC, 2007). Climate change may involve a single parameter such as temperature or rainfall but it usually accompanies more general shifts in weather patterns which might give rise to colder, wetter, cloudier and windier conditions (Burroughs, 2001). When climates change, all species, including humans, must either adapt or migrate if they are to avoid the adverse impacts (Gullett & Skinner, 1992).

Sectors that are sensitive to climate change include: water, energy production, health, tourism, environment and agriculture. The economy of Zimbabwe is mostly depended on agriculture. The country produces many crops but maize is the staple crop and the impact of climate variability and change on maize production is considered in this study. Climate change issues have been extensively investigated in Zimbabwe (Makadho, 1996; Matarira et al., 2004; Murewi, 2009; Sithole, 2009) but the impact of climate variability and change on maize and food production systems has not yet received adequate attention; in particular there is lack of systematic evaluation of climatic-yield trends (Lobell and Asner, 2003), hence the need for this research.

In Zimbabwe, most of the maize is grown in the northeast in an agroecological zone classified as Natural Region 2 (Vincent and Thomas, 1961). Most of the seasons, this region accounts for 75-80 percent of the planted area assigned to crop production in Zimbabwe (FAO, 1999). The cropping systems are based on flue-cured tobacco, maize, cotton, wheat, soybeans, sorghum, groundnuts, seed maize and burley tobacco grown under dry land production as well as with supplementary irrigation in some months. Irrigated crops include wheat and barley grown in the colder and drier months (May-September). This study focuses mainly on maize because it is the primary staple food crop and occupies about half of the agricultural land in Zimbabwe (Matarira et al., 2004). Maize is therefore important to the food security of the country.

This study is a scientific approach to investigate maize production sensitivity to climate variability and change. Modern scientific tools are used to investigate the potential impact of climate change on maize yield. Two major tools are used: Climate Change Explorer (CCE), a software tool that uses downscaled global climate model simulations to explore the historic and future climatic conditions and AquaCrop (Raes et al., 2009), a newly developed crop growth model. The main reason for applying global climate models is their ability to explore different climate scenarios.

These scenarios are able to capture aspects that cannot be directly influenced such as population growth and climate change. In this study, climate projections are derived from Climate Change Explorer (http://wikiadapt.org). The projections are extracted from the highest performing model out of five global climate models based on the A2 climate change scenarios. AquaCrop is used to test maize response to climate change. It uses, as inputs, specified climatic and nonclimatic variables to simulate maize yield. When validated, AquaCrop can be used to make future yield predictions.

The development of statistical crop growth models has increased understanding of the link between climate change and crop productivity. Statistical models which are driven by net radiation and temperature as initial conditions, utilize the carbon budget to predict crop growth. However, they neglect other effects that may cause substantial modifications in crop productivity. Easterling et al. (1989) argued that appropriate soil and technological management as well as genetic improvements are responsible for the observed increase in crop productivity. Moreover, evidence has been found that increased atmospheric carbon dioxide (CO₂) concentration may lead to increased crop productivity, in particular for C₃ plants (e.g. Kinball et al., 1995, Tubiello et al., 2000). Similar work on the impact of climatic variability and change on maize production was done in China. Wang and Lin (1992), using the CERES – maize model and three climate scenarios from doubled CO₂ simulations from three global climate models showed that at most of the 35 investigated sites across China, simulated yields of both rain fed and irrigated maize would decrease under climate change primarily because of increases in temperature which could reduce maize growing period, particularly the grain filling period. Using CERES – maize model and the IPCC A2-based climate change scenarios from a regional climate model, Xiong et al. (2007) showed that maize productivity in north China would decrease by up to 25 % under irrigation conditions; however rain fed maize productivity would increase by up to > 50 % due to CO₂ fertilization effects. This research uses a crop growth model AquaCrop and five downscaled global climate models to carry out similar investigations at five stations in Northeastern Zimbabwe.

1.2 Problem statement

Climate variability and the prospect of future climate change raise serious concerns about the sustainability of maize production in Zimbabwe. The extreme climatic events that are inevitable

consequences of climatic variability and change pose great risks to the successful functioning of agriculture. Maize production is under threat from environmental constraints such as increase in temperature and reduced rainfall. Global Climate Models (GCMs) predict that climate change will bring higher temperatures, altered precipitation and higher levels of atmospheric carbon dioxide (IPCC 2007). According to the IPCC - A2 climate change scenarios, Southern Africa is expected to record a warming of between 0.6 and 0.7 °C by 2020 (Nurmohamed, 2006). These conditions are potentially hazardous to the growth and development of the maize crop, therefore this research seeks to provide an investigation of the future potential productivity of maize under a different climate regime.

In 1982, the population of Zimbabwe was 7 546 071 (CSO, 1989). This population rose from 10 412 548 in 1992 to 11 631 657 in 2002 (CSO, 2004), a rise of about 12 %. If the growth rate observed between 1992 and 2004 continued, the population of Zimbabwe would be expected to double every 23 years (Matarira et al., 2004). Higher population means that more people will be affected by climate change and a growing population also calls for higher demand for food and water. Adverse climatic change impacts include droughts, floods, loss of biodiversity, shifting of agricultural zones and reduction of suitable regions for planting (Lobell et al., 2008; Luo et al., 2005; Richter and Semenov, 2005; Zhang and Liu, 2005). Droughts which occurred during the 1982-83, 1987-88, and 1991-92 rainfall seasons resulted in acute crop failure, which in turn resulted in food insecurity and malnutrition especially among vulnerable rural communities in Zimbabwe (Matarira et al., 2004). There has also been rainfall excesses leading to flooding associated with tropical cyclones such as Bonita in 1995/1996, Eline in 1999/2000, Japhet in 2002/2003 (Tsiko, 2008) and cyclone Ernest in 2004/2005 (Sithole and Murewi, 2009). It is therefore necessary to carry out studies on climatic variability and change and find possible ways of addressing food insecurity in Zimbabwe.

1.3 Objectives of study

The main objective of the study is to investigate the potential impact of climatic variability and change on maize yield in Northeastern Zimbabwe. The specific objectives are:

- ❖ To show the variability and general trends in mean annual rainfall and mean annual air temperature in Natural Region 2 of Zimbabwe for the period 1971 2000;
- to compare five downscaled global climate model simulations and select a model best suited to a particular location;
- to investigate the past and projected climates at five stations using the Climate Change Explorer tool;
- * to validate the AquaCrop model for simulating maize yield in Zimbabwe, and
- to apply the AquaCrop model to simulate maize yield under projected climatic conditions at the five stations.

1.4 Limitations

Some limitations of the research include: (i) there are limited resources available for the work. (ii) the impact on yield due to factors other than weather (e.g. pests, diseases and weeds are not considered in AquaCrop. (iii) it is assumed that there are no changes in soil characteristics and (iv) only a few stations are considered in the study due to data unavailability and the results will be generalized for the whole region.

1.5 Expected benefits

Findings of this research will be provided to agricultural researchers and it is hoped that the information will assist them in researching and breeding for new maize varieties that are suited to particular areas under new climatic regimes. The findings can also be used by policy makers and other stakeholders to device ways of mitigating the negative impacts of climate change. Multilateral agencies and non-governmental organizations can also use the information to plan for drought relief operations if food deficit is anticipated. The results will also be used to educate and advise maize growers on adaptation strategies to moderate the adverse impacts or to benefit from opportunities associated with climate variability and change.

1.6 Thesis layout

The thesis is organized into five chapters. Chapter 1 provides the introduction of the study, its background and justification, objectives and the expected benefits of this research. A detailed literature review of the study and description of the variables included in the study is presented in Chapter 2. Chapter 3 describes the methodology used to carry out the research and the types and sources of data. Chapter 4 provides the results and discussion. Finally Chapter 5 gives conclusions and recommendations.

CHAPTER 2

LITERATURE REVIEW

2.1 Introduction

This chapter presents a review of literature on climate in general and its impact on crop production in Zimbabwe. The maize crop requirements are discussed, focusing mainly on the effect of selected climatic parameters on maize yield. Various types of climate and crop models are discussed. Five global climate models and their predictions of future climate scenarios are also described. The chapter also describes the Climate Change Explorer tool. The functions of the AquaCrop model used in this study are examined.

2.2 Measuring Climate

The climatic variables that are monitored regularly at climatological stations are: temperature (air and soil), rainfall, sunshine hours, wind velocity, cloud cover, atmospheric pressure, humidity and evaporation. When these elements are measured systematically at a site over a period of several years, they eventually accumulate an archive of observations from which people can construct a summary of that place's climate. Using a variety of statistical techniques, it is possible to compute averages for different climate elements as well as measures of variability and frequency of occurrence.

Climate is variable and as a result a single locality's climatic record may show different climates for different periods of time. The likelihood of this is where the climate record is long and substantial changes such as urban growth have altered local conditions. In order to decide which of these climates is the normal climate for a place, Gullett & Skinner (1992) point out that the standard practice is to base the calculations on the last three complete decades. The resulting summaries are referred to as the climate "normals" and they are updated at the beginning of every new decade. The climate record since 1941 for example is covered by sets of normals: 1941-1970, 1951-1980, 1961-1990, 1971-2000 and 1981-2010 (Gullett & Skinner, 1992).

2.3 Climate of Zimbabwe

Although most of the climatic parameters listed in section 2.2 have bearing on the growth and development of maize, temperature and rainfall are the most important factors and so emphasis is placed on these two parameters in this study.

Zimbabwe's main rainfall season starts from mid-November to mid-March (Climate Handbook of Zimbabwe, 1981). The months of December, January and February are the peak rainfall months (Matarira et al., 2004). The mean annual rainfall ranges from about 200 mm in the southern parts of the country to about 3000 mm in the Eastern highlands. Mean annual air temperatures for Zimbabwe range from 15 °C on high ground to above 25 °C in low altitude areas (Climate Handbook of Zimbabwe, 1981).

2.4 Soils of Zimbabwe

About 70 percent of Zimbabwe is covered with sandy soils mostly derived from coarse granite. The sandy soils are low in nitrogen (N), phosphorous (P) and sulphur (S) and in cation exchange capacity (CEC) owing to low clay and organic matter contents (Grant, 1967a, 1967b, 1970; Nyamapfene, 1981). In addition, the sandy soils are generally acidic. According to Grant (1970), many crops on granite sandy soils on the communal lands reveal multiple nutrient deficiencies of N, P, S, magnesium (Mg), potassium (K) and of micronutrients such as zinc (Zn) (FAO, 1999).

2.5 Impact of climate variability and change on crop production

Climate change presents crop production with prospects for both benefits and drawbacks (FAQ, 2008). Although most global climate models (GCMs) predict changes in rainfall and temperature patterns over Zimbabwe, there are several uncertainties that limit the accuracy of current projections. One such uncertainty is related to the degree of temperature increase and its geographic distribution. Another pertains to the accompanying changes likely to occur in the precipitation patterns that determine the water supply to crops and to the evaporative demand imposed on crops by the warmer climate. There is a further uncertainty regarding the physiological response of crops to enriched carbon dioxide (CO₂) in the atmosphere (FAQ, 2008). Climate variability and change also modify the risks of fires, pest and pathogen outbreaks,

negatively affecting the production of food and fibre. However, there are some benefits associated with climate change. If rainfall increases as some GCMs predict, the water can be harnessed and used for a variety of agricultural and other purposes. An increase in temperature may enhance crop production in areas where temperatures are low and limiting.

2.5.1 Factors influencing crop production

Several factors are linked to climate variability and change and crop productivity. Some of them include average temperature increase, changes in rainfall amount and patterns, rising atmospheric concentrations of carbon dioxide and pollution levels such as tropospheric ozone.

2.5.1.1 Average temperature increase

Temperature is an important determinant of the rate at which a plant progresses through various phenological stages towards maturity. Daytime temperatures are critical in determining the growth and development of a crop. The accumulation of biomass is constrained by seasonal variations in daytime temperatures. Higher temperatures above optimum in general slow down plant maturity thus shortening the growth stages during which pods, seeds, grains or bolls can absorb photosynthetic products. An increase in average daytime temperature can shorten the phenological phase i.e. accelerate plant phenology and also adversely affect crops in regions where summer heat already limits production. Daytime temperatures are also important as they determine the rate of evapotranspiration. A large number of GCMs predict a rise in the mean annual temperature over most of Southern Africa in the next few years. Rising temperatures will lead to high rates of evaporation of water from river basins, dams and from the soil and if not matched with precipitation increase, both rain fed agriculture and irrigated crop production will be adversely affected.

2.5.1.2 Changes in rainfall

Although the total rainfall received in a region may be important, crop producers are also interested in the onset, distribution throughout the growing season and cessation of the rains. Rainfall is one of the most important resources in any agricultural region.

It feeds rivers, dams and ground water from which water is extracted for agricultural and other uses. Rainfall replenishes the soil, enabling crops to grow. The onset of the rains in any region is viewed as an important event (Arnetzen et al., 1996). Its total, temporal and spatial variation are however equally important. Changes in the supply of rainfall, whether in the total amount or in its frequency and reliability or changes in the evaporative demand by which water is extracted from the land by the atmosphere have enormous consequences for a wide range of agricultural activities (Arnetzen et al., 1996).

Changes in rainfall can affect soil erosion rates and soil moisture, both of which are important for crop yields. With increasing atmospheric emissions of greenhouse gases, summer rainfall is projected to decrease over subtropical regions of Southern Africa. Over the long-term, it is predicted that much of Southern Africa will become more arid than at present (Clayton, 1997).

GCMs predict that by 2050, the monsoon winds that bring moisture to Sub-Saharan Africa could be 10 to 20 % drier than the 1950-2000 averages. Regions like Zimbabwe that depend on seasonal water supply may experience a shift in the timing of the onset of the rainy season or a shortening or lengthening of that season (Slater, 1981). When the season is shortened, critical phenological stages such as tasselling and grain filling may be adversely affected by moisture deficit thus negatively impacting on crop production.

2.5.1.3 Carbon dioxide concentration

Carbon dioxide in the atmosphere is absorbed by plants during photosynthesis. It has been observed that CO₂ concentration showed a marked increase in the last century mainly due to human activities. Models predict that if industries continue utilizing fossil fuels, the levels of CO₂ will double in the near future. The effect of carbon dioxide enrichment alone would probably be beneficial to some crops. Some studies have demonstrated positive effects of

increasing atmospheric CO₂ concentrations on crop photosynthetic efficiency and water use. According to Easterling et al. (2001), exposure of C₃ plants to elevated CO₂ generally results in stimulated photosynthesis and enhanced growth. As discussed by Long et al. (2006), crops sense and respond directly to rising atmospheric CO₂ concentration through photosynthesis and stomatal conductance and this is the basis for the fertilization effect on yield.

In theory, at 25°C, an increase in atmospheric CO₂ concentration from the present day value to that projected for the year 2050 would increase C₃ photosynthesis by 38 % (IPCC, 2007). Carbon dioxide enrichment studies indicate that at 550 ppm CO₂ concentration, yields increase under unstressed conditions by 10-25 % for C₃ crops and by 0-10 % for C₄ crops (IPCC, 2007). Increased CO₂ concentration is however associated with global warming leading to above average mean air temperatures. Costa et al. (2009) say that for maize, the positive effect of increased CO₂ concentration is not sufficient to compensate the negative effect associated with temperature increase i.e. the CO₂ fertilization effect is much weaker and cannot cancel out the thermal effect. Higher temperatures could also increase the rate of microbial decomposition of organic matter, adversely affecting soil fertility in the long run. In addition, some studies on pests and diseases suggest that temperature increases may extend the geographic range of some insect pests currently limited by temperature (Parry, 1990). Stomata are also known to respond adversely to elevated CO₂ by closing and this can impact on productivity.

2.5.1.4 Effects of pollution

Ozone that is found high in the atmospheric region called the stratosphere is beneficial in that it reacts with harmful ultraviolet radiation. However, the ozone found in the lower levels of the atmosphere is harmful to crops. Increase in ozone levels due to anthropogenic activities is believed to enhance global warming resulting in climate change. Such changes may offset any beneficial yield effects that result from elevated CO₂ levels (IPCC, 2007).

2.6 The maize crop requirements

2.6.1 Soils

Maize can be grown on a variety of soils. It however grows well in deep fertile soils rich in organic matter and with a rich supply of nutrients. Soils should be medium textured, well drained

and with a good water holding capacity. Loam or silt loam surface soil and brown silt clay loam having fairly permeable subsoil are the ideal soil types.

The pH should be between 6.5 to 7.5 along with cation exchange capacity of 20 centimole of charge per kg and base saturation of 70 to 90 percent. Suitable bulk density is 1.3 g/cm³ with water holding capacity of about 0.16 m/m depth (Ikisan, 2000).

2.6.2 Soil moisture

Maize can successfully grow in areas receiving an annual rainfall of 600 mm, which should be well distributed throughout the growing season (Bardzik et al., 1970). The crop needs more than 50 % of its total water requirements in about 30 to 35 days after tasselling and inadequate soil moisture at grain filling stage results in a poor yield of shriveled grains (Ikisan, 2000). The crop is very sensitive to water logging when there is excessive rainfall. In addition, too much precipitation can cause disease infestation. On the other hand, water deficit has an adverse effect on the growth rate of maize and the final yield. Too little precipitation can be detrimental to the crop yields, especially when dry periods occur during critical development stages. Moisture stress during the flowering, pollination and grain-filling stages is harmful to maize (Decker et al., 1985). There is decreased chlorophyll content in maize leaves under water stress resulting in reduced dry matter production (Hejnak, 2009).

2.6.3 Temperature

Maize is a tropical crop that grows best in areas with maximum temperature range of about 30 to 33 °C (Loomis and William, 1963). Critical stages for high temperature injury include seedling emergence, silking and tasselling (Shaw, 1983). Maize is a warm weather loving crop and it stops growing if the night temperature falls below 15° C and can not withstand frost at any stage (Ikisan, 2000).

2.6.3.1 Germination

Temperature is an important ecological requirement for seed germination. Germination is restricted for tropical crops at temperatures lower than 20 °C but takes place satisfactorily at temperatures as high as 40 °C (Goldsworthy and Fisher, 1984).

Temperature also affects the time required for germination; warmer conditions favour more rapid germination. Typical minimum, optimum and maximum temperatures for maize are 9 °C, 33 °C and 42 °C (Mayer et al., 1975). The upper temperature limits for germination, emergence and establishment lies between 40 and 45 °C. The speed of these processes increase with increase in temperature to an optimum of about 30 °C (Nishiyama, 1976).

2.6.3.2 Development of stem and leaves

Growth and development of the above parts of the vegetative plant are determined primarily by the activity of the apical meristem because the leaf primordial is formed here (Lal, 1979). Cell division, expansion and differentiation are controlled to some degree by hormones and these hormones operate within an optimum range of temperatures. Higher temperatures beyond optima slow down hormonal processes. Temperature affects the rate of leaf expansion. In maize, leaf expansion declines sharply at temperatures higher than 35 °C (Lal, 1979). Leaf senescence is however accelerated by high temperatures.

2.6.3.3 Effects of rise in mean temperature during the reproductive phase

In maize, typical florets are initiated at much shorter time intervals than leaves. In tropical maize, the interval between the initiation of successive leaf primordial is between 1.2 and 1.8 days but between 600 and 800 florets may be formed on a single ear in a space of 20 to 40 days depending on temperature and radiation (Goldsworthy and Fisher, 1984). Higher temperatures shorten the duration of floret initiation and so may diminish the number formed. Temperature is also important in the setting of kernels. The kernel set process is vital in determining variability in grain yield. At temperatures above 38 °C, poor seed set in maize is attributed to a direct effect of high temperature (Carberry et al., 1989). Higher mean temperatures tend to reduce the number of grain per plant resulting in a lower final yield.

2.7 Climate change scenarios

Greenhouse gases are those gases that are relatively transparent to short wave radiation that comes from the sun and heats the earth and opaque to longwave radiation.

Such gases include CO₂, methane, nitrous oxide, water vapour, chlorofluorocarbons and ozone. When heated, the earth emits terrestrial or long wave radiation (infrared radiation). Greenhouse gases absorb the long wave radiation and prevent it from escaping into space, so they trap heat near the earth's surface. This is the greenhouse effect. Natural greenhouse gases in the atmosphere are necessary to sustain life as they maintain the earth at a temperature higher than it would be if they were not present (Woodward, 1993). Due to human activities such as burning of fossil fuels and deforestation, the concentration of greenhouse gases in the atmosphere is increasing leading to global warming. CO₂ is the most important of the greenhouse gases as it contributes about 70 % of the greenhouse effect (Houghton, 1999).

Several researchers have presented global scenarios showing variations in emissions of greenhouse gases. Scenarios' output projects climate changes averaged over the entire earth. Regional and local changes are affected by global events. It does not matter where CO₂ is released into the atmosphere; it mixes well so that local concentrations do not vary significantly from global concentrations (CARA, 2006).

Projections of climate change depend upon future human activities thus climate models are run against scenarios. Intergovernmental Panel on Climate Change (IPCC) developed a total of 40 emission scenarios (IPCC, 2009) in its Special Report on Emissions Scenarios (SRES) for use in its Third Assessment Report (TAR). The scenarios were designed to explore potential greenhouse gas and aerosol emissions. There are many different scenarios, each making different assumptions of future greenhouse gas concentration, land-use and other driving forces. Assumptions about future technological development as well as the future economic development are thus made for each scenario (IPCC, 2009). Emission scenarios are organized into families that contain scenarios that are similar to each other in some respects. IPCC assessment report projections for the future are made in the context of a specific scenario family. Amongst the families of scenarios discussed in the IPCC are the A2 and B2 scenarios.

2.7.1 The A2 scenario

The A2 scenario assumes *regional* resilience and adaptation. The fundamental theme of A2 is self-reliance and the preservation of local identities, with economic development being moderate and focused within regions. According to this scenario, global population is expected to increase at a higher rate compared to other scenarios. In addition, the A2 scenario foresees higher energy consumption, higher CO₂ concentrations as well as moderately high changes in land use. It also assumes that resources are scarce and the application of technology is less diverse (CARA, 2006).

2.7.2 The B2 scenario

The B2 scenario assumes *local* resilience and adaptation. This scenario emphasizes environmental preservation and social equity with local solutions to economic, social and environmental sustainability. According to this scenario, global population is expected to increase continuously but more slowly than in scenario A2. Further to this, scenario B2 has a moderate level of economic development (like A2), but requires less energy and less change in land use than A2. CO₂ concentrations are lower than in A2. Resources are more abundant and technological change is more diverse than in A2 (CARA, 2006).

2.7.3 Scenario predictions

Based on a large number of GCMs, annual temperature changes for A2 range from 0.7 °C in 2020 to 2.9 °C in 2080 and for the B2, from 0.6 °C in 2020 to 2.6 °C in 2080 (Nurmohamed, 2006). According to the A2 scenario, the CO₂ concentration is projected to be 440, 559 and 721 ppm in the years 2020, 2050 and 2080 (Costa et al., 2009). The projections according to the B2 scenario are 408, 478 and 559 ppm in 2020, 2050 and 2080 (Travasso et al., 2006). Figure 2.1 shows the global temperature projections for different climate change scenarios.

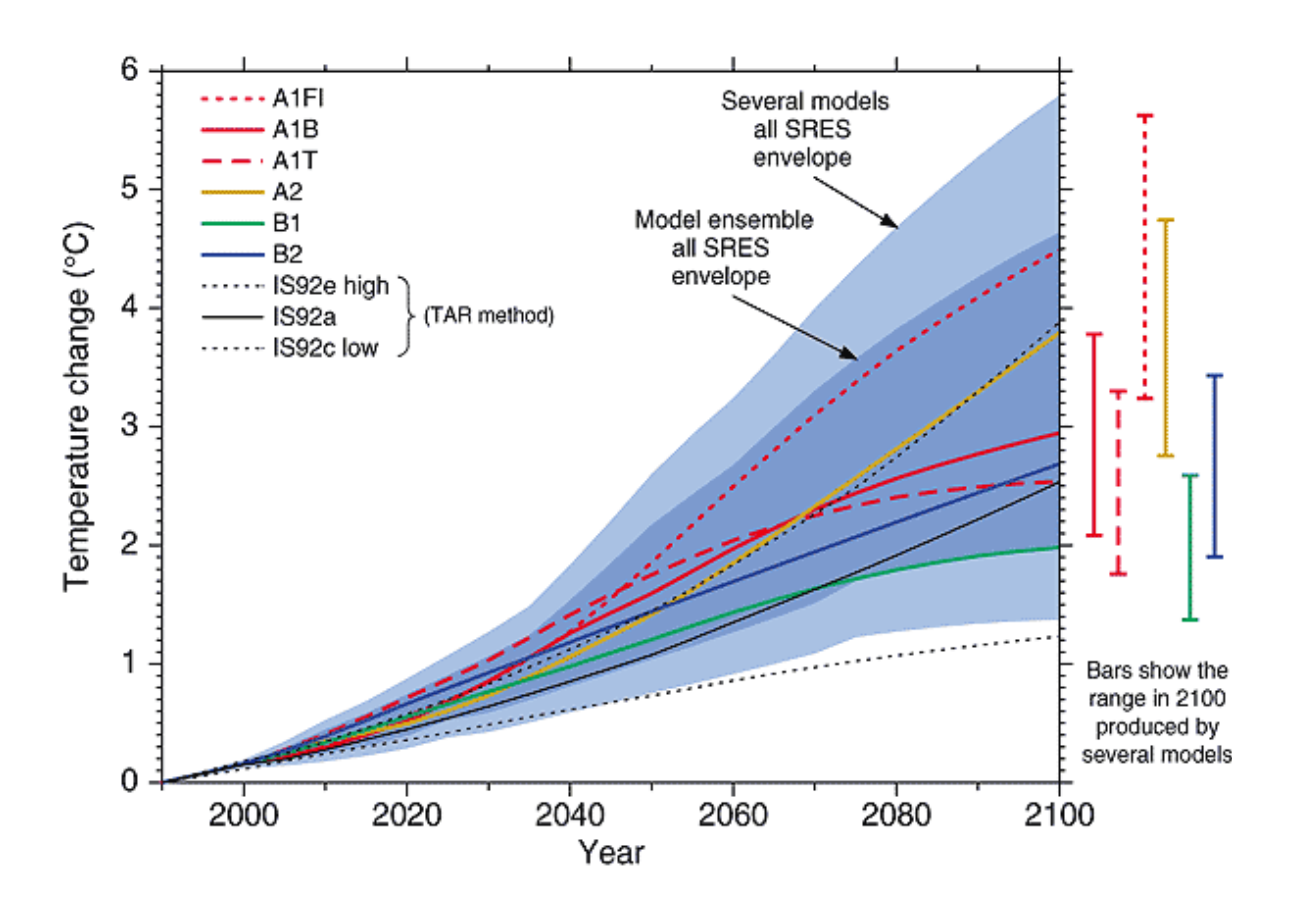


Figure 2.1 Future changes in global mean temperature from different emission scenarios using several different climate models. The bars show the range of simple model results in 2100 Source: (IPCC, 2007)

Other than the A2 and B2 scenarios, other scenario families are also shown in Figure 2.1.

The A1 scenarios are of a more integrated world (IPCC, 2007). There are subsets to the A1 family, based on their technological emphasis:

- A1FI an emphasis is placed on fossil-fuels.
- A1B a balanced emphasis on all energy sources.
- A1T these emphasize on non-fossil energy sources.

The B1 scenarios are also of a world more integrated and more ecologically friendly. B1 scenarios are characterised by rapid economic growth as in A1, but with rapid changes towards a service and information economy (IPCC, 2007).

IS92a: a middle of the range scenario in which global population rises to 11.3 billion by 2100, economic growth averages 2.3 % year⁻¹ between 1990 and 2100 and a mix of conventional and renewable energy sources is used (IPCC, 2007).

IS92c: economic growth averages 1.2 % year⁻¹ between 1990 and 2100 and global population is predicted to be 6.4 billion by 2100, with population decreasing in the 21st century (IPCC, 2007).

IS92e: results in the highest CO₂ emissions. Economic growth averages 3 % year⁻¹, between 1990 and 2100 and global population is predicted to reach 11.3 billion by 2100. Fossil resources are plentiful but, due to assumed improvements in living standards, environmental surcharges are imposed on their use. According to this scenario, nuclear energy is phased out by 2075 (IPCC, 2007).

2.8 Global climate models

Global climate models are computer driven programs for weather forecasting, understanding climate and predicting climate change. The five models used in this study are listed in Table 2.1. The five models were used because they are all based on the A2 climate change scenarios that apply to Southern Africa.

Table 2.1 Global climate models used in the study

Acronym	Name and Institute
CCCMA_CGCM3_1	The third generation coupled global climate model (CGCM3.1 Model,
	T47). Canadian Centre for Climate Modelling and Analysis, Canada.
CSIRO_MK3_5	Mark 3.5 Model. Commonwealth Scientific and Industrial Research
	Organization, Australia.
GFDL_CM2_0	CM2.0 coupled climate model. Geophysical Fluid Dynamics Laboratory,
	United States.
GISS_MODEL_E_R	ModelE20/Russell. Goddard Institute for Space Studies, United States.
MPI_ECHAM5	European Centre Hamburg Model. Max Planck Institute for
	Meteorology, Germany.

Future temperatures and precipitation for the A2 and B2 scenarios for example are estimated by climate models. The Canadian climate change model (CGCM3.1) and the Geophysical Fluid Dynamics Laboratory model (GFDL) predict rises in mean surface air temperature ranging from 2 to 4 °C at doubled CO₂ over most of Southern Africa (Makadho, 1996). GFDL suggests an increase in precipitation of up to 15 % across much of Southern Africa, with temporal and spatial variations over Zimbabwe (Matarira et al., 2004). CGCM3.1 however predicts an average 10 % decline in precipitation for the months September to October; December to February and October to April across Southern Africa (Matarira et al., 2004).

2.9 Downscaling of climatic data

Downscaling climate data is a strategy adopted to generate local data from large-scale information such as global climate model output. The scope behind downscaling is to connect global scale predictions and regional dynamics in order to generate site specific forecasts. The downscaling procedure is based upon developing an empirical relationship between the climatic parameter at a location and the associated large scale atmospheric state. The relationship is determined using historical data records of the parameter concerned at both the location and the atmospheric state. When the relationship has been determined, the future climate atmospheric states can then be substituted for the historical states so as to produce downscaled time series data for a particular parameter such as temperature or rainfall for a given location.

2.10 The Climate Change Explorer Tool

The Climate Change Explorer (CCE) is a software package developed by the Climatic Systems Analysis Group (CSAG) at the University of Cape Town in South Africa. Adaptation to climate variability and change requires an assessment and response to past climatic impacts to increase adaptive capacity and resilience to multiple stresses and to formulate plans and policies in ways that reduce the risk of adverse outcomes in the future (Zermoglio, 2007). A key step is to employ the best available science to contribute to the evaluation of potential exposure to present and future climate hazards. This requires an understanding of present day risks as well as trends in climate and how both may change in years to come (Zermoglio, 2007).

CCE is a climate navigating tool that explores past and future climatic conditions by providing visualizations and analytical routines of climatic variables. Visualizations are graphic and table functions that enable the user to explore the attributes of past and projected climates. The first step in working with the CCE tool is to retrieve climate model output from the CSAG data portal. The CSAG data portal contains downscaled global climate model datasets (scenario/model combinations) for a number of climate variables. The data is downloaded from the site then loaded into the CCE tool for further analysis.

2.11 Crop modelling

2.11.1 Crop growth simulation models and their uses

A model is a set of mathematical equations describing a physical system. In the case of crop growth models, it is the soil–plant–atmosphere system. The model simulates or imitates the behaviour of a real crop by predicting the growth of its components such as leaves, roots, stems and grains. Thus a crop growth model does not only predict the final state of total biomass or harvestable yield but it also contains quantitative information about major processes involved in the growth and development of the crop (Jame and Cutforth, 1996).

Crop growth simulation models are computer programs that integrate information on daily weather, genetics, management and soil characteristics to determine daily plant growth and subsequent yield (Batchelor, 1999). Crop models have many current and potential uses for answering questions in research, crop management and policy (Boote, 1995).

2.11.1.1 Uses of models

Crop models in general integrate current knowledge from various disciplines that include agrometeorology, soil physics, soil chemistry, crop physiology, plant breeding and agronomy into a set of mathematical equations to predict growth, development and yield (Hoogenboom, 2000). One of the main goals of crop simulation models is to estimate crop production as a function of weather, soil conditions and crop management.

Models can be used as tools for assessing agricultural management strategies and their interaction with climatic risk. In this case, the models are used to generate a large set of possible outcomes (Jame and Cutforth, 1996).

Crop models can assist policy makers by predicting effects of soil erosion, leaching of agrichemicals, climatic change as well as predicting yields. They can assist in pre-season and inseason management decisions on cultural practices, fertilization, irrigation and pesticide use (Boote, 1995).

2.11.1.2 Limitations of crop growth models

According to Travasso et al. (2006), the use of a given model for a particular purpose depends on whether the model complexity is appropriate to the problem under investigation and whether the model has been tested in diverse environments. There is need for both simple and complex models in crop simulation studies. In some cases, simple models are inappropriate because they are not programmed to address a particular phenomenon. This means there will be some factors that the model does not address. In other cases, complex models are not appropriate because they may require inputs that are not practical to obtain in a field situation. As the level of mechanism in a crop model increases, so does the requirement for more input data and system parameters and for more detailed experimental data. Such data are often unavailable and may be difficult to obtain experimentally. Thus the main determinant of the level of model simplicity is data availability for running the model. There are still some issues related to climatic variability and change that are not fully understood or missing in crop models and that give some uncertainty about future projections. Examples of such issues include the impact of increasing CO₂, ozone, flooding as well as the interaction with pests, weeds and diseases.

2.11.2 Types of models

2.11.2.1 Empirical and Mechanistic models

An empirical model sets out principally to describe where-as a mechanistic model attempts to give a description with understanding (France and Thorney, 1984). In empirical models, simple empirical functions are used to describe the relationships among the variables involved in the process.

On the other hand, mechanistic equations may be used to express the known or hypothesized theory that relates the variables and attempt to explain their observed behaviour. Thus crop models may range from strictly empirical models that use only a few variables and involve only a few processes to predict crop yield, to very complex models that include detailed biochemical simulations (Jame and Cutforth, 1996).

2.11.2.2 Deterministic and Stochastic models

A deterministic model is one that makes definite predictions for quantities (such as crop yield or rainfall) without an associated probability distribution. A stochastic model on the other hand contains some random elements or probability distributions. Such a model does not only predict the expected value of the quantity but also its variance. The greater the uncertainty in the behaviour of a system, the more important it may be to construct a stochastic model. Stochastic models are used to solve such systems like population dynamics (France and Thorney, 1984).

2.11.2.3 Static and Dynamic Models

A static model is one that does not contain time as a variable. Any time dependent components of the behaviour of the system are ignored. Since many aspects of the world do change at some rate, a static model is always an approximation. A dynamic model on the other hand contains the time variable explicitly. Most dynamic models of crop growth incorporate what are basically static models of light interception by the crop canopy although for crops whose leaves can respond to the light pattern, a dynamic model would be required (France and Thorney, 1984).

2.11.3 Calibration and validation of models

2.11.3.1 Model Calibration

Calibration is a process of adjusting the parameters of the model so that simulated results reach a predetermined level, usually that of an observation. For empirical models, calibration is the only way that system coefficients can be determined. It involves deriving the coefficients which go into the model. Calibration is especially necessary when adapting an existing model to a new environment.

The calibration procedure is conducted using a few well-defined experiments in which the soil and climatic conditions are carefully monitored and the crop growth details are duly recorded. The accuracy of yield prediction from a crop model depends on having an adequate model structure, precise system parameters and accurate environmental data. Once calibrated, a model can be used to evaluate performance of prescriptions over many different weather conditions. Both the comprehensive and simplified crop models have technical problems but they generally can provide reasonably good predictions especially when the model is properly calibrated for a region (Williams et al., 1989).

2.11.3.2 Model Validation

Validating a model is a process by which the model is run to predict an outcome that is already known. Since all practical crop models are limited imitations of the real system, they all need extensive field validation to assess whether they are structurally sound and to assess the extent and limitations of their validity. A practical model should be rigorously validated under widely differing environmental conditions to evaluate its accuracy on overall yield predictions as well as the performance of major processes in the model. Normally, the results from the validation process are used to refine the model or to guide modelers to further experiments that will produce a better model. Only after extensive experimental validation (and after numerous modifications) can a crop model become an actual working tool capable of providing guidance on the practical management of agricultural systems (Williams et al., 1989).

2.12 The AquaCrop model

AquaCrop is a crop water productivity model developed by the Land and Water Division of the Food and Agricultural Organization (FAO). It simulates yield response to water of herbaceous crops and is particularly suited to address conditions where water is a key limiting factor in crop production.

Some applications of AquaCrop include:

* assessing water-limited attainable crop yields at a given geographical location.

- * as a benchmarking tool, comparing the attainable yields against actual yields of a field, farm or region to identify the yield gap and the constraints limiting crop production.
- * assessing rain fed crop production on the long term.
- developing irrigation schedules for maximum production.
- carrying out future climate scenario analysis.
- optimizing a limited amount of water available.
- evaluating the impact of low fertility on yields.
- * assessing actual water productivity at the field and higher scales up to regions.

2.12.1 The evolution of AquaCrop

FAO used one of the empirical function approaches (Doorenbos and Kassam, 1979) to determine the yield response to water of field, vegetable and tree crops. The approach is expressed as:

$$\frac{(Y_x - Y_a)}{Y_x} = K_y \left(\frac{ET_x - ET_a}{ET_x} \right) \tag{2.1}$$

where Y_x and Y_a are the maximum and actual yield, ET_x and ET_a are the maximum and actual evapotranspiration and K_y is the proportionality factor between relative yield loss and relative reduction in evapotranspiration. FAO then revised equation (2.1) so that it could consider field crops and tree crops separately. Equation (2.1) formed the basis of the evolution of the AquaCrop model that was mainly designed for planning, management and scenario simulations. The evolution of AquaCrop saw this new model separating (i) the ET_a into soil evaporation (E) and crop transpiration (T_r) and (ii) the final yield (Y_a) into biomass (B) and harvest index (HI). The separation of ET_a into E and T_r was done to avoid the effect of the non productive consumptive use of water (E). The separation of Y_a into B and HI was done so as to show the difference in the basic functional relations between environment and B from those between environment and HI. These relations would then avoid the effects of water stress on B and on HI (FAO, 2009).

Equation (2.2) became the heart of AquaCrop:

$$\mathbf{B} = \mathbf{WP} \cdot \mathbf{\Sigma} T_r \tag{2.2}$$

where WP is the water productivity parameter with units kgm⁻²mm⁻¹ and T_r is the crop transpiration in mm. Equation (2.1) and equation (2.2) differ in the time scale used in each case. Equation (2.1) is used seasonally or for long periods (of the order of months) while equation (2.2) is used for daily time steps, a period that is closer to the time scale of crop responses to water deficits. Figure 2.2 shows the schematic representation of the evolution of AquaCrop from equation (2.1).

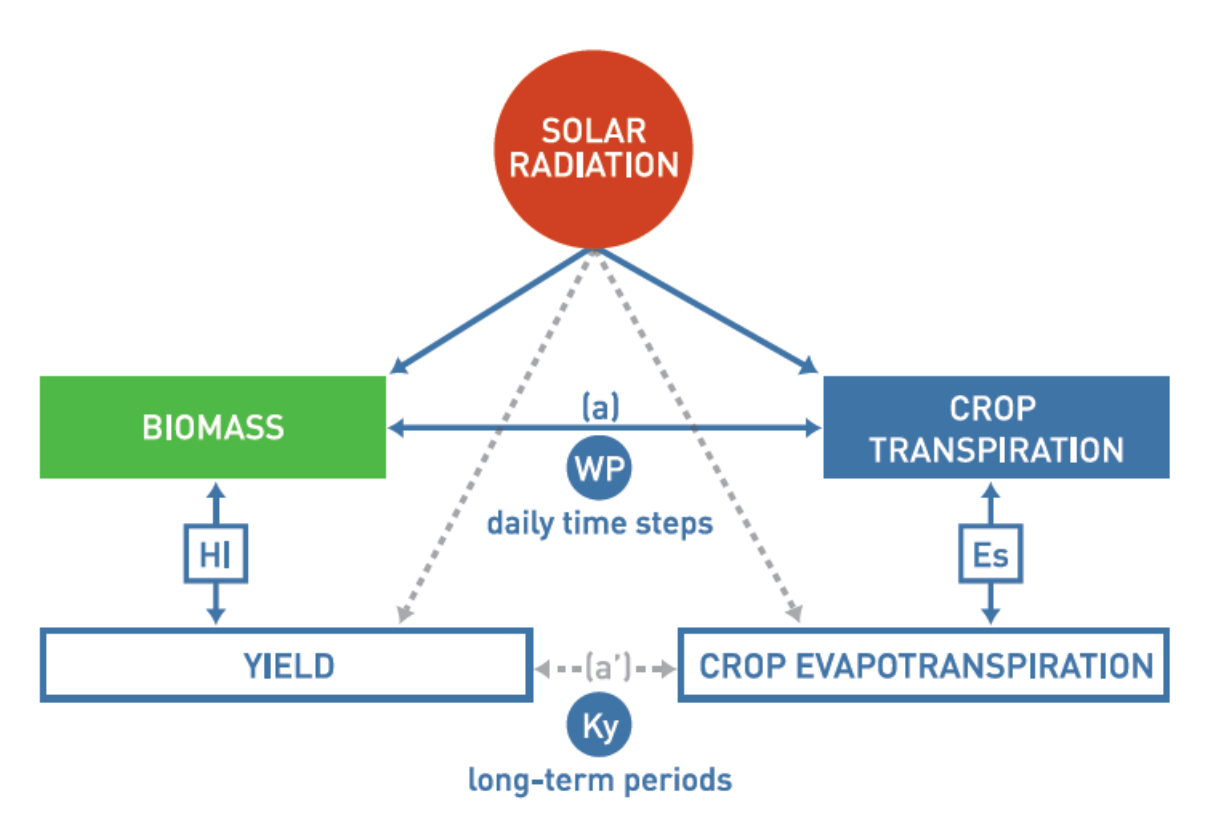


Figure 2.2 Evolution of AquaCrop from equation (2.1), based on the introduction of two intermediary steps: the separation of soil evaporation (E) from crop transpiration (Tr) and the attainment of yield (Ya) from Biomass (B) and harvest index (HI) Source: (FAO, 2009)

2.12.2 Components of the AquaCrop model

The following are the AquaCrop model components:

- soil and its water balance.
- the plant and its processes.
- the atmosphere and its thermal regime.
- rainfall.
- evaporative demand.
- * carbon dioxide concentration.
- * management (e.g. planting date, fertilizer use, irrigation, etc).

The model does not take into consideration such factors like pests, diseases and weeds (FAO, 2009).

Figure 2.3 shows the flowchart of AquaCrop indicating the main components.

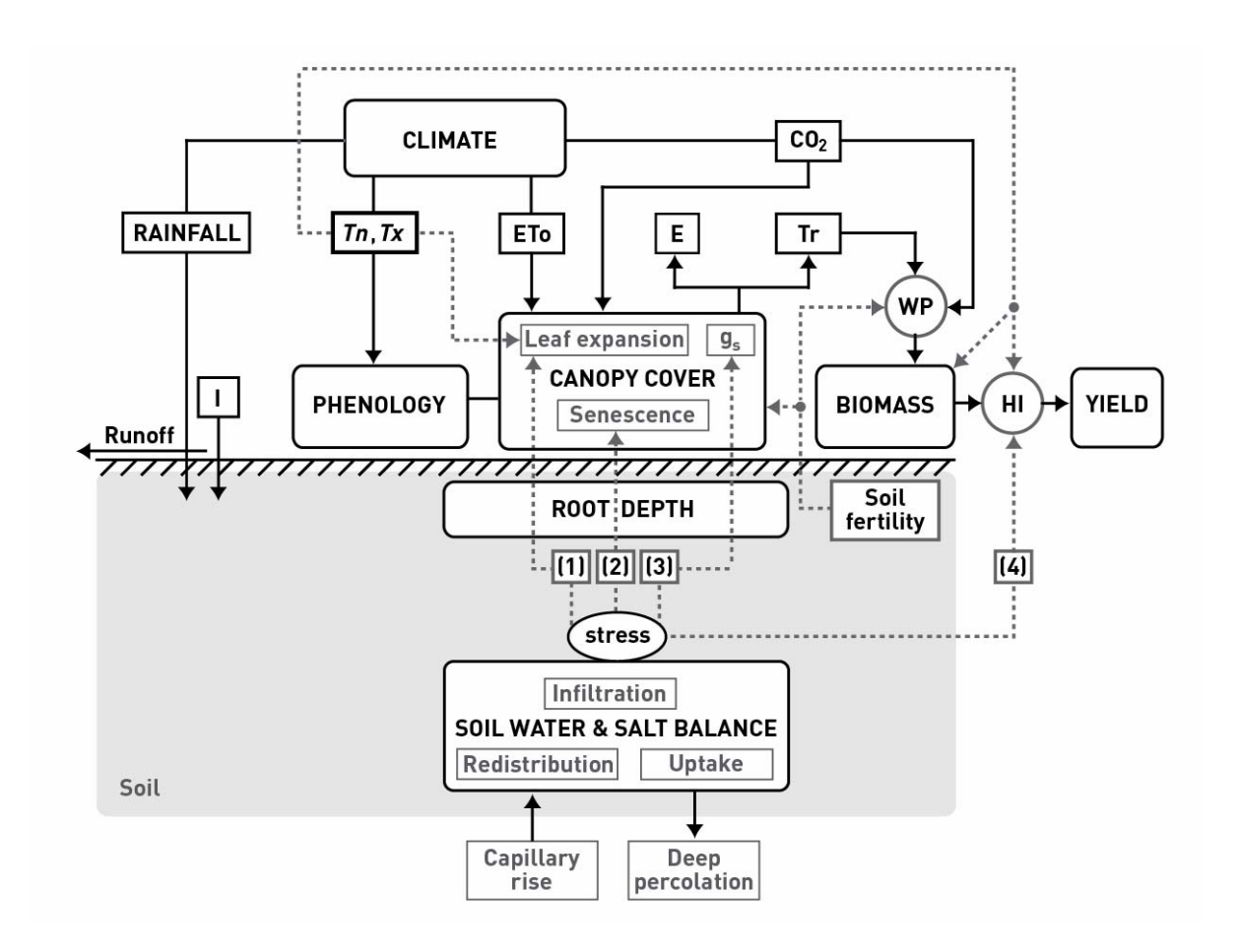


Figure 2.3 Flowchart of AquaCrop indicating the main components of the soil-plant-atmosphere continuum. Source: (FAO, 2009).

2.12.3 Model requirements

2.12.3.1 Climatic data

AquaCrop requires the following daily values as input variables:

- minimum and maximum air temperature,
- reference evapotranspiration (ET_o),
- rainfall and
- mean annual atmospheric CO₂ concentration.

Temperature data are used to calculate growing degree days which determine crop development and phenology and also for making adjustment in biomass production during damaging cold periods. In the absence of daily data, the input may also consist of 10-day or monthly data and the program uses an interpolation procedure to obtain daily temperature from the 10-day or monthly means.

The reference evapotranspiration (ET_o) is used in AquaCrop as a measure of the evaporative demand of the atmosphere. ET_o can be derived from weather station data by means of the FAO Penman-Monteith equation and an ET_o calculator is available for that work.

The use of long-term mean data for rainfall is not recommended because of its non uniform distribution over time. If daily rainfall data is not available, 10-day and monthly data can be used as input.

CO₂ concentration is important as it alters canopy expansion and crop water productivity.

2.12.3.2 Crop characteristics

The number and type of crop parameters varies with crop types. The model uses both conservative and non conservative crop parameters. Conservative parameters are specific for a given crop but do not change with time, management practices, geographic location or climate. These parameters are also assumed to be non cultivar specific. Non conservative parameters are cultivar specific and are affected by the climate, field management or conditions in the soil profile (FAO, 2009).

2.12.3.3 Soil input parameters

AquaCrop requires the following soil input parameters:

- ➤ Saturated hydraulic conductivity (K_{sat})
- \triangleright Volumetric soil water content at saturation (θ_{sat})
- \triangleright Volumetric soil water content at field capacity (θ_{FC})
- \triangleright Volumetric soil water content at permanent wilting point (θ_{pwp})

2.12.4 Biomass production and partitioning

By considering the crop water productivity (WP), the above-ground biomass is derived from the simulated amount of water transpired. The crop water productivity expresses the above-ground dry matter (g or kg) produced per unit land area (m² or ha) per unit of water transpired (mm). The above-ground biomass production for every day of the crop cycle is obtained from the normalized water productivity, the daily crop transpiration for that day and the reference evapotranspiration for that day (FAO, 2009).

The daily above-ground biomass is related to other parameters as:

$$m_i = WP^*_{adj} \left(\frac{T_{ri}}{ET_{oi}}\right) \tag{2.3}$$

where m_i = the daily above-ground biomass production (g/m² or ton/ha), (*i* is the i^{th} day)

 T_{ri} = the daily crop transpiration (mm/day),

 ET_{oi} = the daily reference evapotranspiration (mm/day) and

 WP^*_{adj} = the adjusted normalized crop water productivity (kg/m² or ton/ha) for atmospheric CO₂ concentration for the type of products synthesized during yield formation and for soil fertility.

The dry matter produced on any given day is partitioned between the plant organs that are growing at that time. The partition of biomass into yield part is simulated for fruit or grain producing crops by means of a harvest index (HI). Output from the model includes final grain yield, total biomass and biomass partitioning.

2.12.5 Advantages of the AquaCrop model

Most of the simulation models that quantify the effects of water on yield at the farm level can be valuable tools in water and irrigation management. In the case of maize, many such models have been tested: for example the CERES-Maize model (Jones and Kiniry, 1986), the Muchow–Sinclair–Bennett (MSB) model (Muchow et al., 1990), the EPICphase model (Cavero et al., 2000), CropSyst (Stöckle et al., 2003) and the Hybrid-Maize model (Yang et al., 2004). However these models are quite sophisticated, demand advanced skills for their calibration and operation and require large number of parameters. Some are cultivar-specific and not accessible to endusers. The main advantage of the newly developed AquaCrop model (Raes et al., 2009) is that it is a user-friendly and practitioner-oriented type of model as it maintains an optimal balance between accuracy, robustness, simplicity and requires a relatively small number of parameters. The AquaCrop model also uses input variables that require simple methods for their determination (FAO, 2009).

CHAPTER 3

MATERIALS AND METHODS

3.1 Introduction

This chapter describes the study area, types and sources of data, and the methodology used to carry out the research. Time series analysis of rainfall and temperature is covered in this chapter. The chapter also describes the five global climate models used in the study and the methods used to evaluate and rank them. Also covered in this chapter is the use of Climate Change Explorer (CCE) (version 1.0) in climate navigation. The last section of the chapter presents the validation of the AquaCrop model and its use to predict maize yield under the projected climatic conditions at each station.

3.2 The study area

The study was carried out in Natural Region 2 which is located in the middle of the north of Zimbabwe, covering parts of Harare, Mashonaland East, Mashonaland West, Mashonaland Central and Manicaland provinces. The region has a total area of 58600 km² which is about 15 % of the total area of Zimbabwe (Rukuni and Eicher, 1994). Data from five climatic stations: Karoi, Mutoko, Mt Darwin, Rusape, Wedza and one research station, Agricultural Research Trust (ART) Farm were used in this research. Of the six stations, five are within the region while Mutoko is adjacent to the region in Region 3. The choice of these stations was mainly based on data availability.

Figure 3.1 is a map of Zimbabwe showing all the natural regions with locations of the climatological stations overlaid. The positioning of the climatological stations on the agroecological map was done in the Department of Geography and Environmental Science at the University of Zimbabwe.

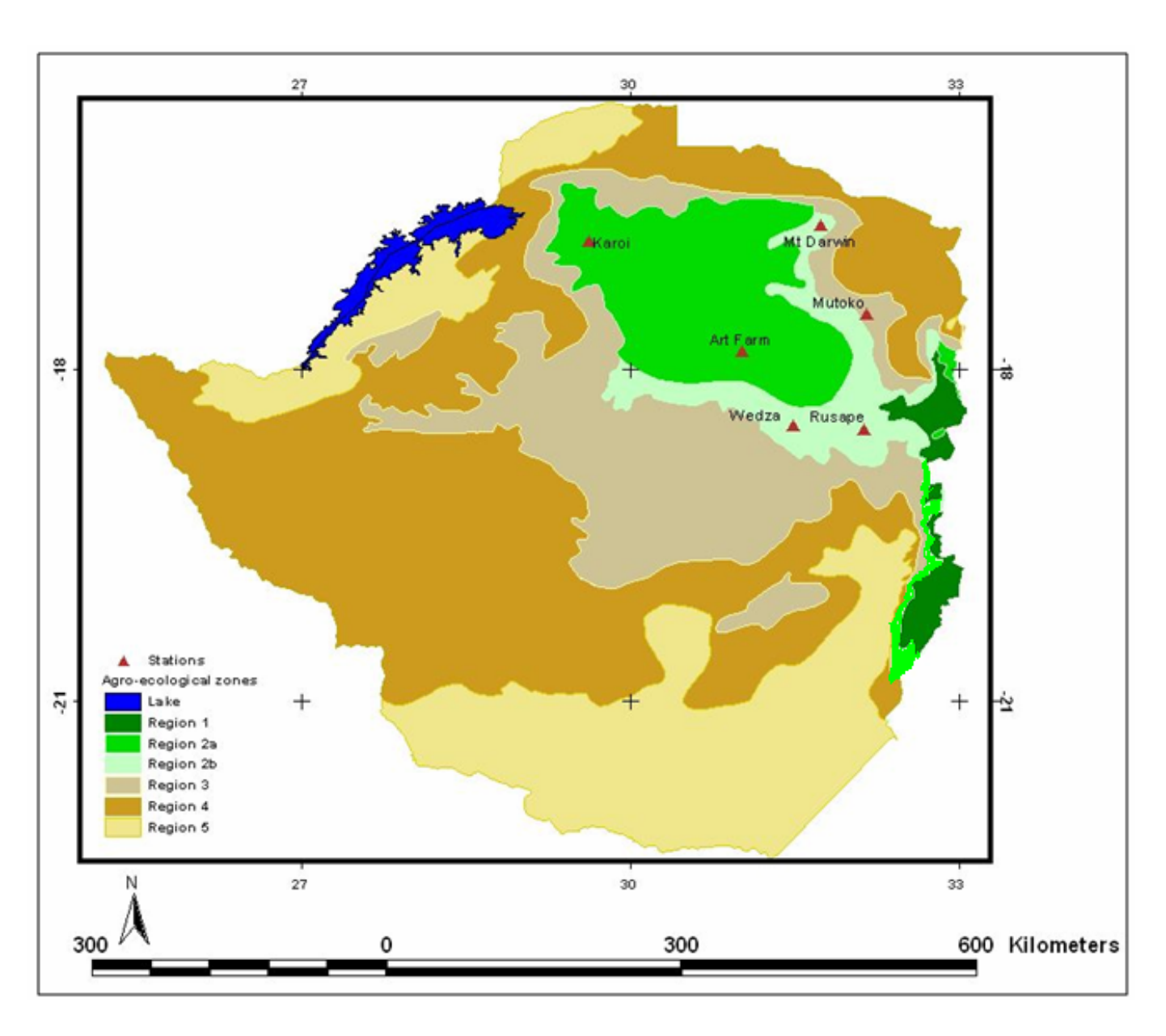


Figure 3.1 The study area Source: Department of Geography and Environmental Science, University of Zimbabwe.

Characteristics of the stations used in the study are shown in Table 3.1.

Table 3.1 Characteristics of the stations used in the study

Station	Region	Loca	ation	Altitude (m)
Karoi	2a	16° 50′S	29° 37′E	1343
Wedza	2b	18° 37′S	31° 34′E	1384
Rusape	2b	18° 32′S	32° 08′E	1430
Mt Darwin	2b	16° 47′S	31° 35′E	965
ART Farm	2a	17° 50′S	31° 01′E	1471
Mutoko	3	17° 25′S	32° 13′E	1244

3.3 Types and sources of data

3.3.1 Climatic data

Climatic data used in this study consist of observed data as well as model data. Observed data was provided by the Zimbabwe Meteorological Services Department (ZMSD) and by ART Farm which is in Harare. Model data was provided by the Climatic Systems Analysis Group (CSAG) in South Africa. The data was downloaded from the CSAG data portal at http://data.csag.uct.ac.za/

3.3.1.1 Rainfall

Daily rainfall data for the period 1971 - 2000 for Wedza, Rusape, Mt Darwin and monthly rainfall for Mutoko was provided by the ZMSD. ART Farm provided daily rainfall data for the period 1971 - 2006. CSAG model data consist of daily and monthly totals for three time periods: 1961 - 2000, 2046 - 2065 and 2081 - 2100 for the following stations: Karoi, Mutoko, Mt Darwin, Rusape and Wedza. ART Farm was not contained in the CSAG data base so there was no model data for this station.

3.3.1.2 Temperature

Mean monthly minimum and maximum temperature data for the period 1971 - 2000 for Karoi, Mt Darwin, Rusape and Wedza was provided by the ZMSD. ART Farm provided daily minimum and maximum temperature data for the period 2000 - 2006 as well as mean monthly minimum and maximum temperatures for the period 1971-2000 at the station. The downloaded temperature data are average daily and monthly minimum and maximum temperatures for the same period and stations as rainfall.

3.3.1.3 Reference evapotranspiration (ET₀)

ET_o data for ART Farm was provided together with temperature and rainfall data. For the remaining stations, ET_o data was calculated using the ET_o calculator software (Raes, 2007) applying the Hargreaves method. Reference evapotranspiration can be determined using a variety of approaches if the required data is available. The Hargreaves method requires minimum and maximum air temperature to estimate ET_o. This was the only usable data available for all stations hence its choice.

3.3.1.4 Homogeneity test of rainfall data

A reliable assessment of historical climate trends and variability requires a long-term, homogeneous time series of climate data. A homogeneous climate time series is one where the variations are caused by variations in climate only. However, data of high quality usually do not exist in practice. Such long series exhibit inconsistencies and non-homogeneities arising from a wide variety of non-climatic factors. These factors include changes in instruments, observation procedures, monitoring station relocations, changes of the surroundings, changes in calculation procedures etc. Non-climatic factors make data unrepresentative of the actual climate variation and thus the conclusions of climatic studies are potentially biased. Statistical tests can be used to identify non-climatic inhomogeneities. In this study, RAINBOW (Raes, 2006) was used to test homogeneity of rainfall data for each station. Figure 3.2 shows the main menu of RAINBOW.

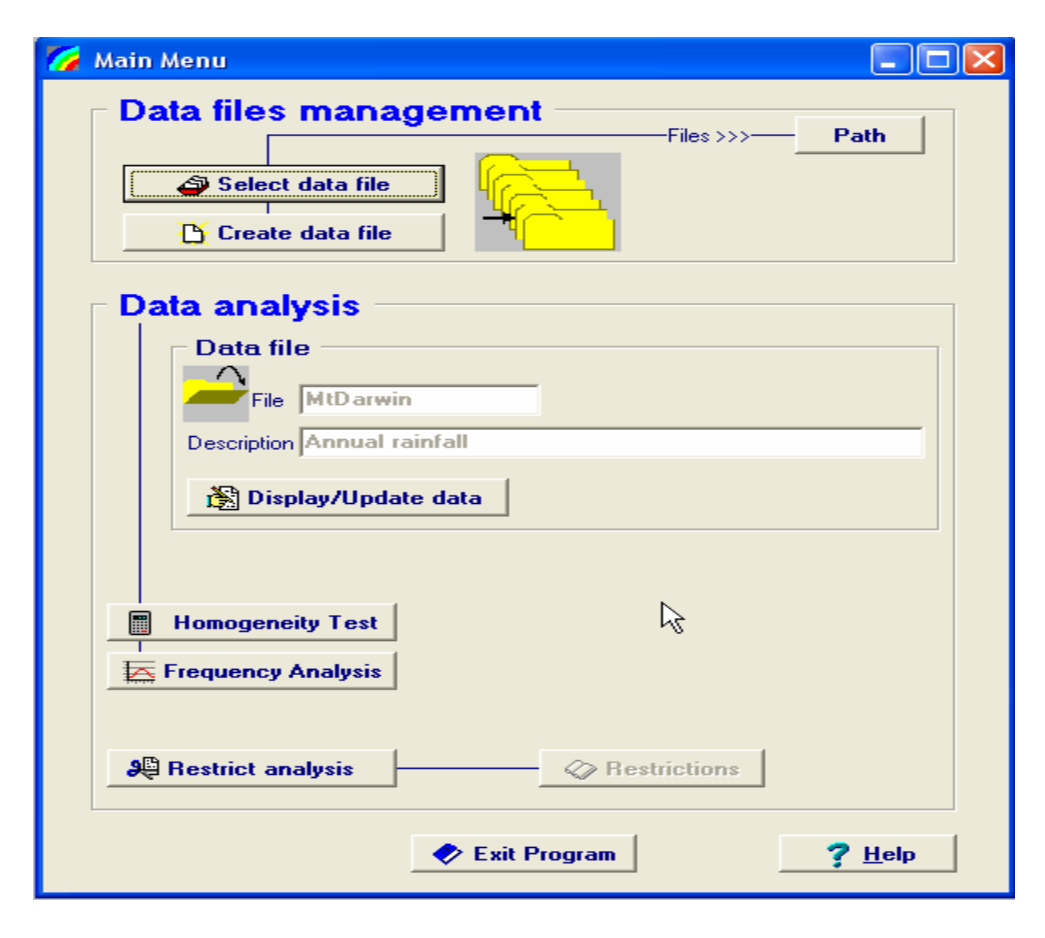


Figure 3.2 The main menu of RAINBOW

Data files were created and selected in the panels shown in Figure 3.2. When the files had been created and the climatic data loaded, a test for homogeneity was done by clicking on the "Homogeneity Test" button.

One of the tests of homogeneity (Buishand, 1982) is based on the cumulative deviations from the mean S_k :

$$S_k \otimes \text{EMBED Equation. 3 } \mathbb{D} \otimes \mathbb{D} \left(X_i - \overline{X} \right) \qquad k = 1, \dots, n$$
 (3.1)

where X_i are the records from the series $X_1, X_2, ..., X_n$ and \overline{X} is the mean. The initial value of $S_{k=0}$ and the last value $S_{k=n}$ are equal to zero. When plotting the S_k 's, changes in the mean are easily detected.

For a record X_i above normal the $S_{k=i}$ increases, while for a record below normal $S_{k=i}$ decreases. If a data set is homogeneous, the S_k 's fluctuate around zero because there is no systematic pattern in the deviations of the X_i 's from their average values \overline{X} (Raes et al., 2006). When a data set is tested for homogeneity, RAINBOW rescales the cumulative deviations by dividing the S_k 's by the sample standard deviation value. It then evaluates the maximum (Q) and the range (R) of the rescaled cumulative deviations from the mean thereby testing the homogeneity of the dataset. High values of Q or R are an indication that the data of the time series is not from the same population and that the fluctuations are not purely random (Raes et al., 2006).

3.3.1.5 Frequency analysis test of rainfall data

A frequency analysis requires statistical parameters describing the characteristics of the data set. The parameters are the mean and standard deviation. RAINBOW ranks the historical data in descending order and assigns a serial rank that ranges from 1 to n where n is the number of observations. The ranking is done by estimating the probability of exceedance of the rainfall data. From frequency analysis, the estimates of rainfall depths for selected probabilities of return periods are obtained (Raes et al., 2006).

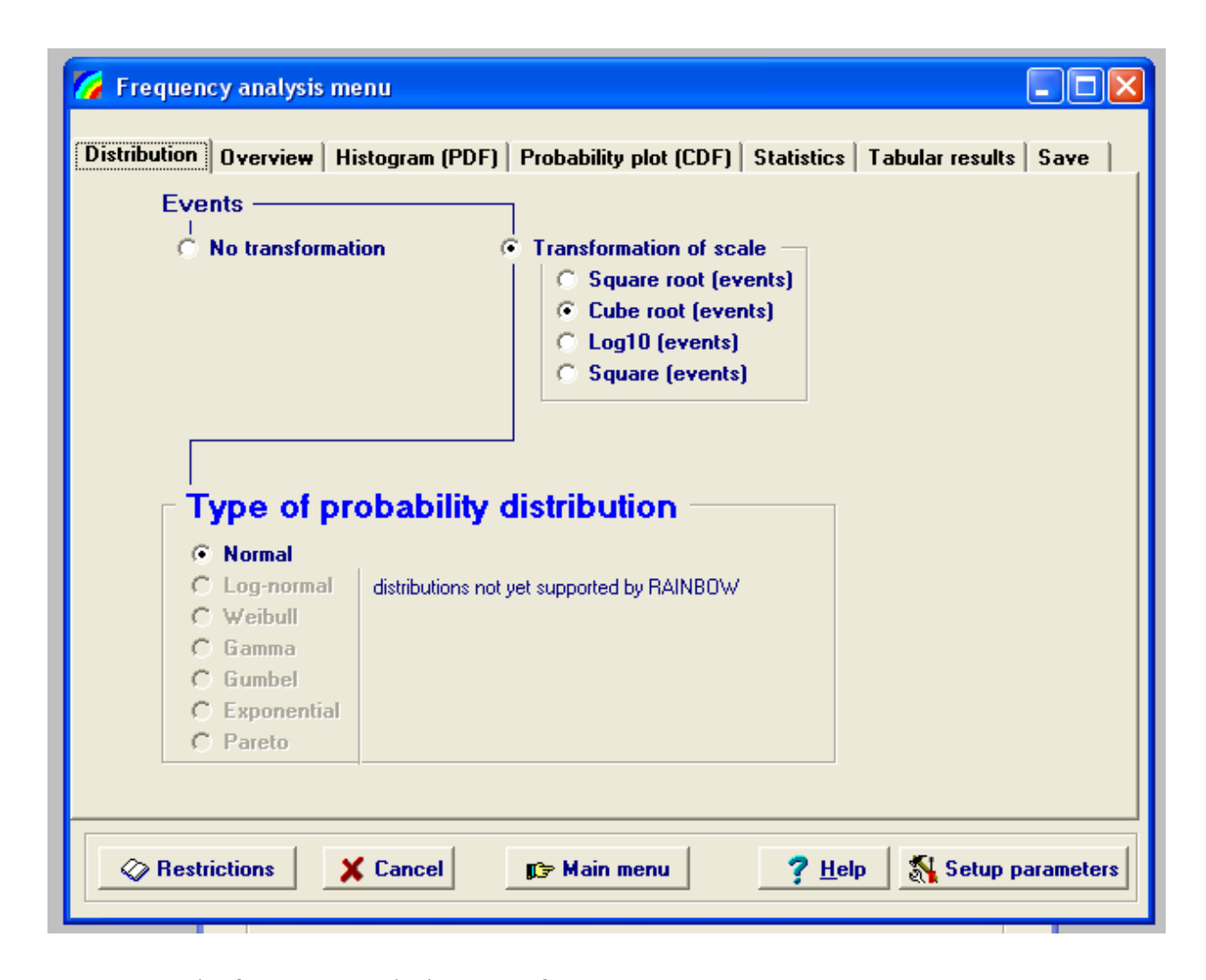


Figure 3.3 The frequency analysis menu of RAINBOW

The panel shown in Figure 3.3 contains various folders where options were selected and the results viewed.

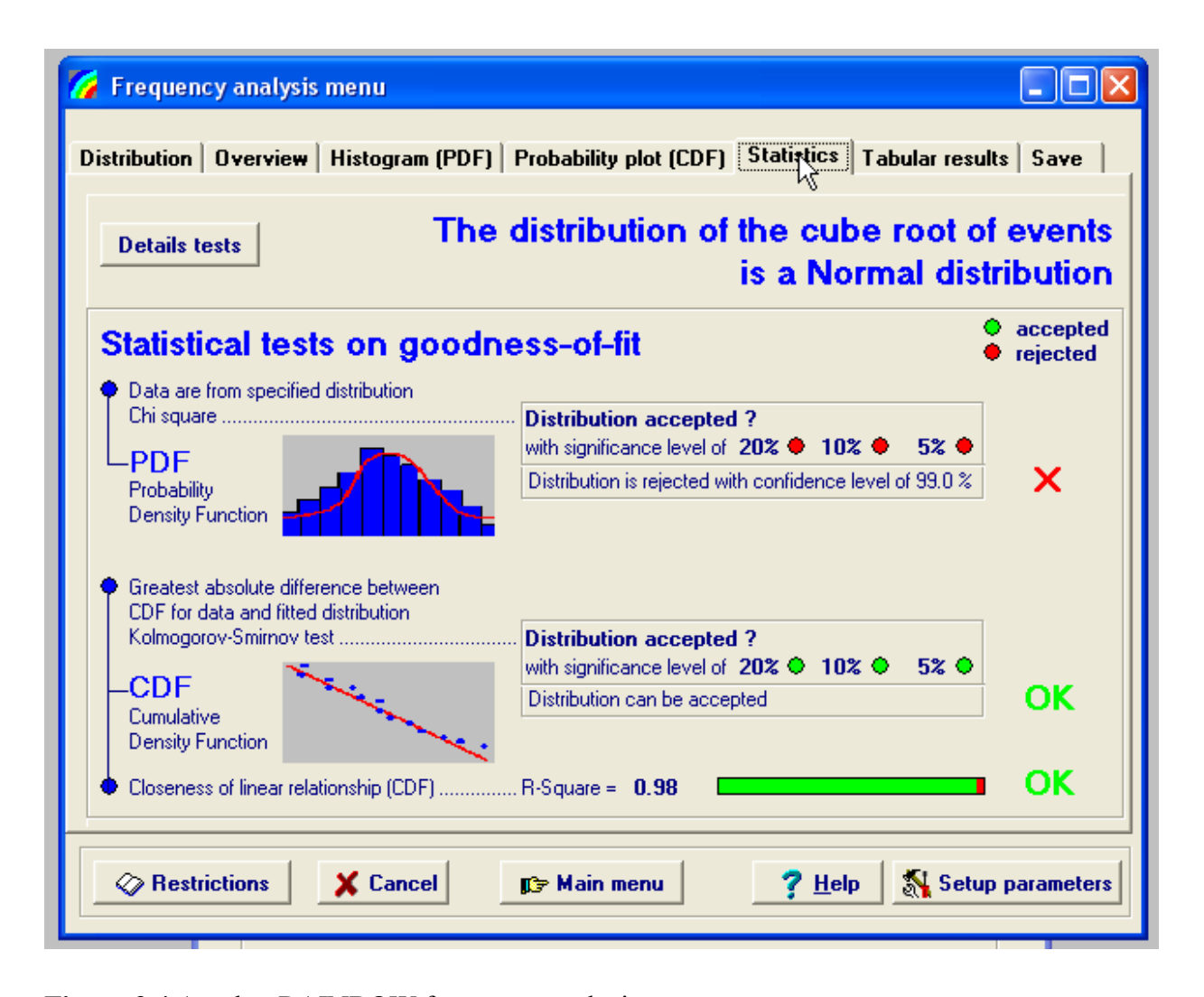


Figure 3.4 Another RAINBOW frequency analysis menu

The panel in Figure 3.4 contains the results from statistical tests evaluating the goodness of fit for the normal distribution of annual rainfall (1971-2000) for a particular station.

3.3.2 Nonclimatic data

In addition to climatic variables, the AquaCrop model also requires nonclimatic input parameters such as soil, crop, CO₂ concentration, yield and management.

3.3.2.1 Soil data

The most common soil type in Natural Region 2 is sandy loam and its characteristics are given in Table 3.2.

Table 3.2 General physical properties of the sandy loam soil predominant in Natural Region 2 of Zimbabwe

Property	Value	Units
Bulk density	1.51	gcm ⁻³
Soil water content at saturation (θ_{sat})	42.8	(vol %)
Soil water content at field capacity (θ_{FC})	24.4	(vol %)
Soil water content at wilting point(θ_{pwp})	10.6	(vol %)
Total available water (TAW)	13.8	(mm/m)

(Adapted from Sithole, 2003)

3.3.2.2 Crop data

Crop characteristics used to validate the AquaCrop model are shown in Tables 3.3 to 3.8 Cultivar specific characteristics for the SC513, SC633/635 and SC715/719 varieties were provided by SeedCo.

Table 3.3 Cultivar specific crop characteristics used to validate the AquaCrop model

Category	Variety	Time to maturity	Time to silking	Potential yield
		(days)	(days)	range (ton/ha)
Early maturity	SC513	137	68	4-8
Medium	SC633	140	69	6-12
maturity	SC635	142	67	5-10
Late maturity	SC715	152	73	6-11
	SC719	158	72	7-13

(Adapted from SeedCo, 2008)

Table 3.4 Growth stages and crop coefficient (K_c) factors for a 140-day maize

Stage of growth	Length	K _c
	(days)	
Initial	25	0.17-0.10
Crop development	40	0.17
Mid-season	45	1.20
Late season	30	0.35

(Adapted from Sithole, 2003)

Table 3.5 Growth stages and yield response factors (K_v) for a 140-day maize

Growth stage	Length	K_{y}
	(days)	
Establishment	20	1.00
Vegetative (early)	20	0.40
Vegetative (late)	20	0.40
Flowering	20	1.50
Yield formation	45	0.50
Ripening/drying	15	0.20

(Adapted from Sithole, 2003)

Table 3.6 Conservative crop characteristics considered for the SC513 cultivar

Description	Value
Plant density	37037 plants/ha
Maximum canopy cover	80 %
Maximum rooting depth	1.5 m

Table 3.7 Conservative crop characteristics considered for the SC633 cultivar

Description	Value
Plant density	37037 plants/ha
Maximum canopy cover	80 %
Maximum rooting depth	1.55 m

Table 3.8 Conservative crop characteristics considered for the SC715 cultivar

Description	Value
Plant density	37037 plants/ha
Maximum canopy cover	80 %
Maximum rooting depth	1.60 m

3.3.2.3 Carbon dioxide data

 CO_2 concentrations were based on measurements done at Mauna Loa Observatory in Hawaii, China. The data is calibrated within the AquaCrop model.

3.3.2.4 Historical maize yield data

Maize yield data required to validate the AquaCrop model was provided by ART Farm and it is given in Tables 3.9, 3.10 and 3.11. Yield data was provided together with sowing dates. The maize cultivars mainly considered were the SC513, SC633 and SC715 because these are the most common varieties grown in Northeastern Zimbabwe. The SC635 and SC719 were considered for the seasons in which data was not provided for the SC633 and SC715 varieties respectively.

Table 3.9 Observed yield and planting dates for the SC513 maize variety at ART Farm

Season	Planting date	Observed yield
	(date/month/year)	(ton/ha)
2000-2001	31/10/2000	10.86
2002-2003	28/10/2002	7.76
2003-2004	28/10/2003	11.30
2004-2005	27/10/2004	11.18
2005-2006	31/10/2005	10.10

Table 3.10 Observed yield and planting dates for the SC633 maize variety at ART Farm

Season	Planting date	Observed yield
	(date/month/year)	(ton/ha)
2000-2001	31/10/2000	10.51
2002-2003	28/10/2002	10.16
2003-2004	28/10/2003	14.15
2004-2005	27/10/2004	11.69
2005-2006 (SC635)	31/10/2005	13.77

Table 3.11 Observed yield and planting dates for the SC715 maize variety at ART Farm

Season	Planting date	Observed yield
	(date/month/year)	(ton/ha)
2000-2001	31/10/2000	9.11
2002-2003	28/10/2002	7.17
2003-2004	28/10/2003	11.73
2004-2005	27/10/2004	10.85
2005-2006 (SC719)	31/10/2005	14.78

3.4 Time series analysis of rainfall and temperature

Time series analysis of any climatic parameter shows the variabilities and general trends in the parameter. It is from time series plots of rainfall that seasons are identified as above normal or below normal rainfall seasons. The occurrence of extreme events is also evident from time series plots. Time series analysis was done using observed annual rainfall and observed mean annual temperature for the period 1971-2000. No data was available at some of the stations used in the study beyond 2000. ART Farm, Wedza, Rusape and Mutoko had rainfall data beyond 2000. For Mt Darwin, only maximum temperatures were available for temperature data. Time series analysis was done using Microsoft EXCEL.

3.5 Model data acquisition

The CSAG data portal contained a number of climatic stations in Zimbabwe. At the time of downloading, there were sixteen stations and more than ten global climate models present at the site. Access to the site was possible after having entered the necessary username and password. A list of climatic stations in Zimbabwe was provided from which one would choose stations of interest. Each station contained data that is downscaled from the climate models present. Four stations (listed in section 3.3) in Natural Region 2, and Mutoko in Region 3 were selected. The data was downloaded and then loaded into the Climate Change Explorer tool.

3.6 Model selection

A wide range of global climate models was available. From the list, five models were selected for use in this research. The reason for choosing five models was to capture the relevant uncertainties in climate projections arising from uncertainties in future greenhouse gas emissions and also uncertainties in earth-ocean-atmosphere feedback mechanisms. This also provided a wide range of models from which the most suitable one(s) could be selected. The choice of the five models may be justified by the fact that they are all based on the A2 family of climate change scenarios that apply to Southern Africa (Matarira et al., 1994). The five models used in this study are listed in Table 3.12.

Table 3.12 Characteristics of the global climate models used in the study

Name	Atmospheric resolution
	(latitude x longitude)
CCCMA_CGCM3_1	3.75 ° x 3.75 °
CSIRO_MK3_5	1.88 ° x 1.88 °
GFDL_CM2_0	2.0 ° x 2.5 °
GISS_MODEL_E_R	4.0 ° x 5.0 °
MPI_ECHAM5	1.88 ° x 1.88 °

Source: (Dai, 2006)

3.7 Comparison of global climate model performance

Each of the five global climate models listed in Table 3.12 is based upon a certain climate scenario that is different from the other four. The models need to be compared in order to assess their ability to simulate real observations in different geographic and climatic ranges. Comparison is important for two main reasons: first to find out whether the models are usable and second to test the performance of each model in predicting future climates. In this study, each model data set was compared with observational data and the results statistically analyzed. The goal was to rank the models and to be able to select one model best suited to a particular station and then all further analysis at that station would be based on that model. Comparison of the models was done using three different classical statistics for both temperature and rainfall data.

3.7.1 Regression analysis

Regression analysis was performed for both minimum and maximum temperature and rainfall data. The analysis was done using Microsoft EXCEL. Observed data was plotted against model control data to observe the relationship between the two variables. The closeness of the relationship was assessed by the coefficient of determination (R²).

3.7.2 Model efficiency (ME)

This approach was applied for temperature data. The efficiency of each model to simulate minimum and maximum temperature was calculated for each of the five models. The ME approach (Nash and Sutcliffe, 1970) is computed as:

$$\mathbf{ME} = \mathbf{1} - \frac{\mathbf{B} \ \mathbf{EMBED} \ \mathbf{Equation.3} \ \mathbf{BBB} \ \mathbf{C}(O_i - M_i)^2}{\mathbf{B} \ \mathbf{EMBED} \ \mathbf{Equation.3} \ \mathbf{BBB} \ \mathbf{C}(O_i - \bar{O}_i)^2}$$

$$(3.2)$$

where ME is model efficiency, Q_i is an elementary observation in the observed data set (n observations), \overline{Q}_i is the mean of i observations and M_i represents an elementary observation in the modelled dataset (n predictions).

3.7.3 Root mean square error (RMSE)

The analysis was applied for both rainfall and temperature data. The RMSE for each model was calculated for simulating minimum and maximum temperature and rainfall. The RMSE approach is computed as:

RMSE =
$$\sqrt{\frac{\text{DEMBED Equation. 3 DDD}(O_i - M_i)^2}{n}}$$
(3.3)

3.7.4 Frequency analysis

For rainfall, a frequency analysis test was performed at 50 % probability of exceedance using RAINBOW (Raes, 2006). The model that best resembled observed data was identified by inspection from the curves obtained.

3.7.5 Significance testing

A t-test was carried out at 5 % level of significance to assess the reliability of the null hypothesis H_o which was formulated as follows: there is no significant difference between observed data and simulated data. A two tailed test was performed for each pair of data set. The hypothesis was rejected when the t-value obtained (t_{stat}) was greater than t-critical (t_α) . That is, H_o was rejected when $|t_{stat}| > t_\alpha$ otherwise the null hypothesis was accepted.

3.7.6 Ranking of the models

The models were ranked on the basis of the values of R², ME and RMSE obtained for each model and the results of significance testing of the correlation between observed and simulated data. The model that obtained the highest rank for a given station was then considered the basis for further analysis at that station.

3.8 Application of the Climate Change Explorer tool

The climatic data that was downloaded from the CSAG data portal was loaded into the Climate Change Explorer tool. The tool (version1.0) uses historical and projected climatic data and explores various futures based on the global climate models considered. Each historical dataset had a corresponding future dataset and both were based upon a particular global climate model. The version used in this study uses the 1961-2000 historical climatic data and projected data for the periods 2046-2065 and 2081-2100. There were therefore three datasets for each model, the historical (control) and two futures (a) and (b). The control data covers the period 1961 - 2000 while the two futures (a) and (b) are for the periods 2046 - 2065 and 2081 - 2100 respectively. This study used the control and the future (a) datasets.

In the study, temperature and rainfall downscaled from the best out of five global climate models were used to investigate the past and future climates at Mt Darwin, Mutoko, Rusape, Karoi and Wedza. The main menu of CCE is shown in Figure 3.5.

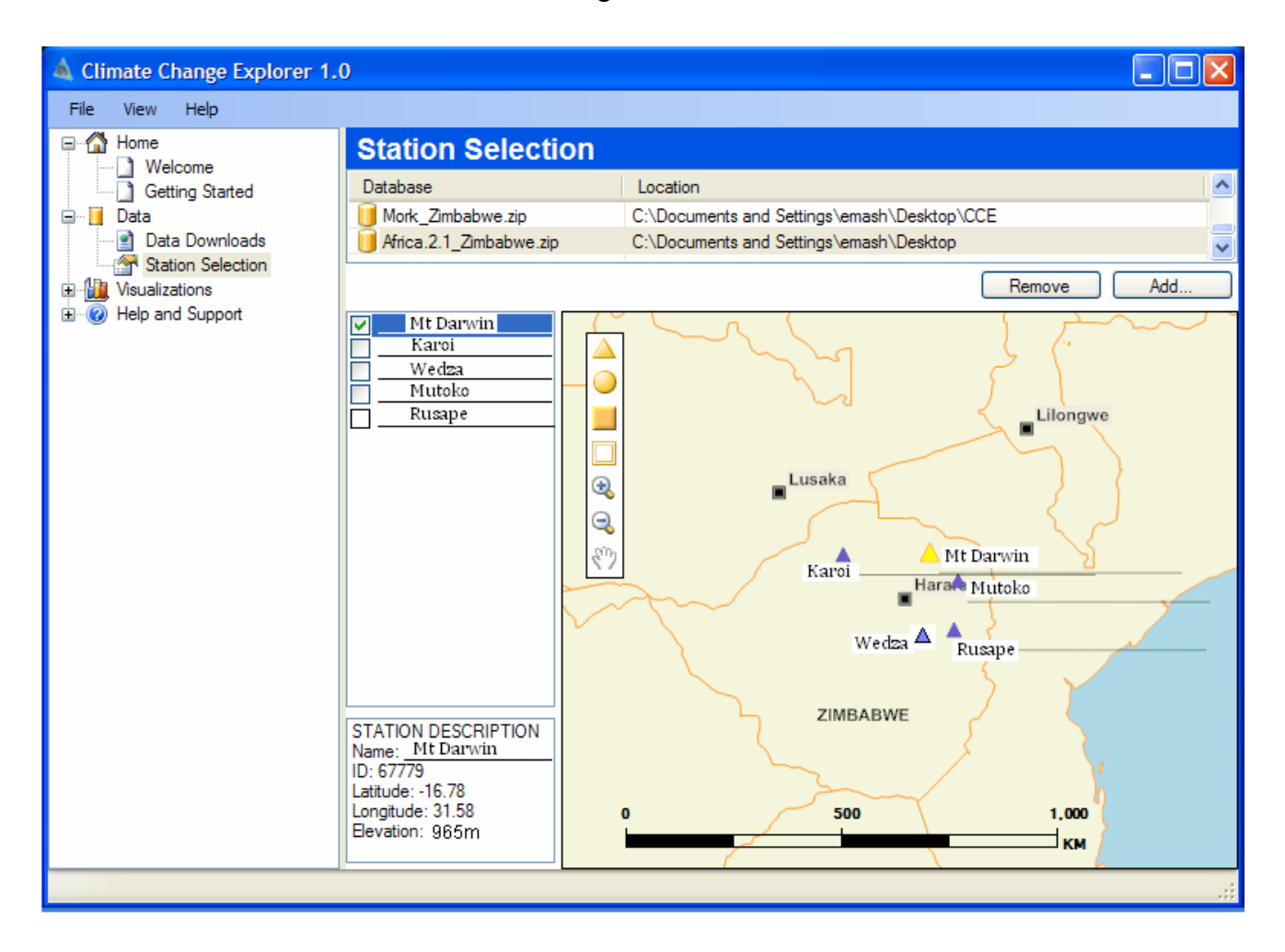


Figure 3.5 The main menu of CCE

In this panel (Figure 3.5), the downloaded data contained in the folder named Africa.2.1_Zimbabwe.zip (under Database) was loaded to the database by clicking on the "Add" button. Stations of interest were selected by clicking on the "Station Selection" function and clicking on the small square next to its name. A station when selected would be highlighted such as Mt Darwin and its position was also highlighted on the map of Zimbabwe as shown in Figure 3.5.

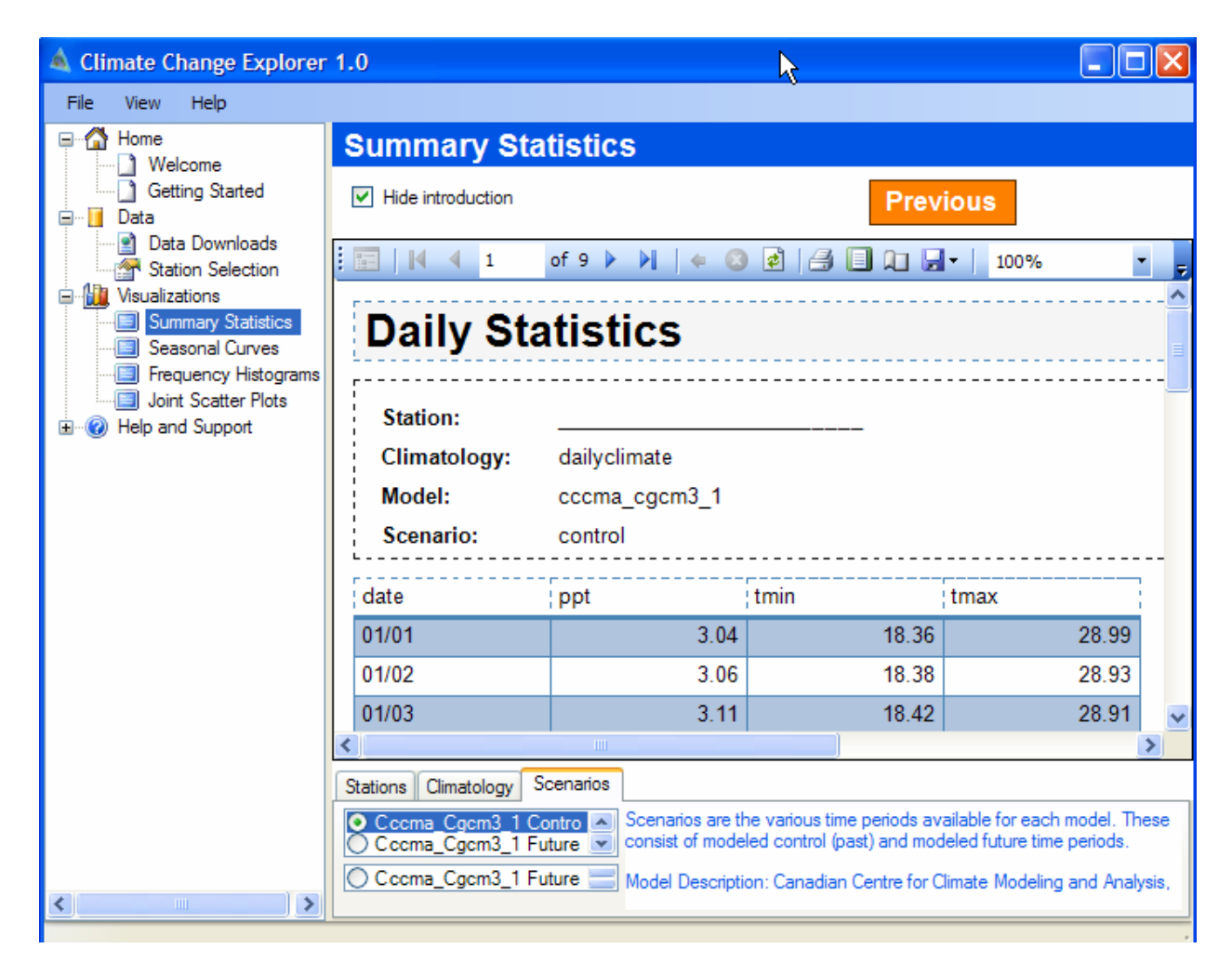


Figure 3.6 The Summary Statistics panel

The Summary Statistics panel contains downscaled data, and options to use either daily or monthly variables. In this study, monthly data was used and it was selected by clicking on the "Climatology" button in Figure 3.6. Global climate models were also selected here by clicking on the "Scenarios" button. This is where the control and future scenarios for a specified model were selected.

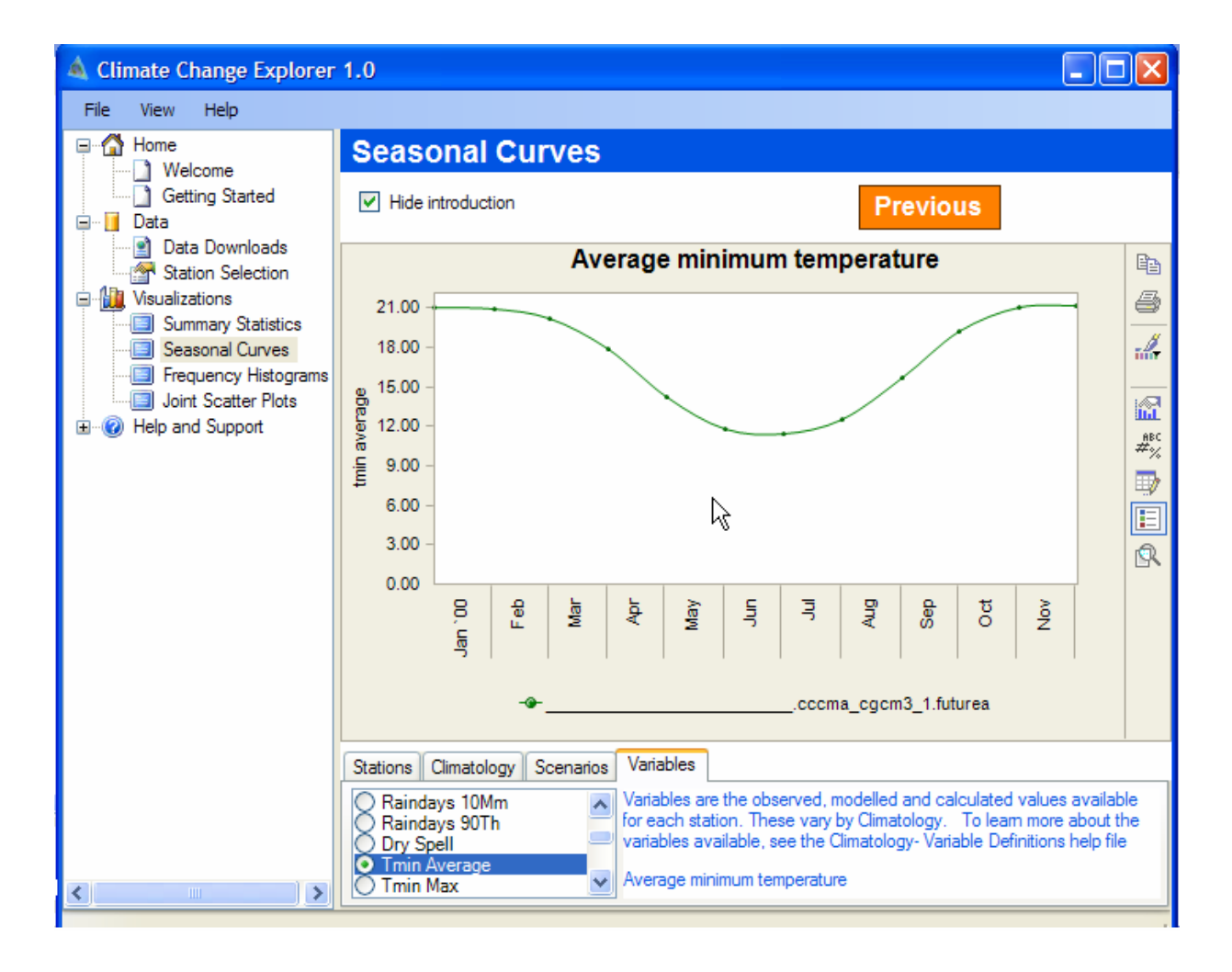


Figure 3.7 The Seasonal Curves panel

The variables of interest, such as the average minimum temperature (Tmin Average highlighted in Figure 3.7, bottom left), were also selected in this panel by clicking on the "Variables" button. The tool would display the mean monthly variation of the variable of interest as shown in Figure 3.7. This panel was used to construct baseline climates for the stations as well as the projected future anomalies in temperature and rainfall. This was done by exporting data from the panel to Microsoft EXCEL where the graphics were done.

3.8.1 Baseline climates

The CCE tool was used to construct baseline climates for Karoi, Wedza, Rusape, Mt Darwin and Mutoko based on the most suitable model(s) obtained in Section 3.7. Here, the CCE tool was used to show the climate at each station averaged over 30 years.

3.8.2 Projected changes in temperature and rainfall

The CCE tool was used to investigate how the best model for use in the study predicts the change in temperature and rainfall above or below baseline. To do this, data from the tool was used to construct future anomalies in temperature and rainfall for each station. The procedure was the same as that described in Figure 3.7. The anomalies in temperature were used to depict the magnitude of any warming at each station in the period 2046-2065. Anomalies in rainfall were used to show the expected monthly variabilities in rainfall at each station also in the 2046-2065 regime. The anomalies were also used to indicate the variation in predictions across the models.

3.8.3 Dry spell analysis

The CCE tool was used to compare the mean dry spells experienced in the period 1971 - 2000 and the dry spells expected in the 2046-2065 regime. To do this, data from the CCE tool was used to construct frequency polygons in Microsoft EXCEL from which the past and future dry spells were compared. The best model suited for each station was used for this analysis.

3.9 Validation of the AquaCrop model

3.9.1 The validation procedure

The following parameters were used: daily rainfall, minimum and maximum temperature and reference evapotranspiration. Crop parameters used are shown in section 3.3.2.2. Soil parameters used are shown in Table 3.2. Management parameters were also used. These parameters were fed into the model and the model was run for each season between the years 2000 and 2006 for each cultivar using the sowing dates provided. The initial rooting depth was 0.3 m for each simulation. The soil depth was 2 m.

Each simulation was done with soil moisture initially at field capacity. The output yields from the model were then regressed with the observed yields shown in Tables 3.9, 3.10 and 3.11. Regression was done using Microsoft EXCEL. To assess how well the model simulated observed yields, the coefficient of determination, R², the root mean square error RMSE and the slope were used. Figure 3.8 shows the main menu of the AquaCrop model.

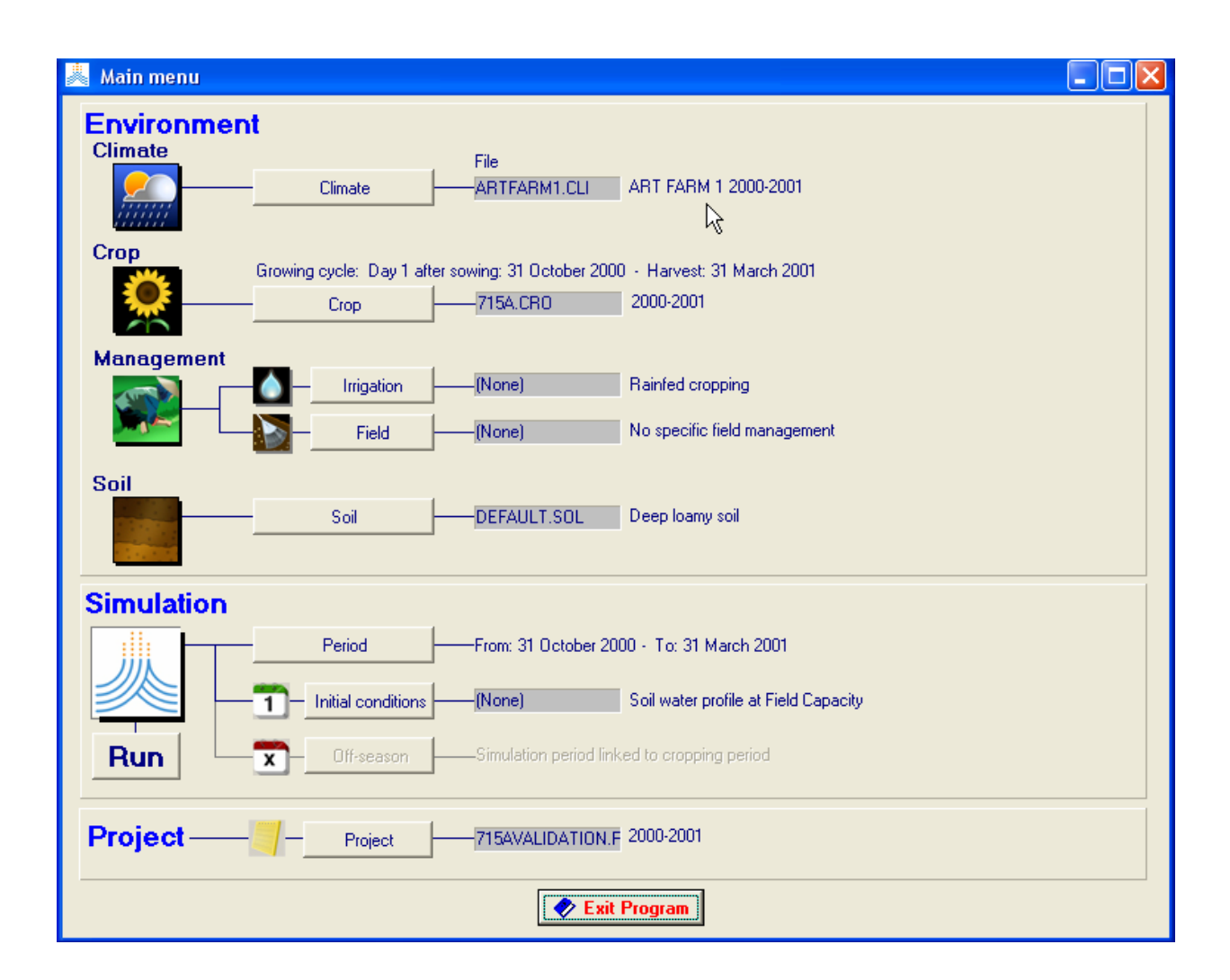


Figure 3.8 The main menu of AquaCrop

There are three panels on the main menu where the names and descriptions of the selected input files are displayed as shown in Figure 3.8.

3.9.2 Environment panel

This is where Climate (Temperature, ET_o, Rain, CO₂), Crop, Management (Irrigation and Field) and Soil profile files were created or selected and updated. The start of the growing season was also specified in this panel.

3.9.3 Simulation panel

In this panel, the following were specified:

- (i) the simulation period,
- (ii) the initial conditions for a simulation run and
- (iii) the off-season conditions when the simulation period exceeds the growing period.

It is in this panel where simulations were run for the specified environment, period and conditions.

3.9.4 Project panel

This is where the project was saved and project files retrieved. By selecting the "Save project" command in the "Simulation run" menu, the characteristics of the environment, the initial and off-season conditions and program settings were saved as a project file.

3.9.5 Significance testing

A t-test was performed at 5 % level of significance to assess the significance of the correlation between observed and simulated yield. The null hypothesis H_o used was: there is no significant difference between observed and simulated yield. The alternative hypothesis was: the observed and simulated yields are significantly different. For each pair of dataset, a two-tailed test was performed. The null hypothesis was rejected when $|t_{start}| > t_{\alpha}$ otherwise H_o was accepted.

3.10 Modelling to simulate historic and future maize yields

The validated AquaCrop model was used. The input parameters used were the same as the ones used in Section 3.9 except for climatic variables and the planting dates. Soil fertility levels were

also adjusted so as to take into account the conditions of soils in rural areas. Climatic variables were based on the best model found in Section 3.7.

Current planting dates were based on optimal planting dates in Zimbabwe that were found by Sithole (2003). The optimal planting date for maize in Natural Region 2(b) of Zimbabwe was found to be between 18 October (earliest) and 5 December (late) and the best suiting crop varieties are the 100 day and 150 day (Sithole, 2003). In this study, these dates apply for Wedza, Rusape and Mt Darwin. In Region 3, the recommended planting dates are 24 October to 16 December with the season length of between 108 to 153 days (Sithole, 2003). The dates apply for Mutoko. At Karoi, the planting date was found to be between 20 October and 5 November (Sithole, 2003). The model was run to predict yields under three different conditions:

3.10.1 Simulations under baseline conditions and current planting dates

AquaCrop was run using the baseline (1971-2000) values of monthly rainfall, monthly minimum and maximum temperature and monthly ET_o. The ET_o values were generated using the ET_o calculator applying the Hargreaves method. Other parameters were as used in Section 3.9

3.10.2 Simulations under future conditions maintaining current planting dates

With all other variables unchanged, the model was run again using the values of temperature and rainfall projected in the near future, (2046-2065) period. These simulations were done to find out how the yields would change if the current planting dates are maintained in the 2046-2065 period.

3.10.3 Simulations under future conditions using generated planting dates

Another set of planting dates was generated for the 2046-2065 regime. The planting dates were generated using the AquaCrop model based on the AREX criterion (25 mm of rainfall in 7 days) for the first planting date. The set of planting dates used for these simulations is shown in Table 3.13. The simulations had to include different planting dates because the date of sowing is a factor that affects yields significantly under rain-fed conditions in Zimbabwe (Makadho, 1996).

Table 3.13 Planting dates generated for the period 2046-2065

Station		Planting date	
	Early	Mid	Late
Wedza	27 November	4 December	11 December
Rusape	6 December	13 December	19 December
Mutoko	4 January	11 January	17 January
Mt Darwin	4 January	10 January	16 January
Karoi	17 December	24 December	31 December

The historic yields were then compared with the predicted future yields to investigate the potential impact of climate change on maize yield.

CHAPTER 4

RESULTS AND DISCUSSION

4.1 Introduction

The results of the research are presented and discussed in three sections. The first section discusses the results obtained in the homogeneity test as well as frequency analysis of rainfall data and the results of time series analysis of rainfall and temperature. The second section presents the evaluation and ranking of the five global climate models and also the application of the Climate Change Explorer (CCE) tool. Finally, the third section outlines the validation of AquaCrop model and its application in estimating maize yield based on the baseline climate as well as on climate projections from the highest performing model for simulating temperature and for simulating rainfall.

4.2 Homogeneity testing

The distribution of temperature and rainfall is different. Rainfall can be normally distributed but temperature does not follow the same distribution. In the study, homogeneity test was applied for rainfall data only because it assumes the normal distribution of rainfall. Confirmation of homogeneity of rainfall data was found at all stations. Figure 4.1 shows the results obtained in the homogeneity test of rainfall at Rusape.

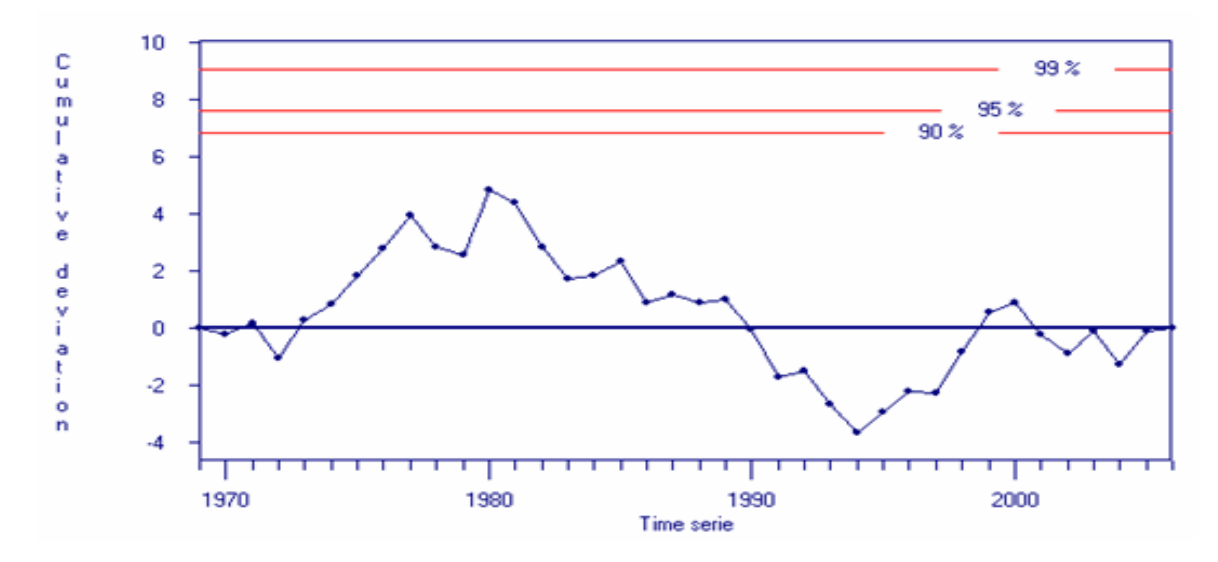


Figure 4.1 Cumulative deviations from mean total annual rainfall for Rusape for the period 1971-2006 Source: (Raes 2006)

Figure 4.1 shows the cumulative deviations of rainfall from the long term mean. For a homogeneous dataset, the deviations fluctuate about the horizontal axis without crossing the horizontal lines labeled 90, 95 and 99%. When the deviations cross one of these lines, the hypothesis of homogeneity of the dataset is rejected with respectively 90, 95 and 99% probability. In all the analysis, homogeneity was not rejected showing that the data statistically belonged to the same population. The change in rainfall was therefore caused by variations in climate only and so the rainfall data used was reliable.

4.3 Climate characterization

4.3.1 Rainfall

Figures 4.2 to 4.7 show the time series plots of annual rainfall and rainfall anomalies at Mt Darwin, Wedza, Rusape, Karoi, Agricultural Research Trust (ART) Farm and Mutoko.

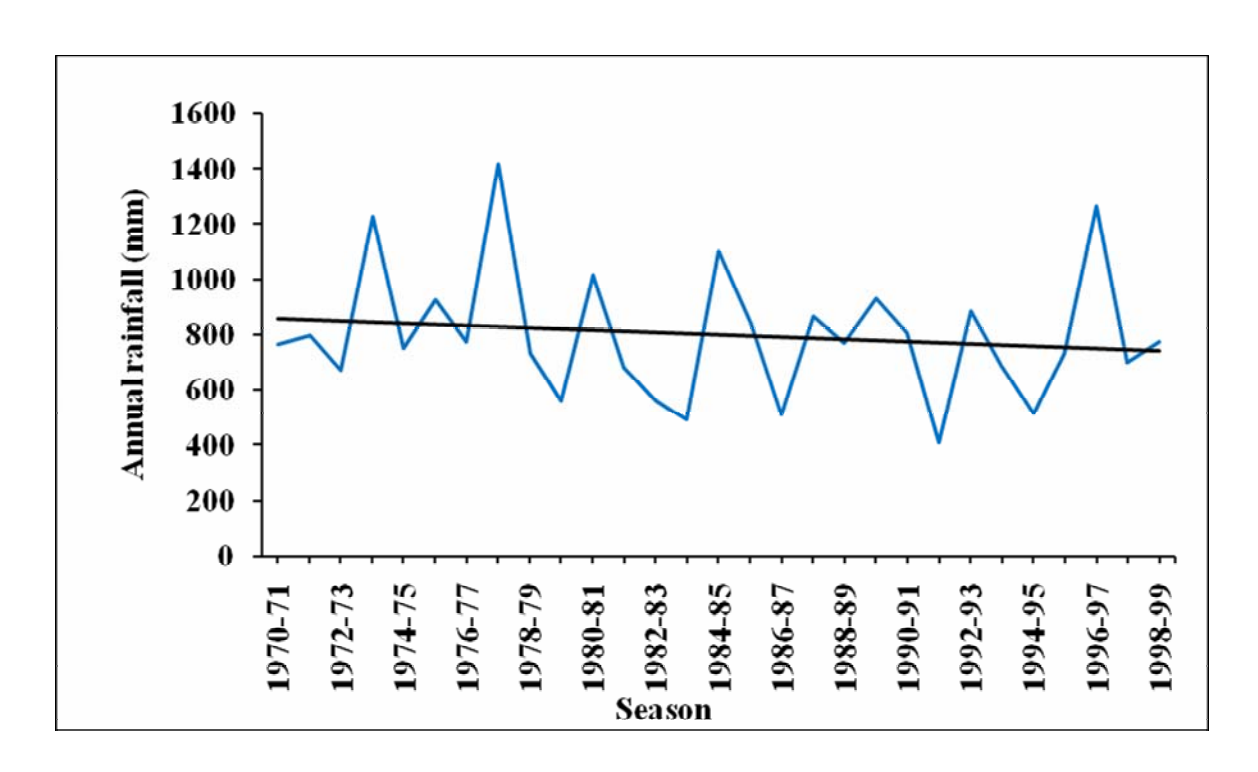


Figure 4.2(a) Time series for annual rainfall at Mt Darwin for the period 1970-1999

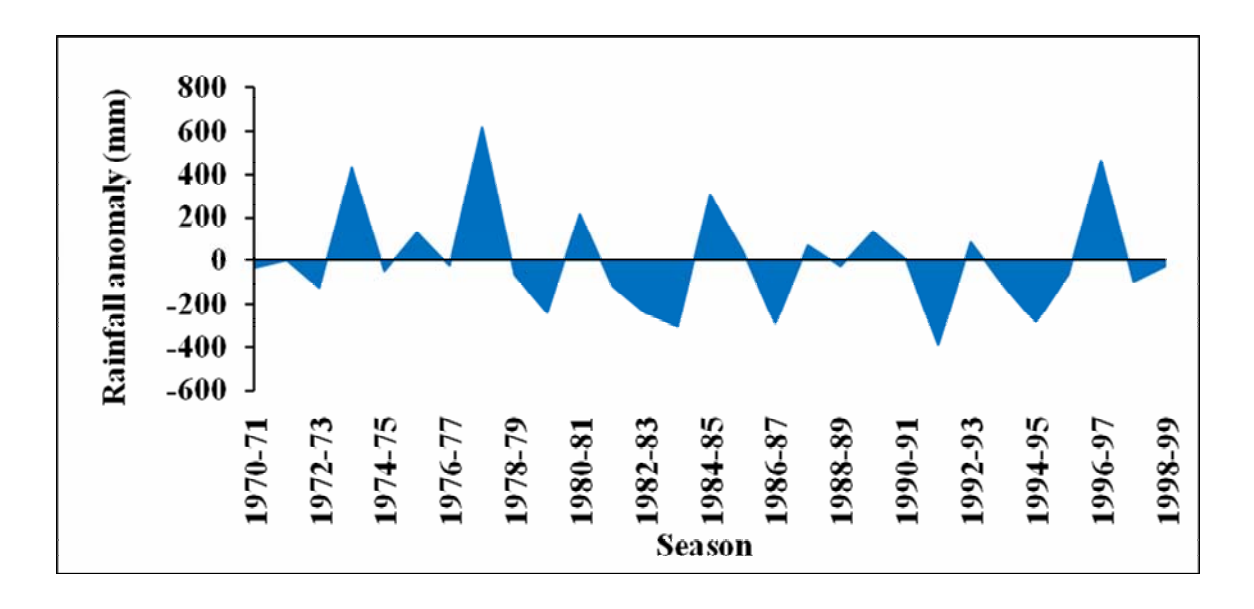


Figure 4.2(b) Rainfall anomalies at Mt Darwin for the period 1970-1999

Figure 4.2(a) shows that the mean annual rainfall has been on a downward trend at Mt Darwin between the years 1970 and 1999. The rainfall anomalies (shaded areas) in Figure 4.2(b) are deviations from the long term mean rainfall. Areas above the horizontal axis indicate a positive

anomaly, that is above normal rainfall seasons while areas below the horizontal axis are negative anomalies and they indicate below normal rainfall seasons. Most of the years between 1986 and 1996 were characterised by below normal rainfall seasons at Mt Darwin as shown in Figure 4.2(b).

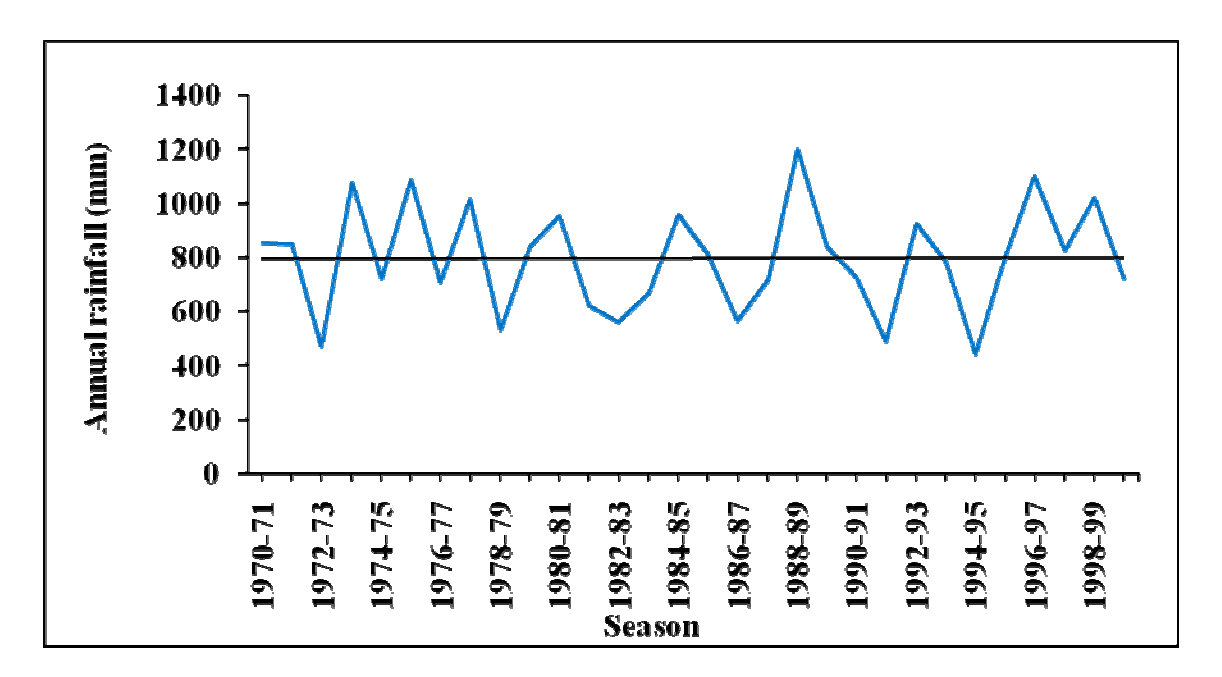


Figure 4.3(a) Time series for annual rainfall at Karoi for the period 1970-2000

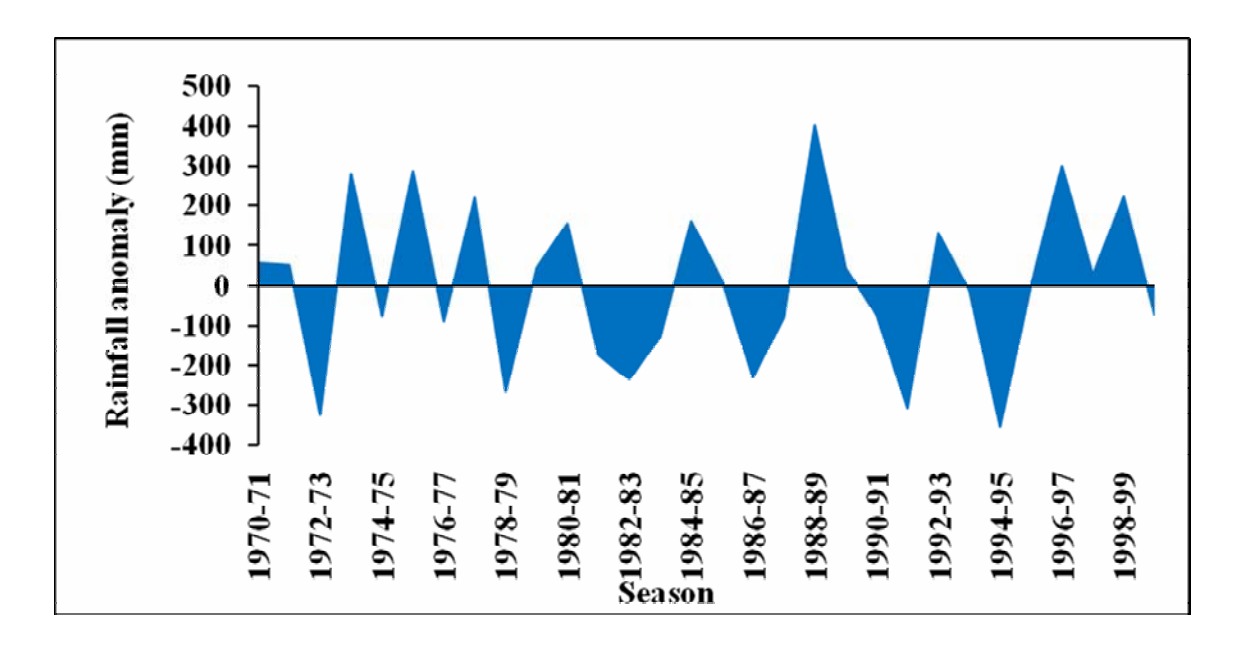


Figure 4.3(b) Rainfall anomalies at Karoi for the period 1970-2000

There has been no significant change in mean annual rainfall at Karoi; however rainfall variability is evident from Figure 4.3(a). For the period under review, the highest rainfall amount was experienced in the 1988/89 season when the rainfall recorded about 1200 mm. The lowest amount was received in the 1994/95 season when the rainfall recorded slightly above 400 mm.

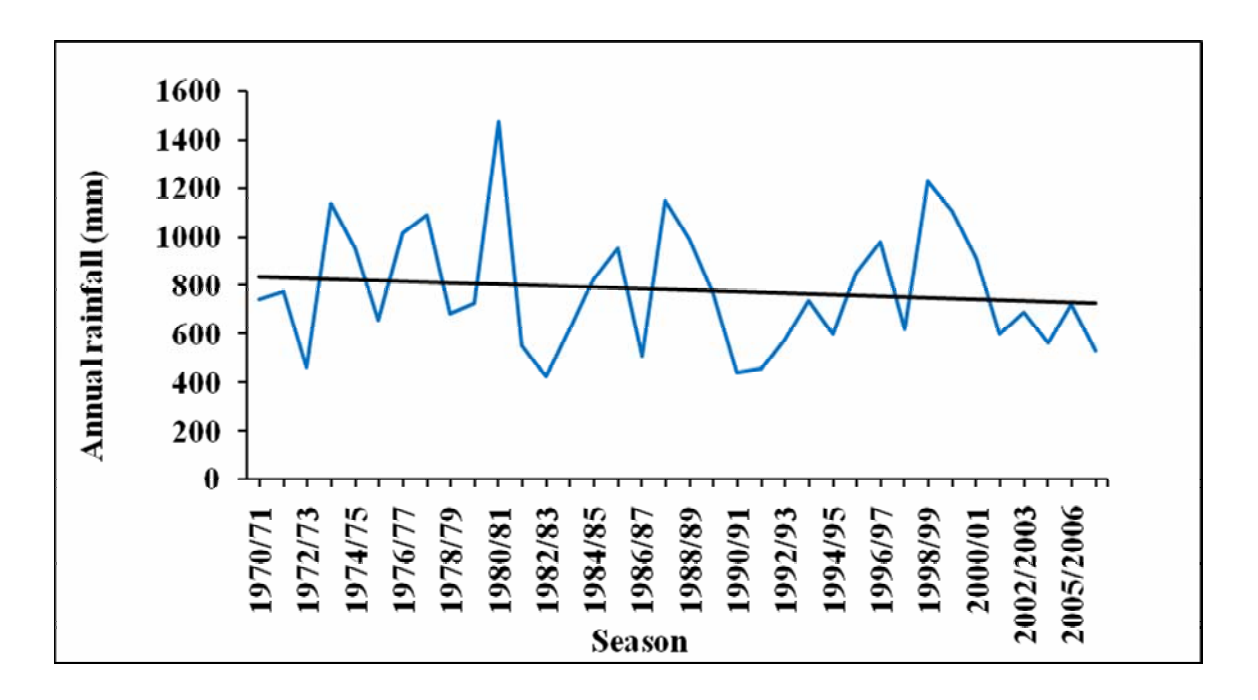


Figure 4.4(a) Time series for annual rainfall at Wedza for the period 1970-2007

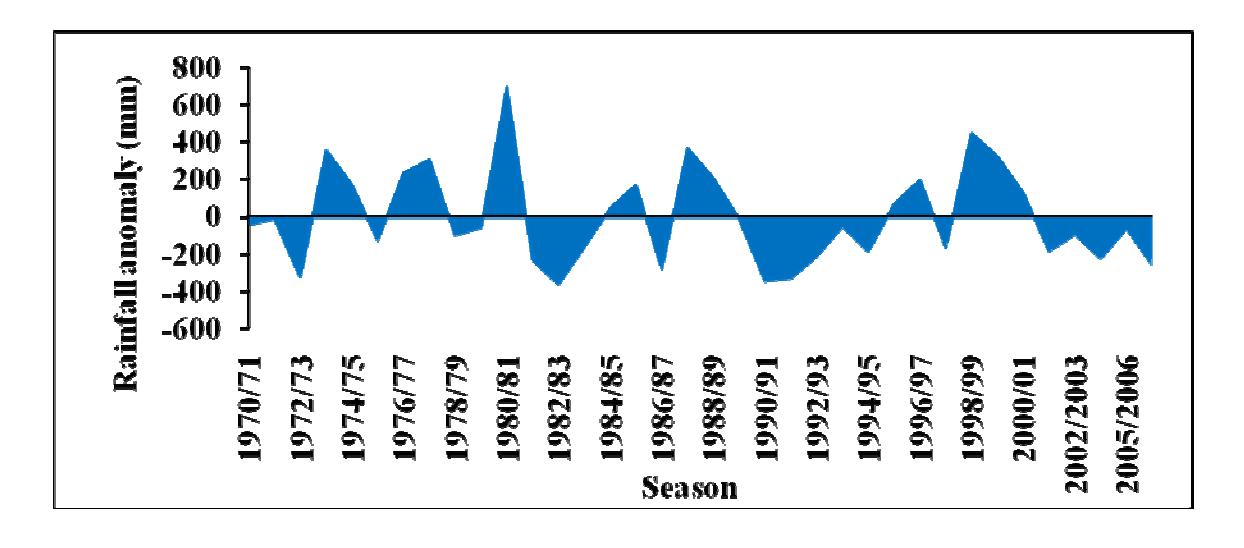


Figure 4.4(b) Rainfall anomalies at Wedza for the period 1970-2006

Figure 4.4(a) shows a downward trend of mean annual rainfall at Wedza as was observed at Mt Darwin. Wedza however recorded above normal rainfall in the 1999/2000 season as shown in Figure 4.4(b). These rains were induced by tropical cyclone Eline which caused floods in various parts of Zimbabwe in the year 2000.

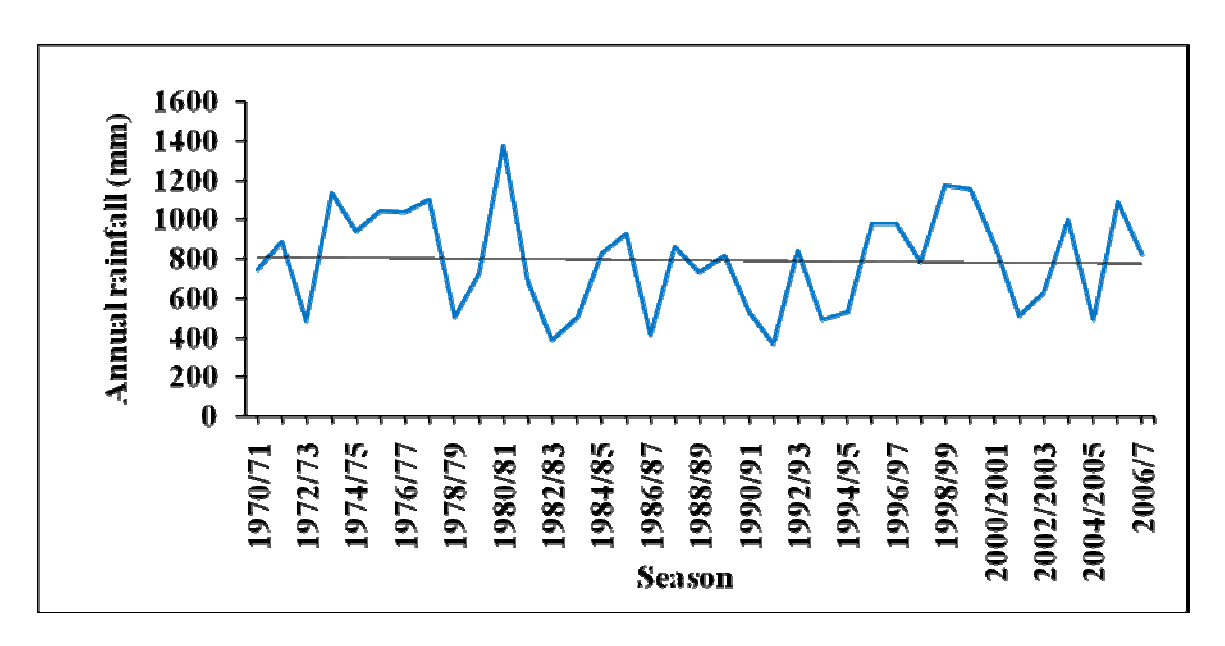


Figure 4.5(a) Time series for annual rainfall at Rusape for the period 1970-2007

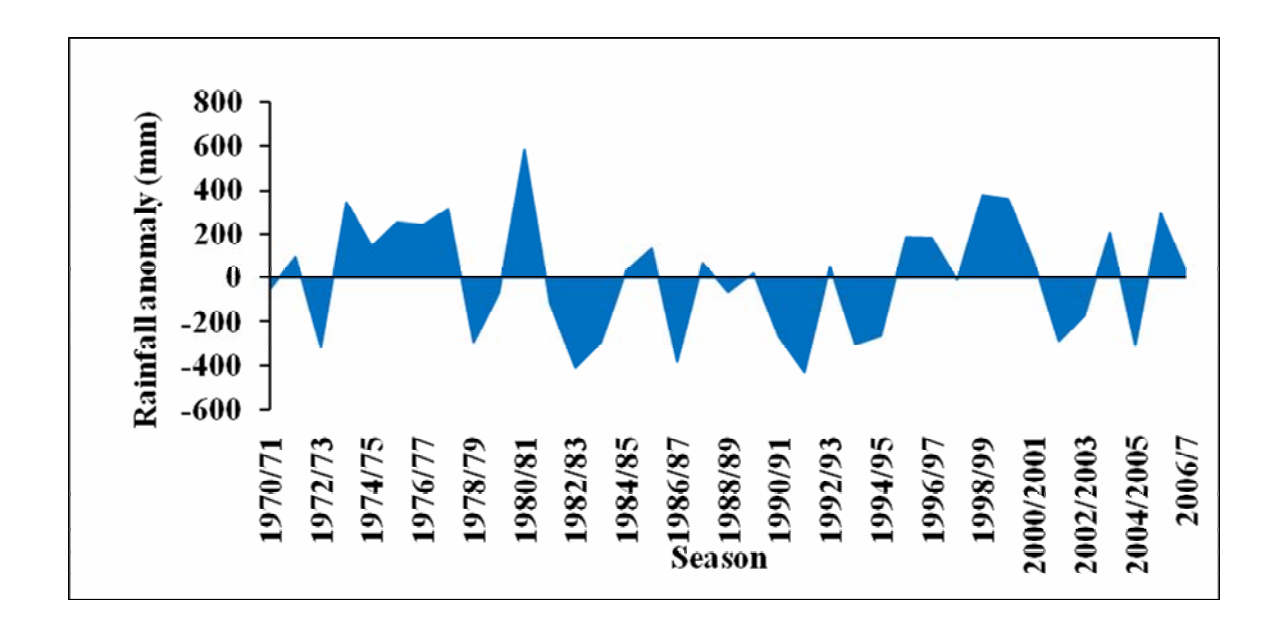


Figure 4.5(b) Rainfall anomalies at Rusape for the period 1970-2007

Mean annual rainfall at Rusape also shows a downward trend (Figure 4.5(a)), that is however slight as compared to that observed at Mt Darwin and Wedza. Rusape has experienced very erratic rains consecutively for about 15 years from 1980-1995 as shown in Figure 4.5(b). As was observed at Wedza, Rusape also recorded above normal rainfall in the 1999/2000 season. These rains were also associated with tropical cyclone Eline.

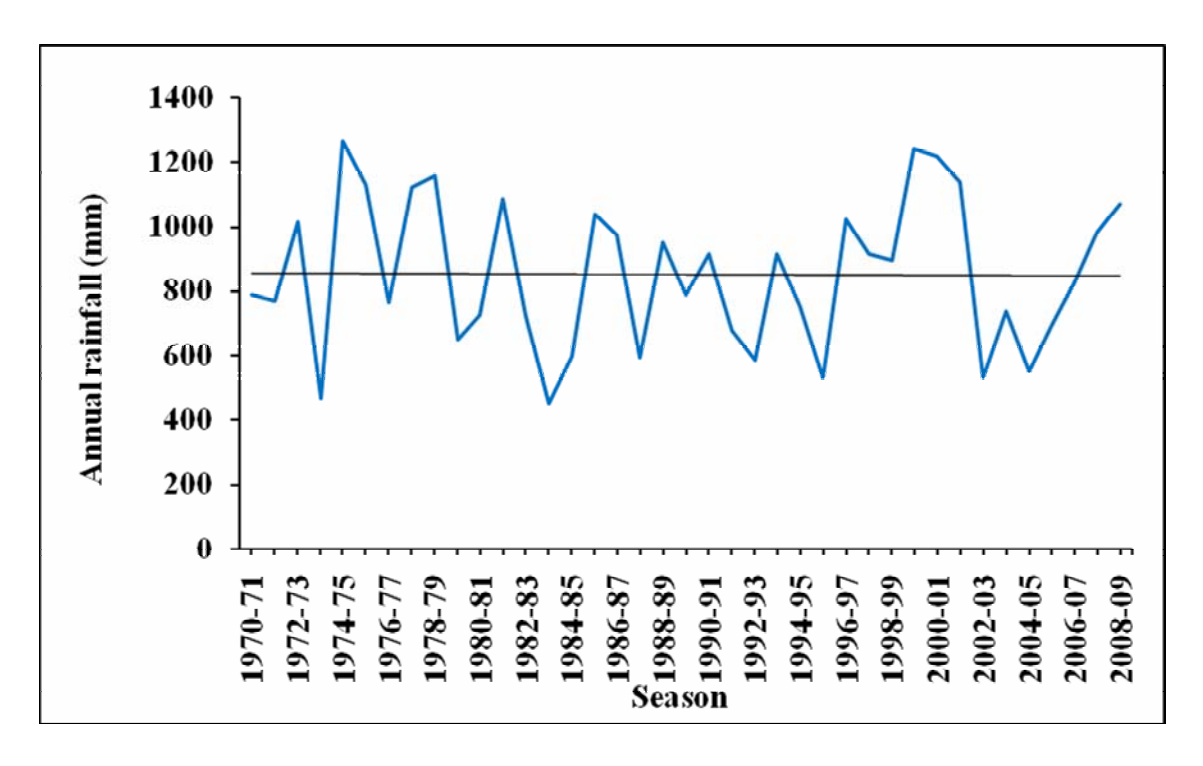


Figure 4.6(a) Time series for annual rainfall at ART Farm for the period 1970-2009

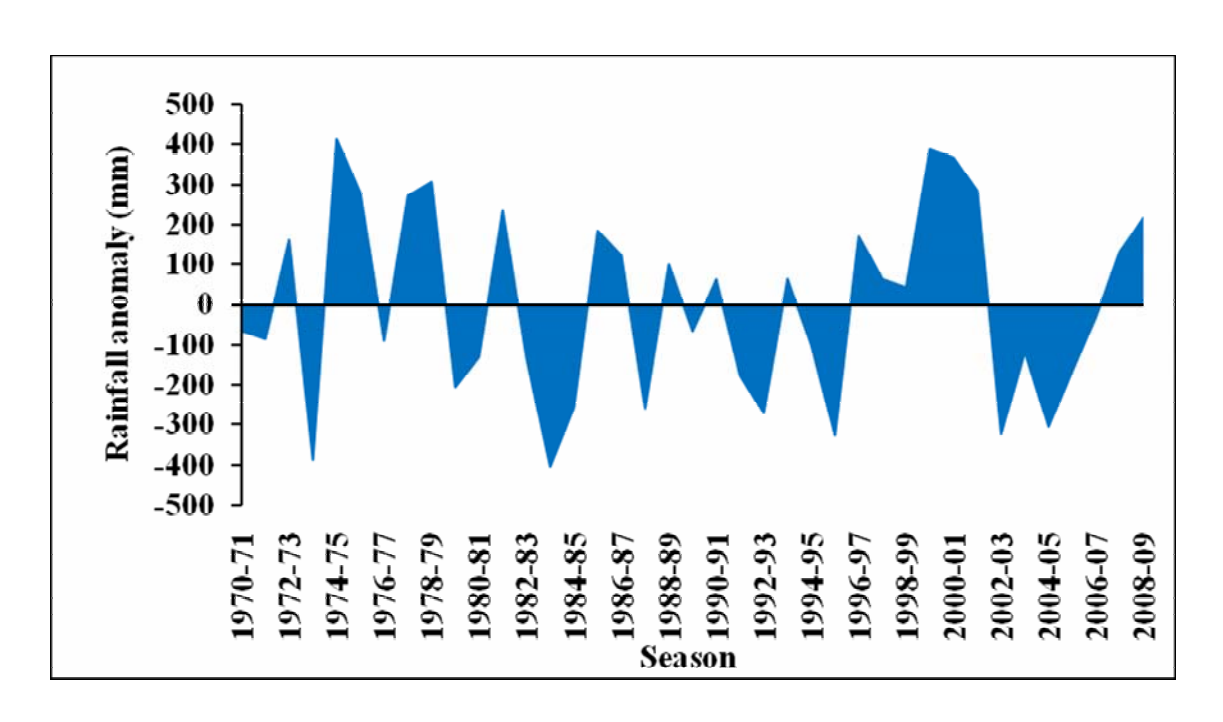


Figure 4.6(b) Rainfall anomalies at ART Farm for the period 1970-2009

The mean annual rainfall at ART Farm (Figure 4.6(a)) does not show any significant change over the period 1970-2009. ART Farm recorded above normal rainfall in the 1999/2000 season as shown in Figure 4.6(b). This anomalously wet season is also attributed to the occurrence of tropical cyclone Eline.

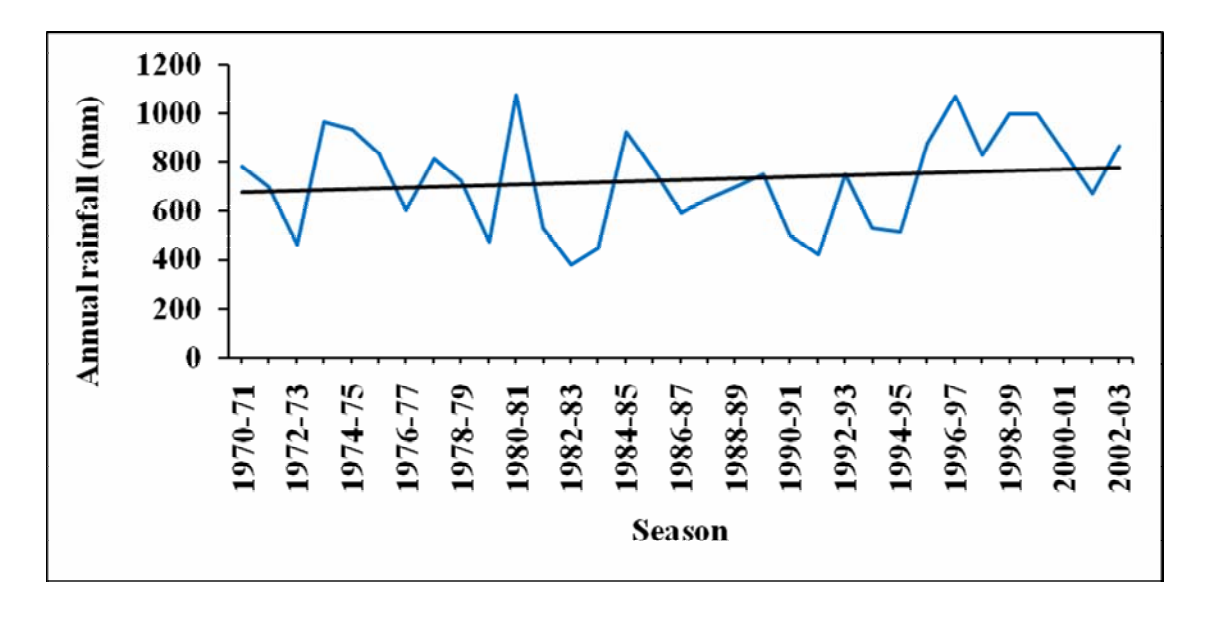


Figure 4.7(a) Time series for annual rainfall at Mutoko for the period 1970-2003

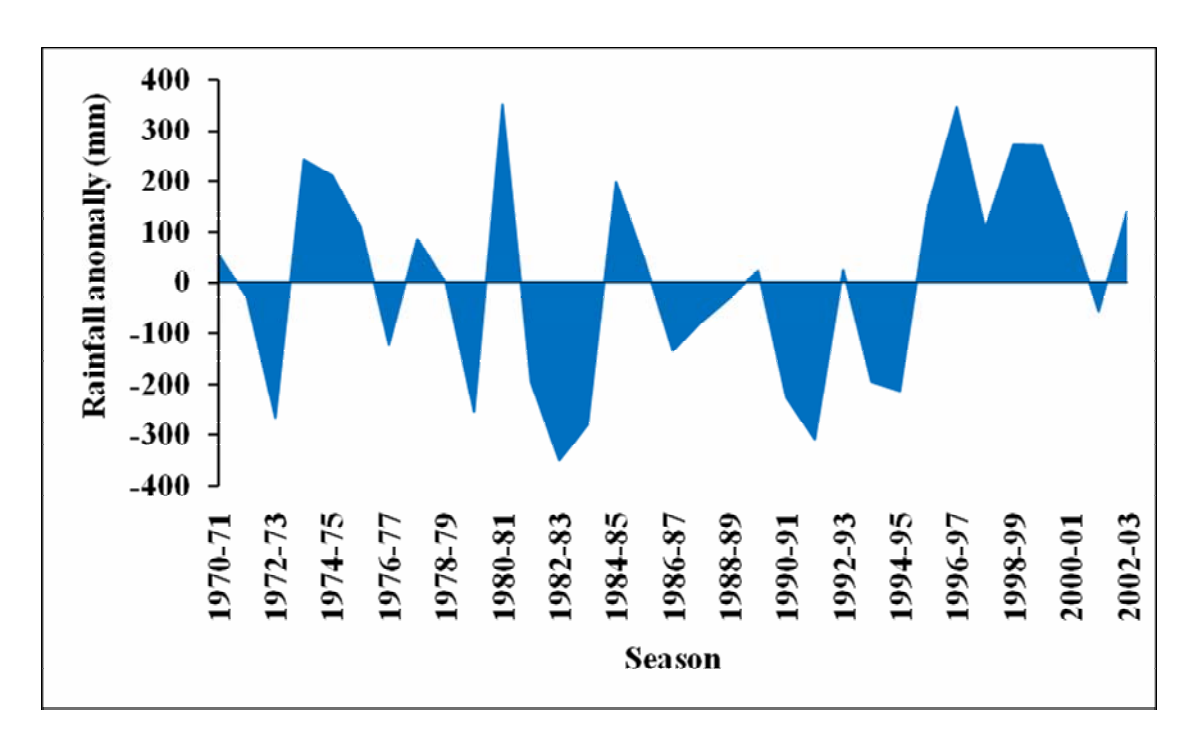


Figure 4.7(b) Rainfall anomalies at Mutoko for the period 1970-2003

Figure 4.7(a) shows that the mean annual rainfall has been on an upward trend at Mutoko between the years 1970 and 2003. The years between 1986 and 1995 have been characterised by below normal rainfall seasons. This is shown in Figure 4.7(b). All stations received below normal rainfall in the 1982/83 and 1992/93 seasons, a clear confirmation of the famous 1982 and 1992 droughts in Zimbabwe.

4.3.2 Temperature

Figures 4.8 to 4.11 show time series plots of mean annual temperature at Wedza, Rusape, Karoi and ART Farm and general trends in temperature.

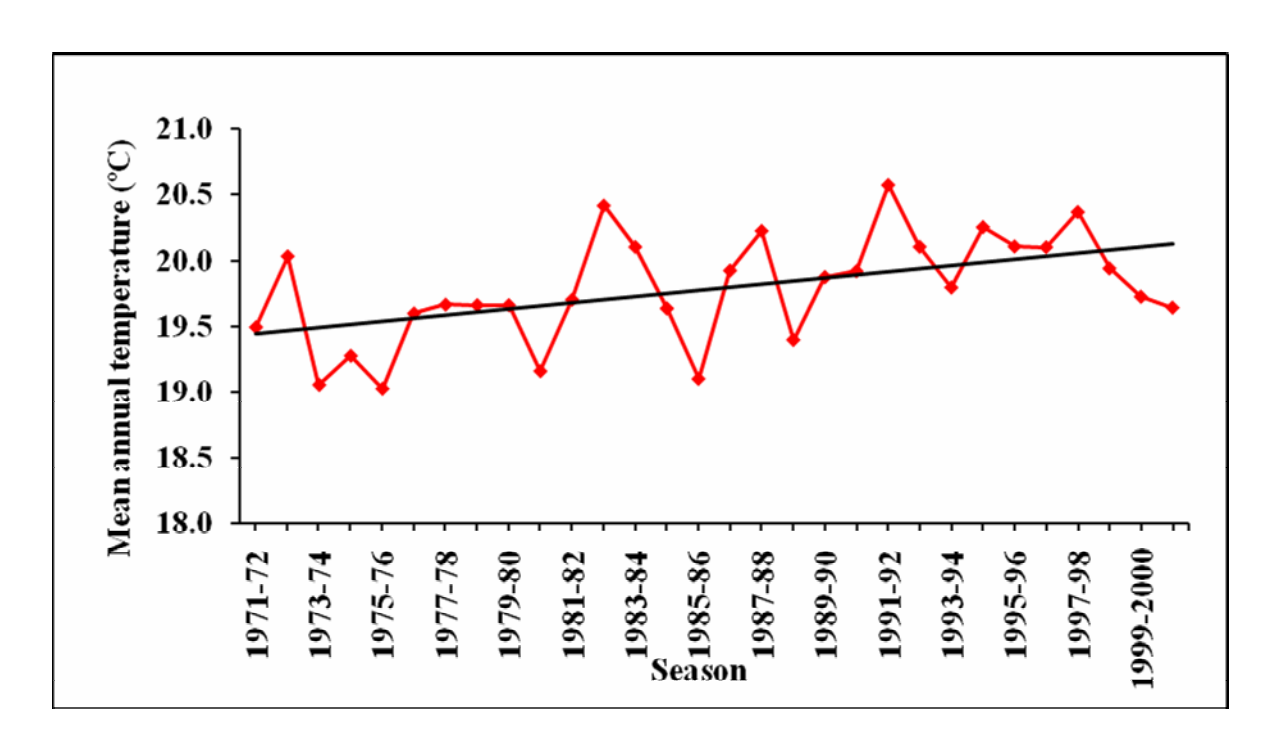
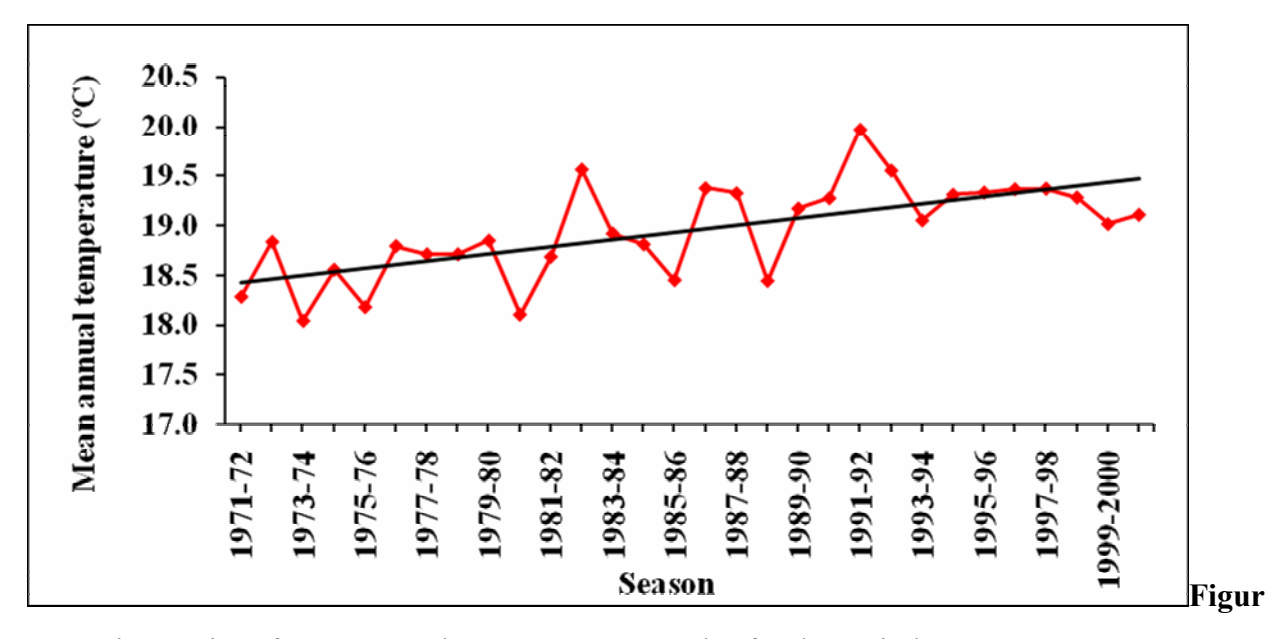


Figure 4.8 Time series of mean annual temperature at Karoi for the period 1971-2000

The mean annual temperature at Karoi has been increasing from 1971 to 2000. On average, the period 1971-2000 shows a positive temperature anomaly of about 0.5 °C at Karoi. The 1991/92 season recorded the greatest mean annual temperature of about 20.5 °C. This is shown in Figure 4.8.



e 4.9 Time series of mean annual temperature at Wedza for the period 1971-2000

At Wedza, there has also been an upward trend in mean annual temperature for the period 1971-2000. The rate of increase has been higher than that observed at Karoi. The period under review has seen an increase in mean annual temperature of about 1°C as compared to about 0.5 °C at Karoi. This information is shown in Figure 4.9.

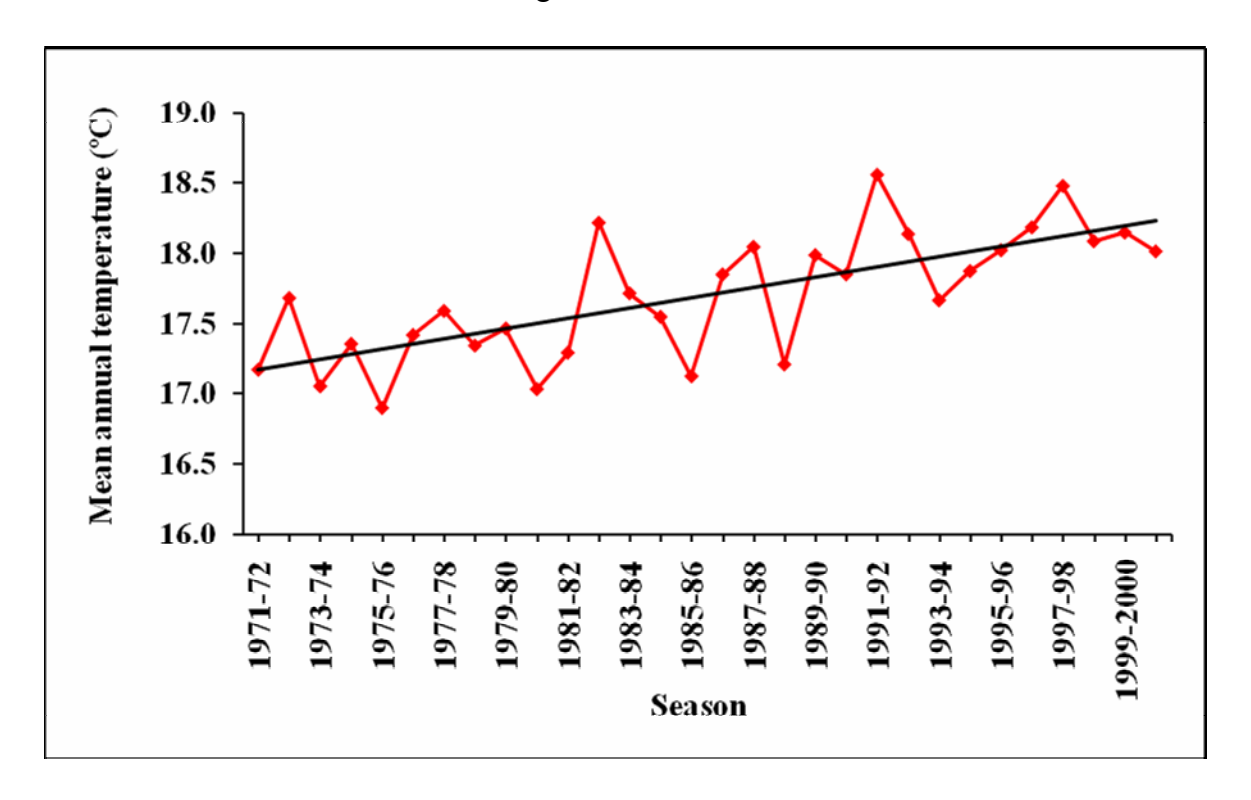


Figure 4.10 Time series of mean annual temperature at Rusape for the period 1971-2000

Rusape also shows a similar upward trend in mean annual temperature with a positive temperature anomaly of about 1°C. The highest mean annual temperature recorded at Rusape was about 18.5 °C and this was in the 1991/92 season as shown in Figure 4.10.

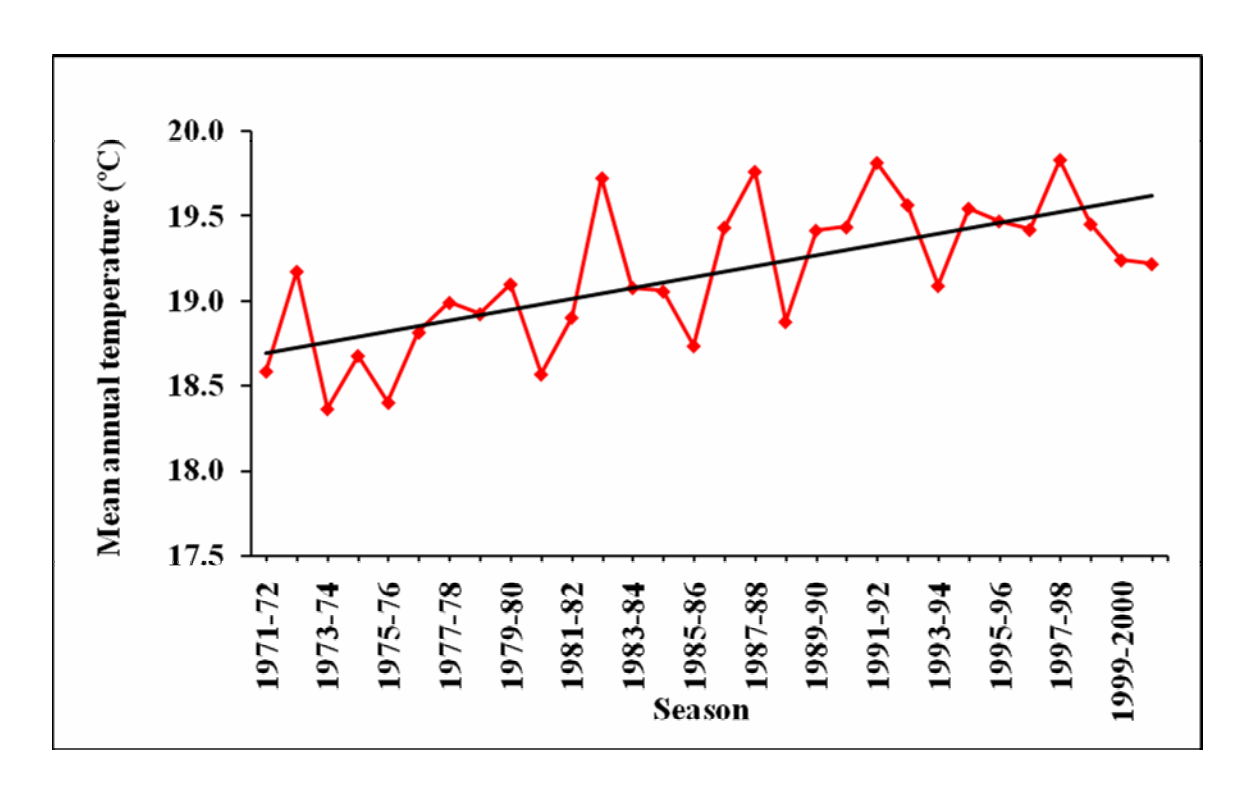


Figure 4.11 Time series of mean annual temperature at ART Farm for the period 1971-2000

The mean annual temperatures recorded at ART Farm have also increased from 1971 to 2000. The temperature anomaly is in the range of about 0.8 - 1.0 °C. Three seasons, 1982/83, 1987/88 and 1991/92 have been anomalously hot as compared to all other years. This is shown in Figure 4.11.

At all stations, the mean annual temperature shows an upward trend though the rates of increases are different. This shows that Natural Region 2 of Zimbabwe has experienced a warming in the period under review. It is difficult to ascertain whether the warming is part of climate variability or climate change. It can only be assumed that if the trend and the level of temperature anomaly observed in this study have continued beyond 2000, then Zimbabwe's climate will change. However, some sources say there has been climate change in Zimbabwe. The Intergovernmental Panel on Climate Change (IPCC) Fourth Assessment Report (IPCC, 2007) reports that the average global mean surface temperature has increased by between 0.3 and 0.6 °C due to anthropogenic activities. According to Unganayi (2010), mean annual temperatures have increased globally between 1900 and 2000 by 0.7 °C with Zimbabwe and Harare recording increases of 0.4 °C and 1 °C respectively.

4.4 Evaluation of global climate models

Climatic data was downloaded from the Climatic Systems Analysis Group (CSAG) data portal. The data was loaded into the CCE tool. The five global climate models were compared using the following statistical techniques: Regression analysis, Model efficiency, Root mean square error and Frequency analysis (rainfall data). Model performance was judged by the magnitude of the coefficient of determination (R²), root mean square error (RMSE) and the model efficiency (ME). The models were then ranked according to their performances.

4.4.1 Minimum air temperature

The statistics used to assess global climate model performance in simulating minimum temperature are shown in Tables 4.1(a) to 4.1(c). The null hypothesis H_o that the observed and simulated data are not significantly different was accepted when the magnitude of the t-value (t_{stat}) was greater than t-critical (t_{α}) otherwise H_o was rejected. The value of t_{α} was 2.25

Table 4.1(a) Quantitative measures of the performance of the five global climate models for simulating minimum temperature at Karoi

Model	R^2	ME (%)	RMSE (°C)	$t_{\rm stat}$
CCCMA_CGCM3_1	0.92	91.72	3.21	-0.07
CSIRO_MK3_5	0.89	87.17	3.08	7.23
GFDL_CM2_0	0.82	78.23	2.58	-5.60
GISS_MODEL_E_R	0.69	66.05	2.32	-2.34
MPI_ECHAM5	0.88	85.90	2.88	-5.50

At Karoi, the CCCMA_CGCM3_1 model showed the greatest values of R^2 and ME as shown in Table 4.1(a). The null hypothesis was also accepted. The model therefore obtained the highest ranking for simulating minimum temperatures at this station. The GISS_MODEL_E_R model showed the smallest values of R^2 and ME. The RMSE value for this model is the smallest, however H_o was rejected. For the remaining models, H_o was rejected at Karoi indicating that they did not perform well in simulating minimum temperature at the station.

Table 4.1(b) Quantitative measures of the performance of the five global climate models for simulating minimum temperature at Wedza.

Model	R^2	ME	RMSE	t_{stat}
		(%)	(°C)	
CCCMA_CGCM3_1	0.89	88.89	2.88	-2.10
CSIRO_MK3_5	0.76	74.33	2.48	-1.69
GFDL_CM2_0	0.79	74.98	2.46	-6.06
GISS_MODEL_E_R	0.73	71.36	2.36	-0.64
MPI_ECHAM5	0.85	82.86	2.66	-6.04

Table 4.1(b) shows that the R² and ME values were greatest for the CCCMA_CGCM3_1 model at Wedza and H_o was also accepted for this model. H_o was also accepted for the CSIRO_MK3_5 and the GISS_MODEL_E_R models; however the coefficient of determination and model efficiency values were smaller that those obtained for the CCCMA_CGCM3_1 model. The CCCMA_CGCM3_1 model therefore was most suitable for simulating minimum temperatures at Wedza.

Table 4.1(c) Quantitative measures of the performance of the five global climate models for simulating minimum temperature at Rusape.

Model	R^2	ME	RMSE	t _{stat}
CCCMA CGCM3 1	0.87	(%) 86.73	(°C) 3.81	-1.76
CCCIVIA_CGCIVI3_1	0.07	80.73	3.01	-1.70
CSIRO_MK3_5	0.84	83.44	3.47	4.61
GFDL_CM2_0	0.81	77.13	3.19	-6.44
GISS_MODEL_E_R	0.69	67.20	2.89	-2.09
MPI_ECHAM5	0.84	81.56	3.30	-6.44

Rusape minimum temperatures were best simulated by the CCCMA_CGCM3_1 model. This is shown by the statistics in Table 4.1(c). Although H_o was accepted for the GISS MODEL E R

model at Rusape, the R² and ME values for this model are weaker than those of the former, thus making the CCCMA_CGCM3_1 model most suitable.

4.4.2 Maximum air temperature

The statistics used to assess global climate model performance in simulating maximum temperature are shown in Table 4.2(a) to 4.2(e).

Table 4.2(a) Quantitative measures of the performance of the five global climate models for simulating maximum temperature at Mt Darwin.

Model	R^2	ME (%)	RMSE (°C)	$t_{\rm stat}$
CCCMA_CGCM3_1	0.68	63.95	2.55	2.21
CSIRO_MK3_5	0.60	44.55	1.61	10.90
GFDL_CM2_0	0.42	41.27	1.89	-0.63
GISS_MODEL_E_R	0.54	52.37	1.81	3.60
MPI_ECHAM5	0.62	61.79	2.05	-0.05

Maximum temperatures at Mt Darwin were best simulated by the CCCMA_CGCM3_1 model as shown by the statistics in Table 4.2(a). All other models performed poorly in simulating the temperatures at Mt Darwin. The CCCMA_CGCM3_1 model however showed weaker values of R² and ME in simulating maximum temperature as compared to the same statistical quantities for simulating minimum temperature.

Table 4.2(b) Quantitative measures of the performance of the five global climate models for simulating maximum temperature at Karoi.

Model	R^2	ME	RMSE	t _{stat}
		(%)	(°C)	
CCCMA_CGCM3_1	0.67	64.60	2.31	-1.48
CSIRO_MK3_5	0.61	49.15	1.58	9.73
GFDL_CM2_0	0.40	37.33	1.77	-3.24
GISS_MODEL_E_R	0.56	54.68	1.49	0.81
MPI_ECHAM5	0.61	60.24	1.91	-3.23

At Karoi, the CCCMA_CGCM3_1 model best resembled observations, making it the most suitable model for simulating maximum temperatures at the station. This is shown by the statistical parameters in Table 4.2(b). H_o was accepted for the GISS_MODEL_E_R model; however the weaker R² and ME values made it unsuitable for the simulations at the station.

Table 4.2(c) Quantitative measures of the performance of the five global climate models for simulating maximum temperature at Wedza.

Model	R^2	ME (%)	RMSE	t _{stat}
CCCMA_CGCM3_1	0.69	60.78	2.74	-2.22
CSIRO_MK3_5	0.63	60.45	2.19	-4.54
GFDL_CM2_0	0.33	28.48	1.98	-3.58
GISS_MODEL_E_R	0.58	57.82	2.09	-0.86
MPI_ECHAM5	0.56	54.57	2.18	-3.53

The greatest values of R² and ME for the CCCMA_CGCM3_1 model that are shown in Table 4.2(c) made this model the best for simulating maximum temperatures at Wedza.

Table 4.2(d) Quantitative measures of the performance of the five global climate models for simulating maximum temperature at Rusape.

Model	R^2	ME	RMSE	t _{stat}
		(%)	(°C)	
CCCMA_CGCM3_1	0.67	62.36	2.74	-0.91
CSIRO_MK3_5	0.60	55.28	1.92	6.38
GFDL_CM2_0	0.38	36.66	1.93	-3.08
GISS_MODEL_E_R	0.60	59.90	1.97	0.17
MPI_ECHAM5	0.59	58.24	2.16	-2.66

At Rusape, all other models did not perform well in simulating maximum temperatures at the station and of the five models, the CCCMA_CGCM3_1 model was the best. This is shown by the statistical indicators in Table 4.2(d). Although the null hypothesis was accepted for the GISS_MODEL_E_R model, its statistical measures were weaker than those of the CCCMA_CGCM3_1 model.

Table 4.2(e) Quantitative measures of the performance of the five global climate models for simulating maximum temperature at Mutoko

Model	R^2	ME (%)	RMSE (°C)	$\mathbf{t}_{\mathrm{stat}}$
CCCMA_CGCM3_1	0.78	68.20	2.41	2.11
CSIRO_MK3_5	0.68	57.83	1.71	-4.95
GFDL_CM2_0	0.62	50.24	1.75	3.91
GISS_MODEL_E_R	0.66	64.35	1.83	-0.31
MPI_ECHAM5	0.71	65.11	1.99	3.62

The CCCMA_CGCM3_1 model was the best for simulating maximum temperatures at Mutoko as shown by the statistical measures in Table 4.2(e).

The null hypothesis was accepted at all stations for the CCCMA_CGCM3_1 model. This is confirmed by the t-values obtained in the significance test. The CCCMA_CGCM3_1 model therefore obtained the highest ranking for simulating both minimum and maximum temperature at all stations. The GISS_MODEL_E_R model showed weaker values of R² and ME; however for this model, H₀ was accepted at Wedza and Rusape for simulating minimum temperature and was also accepted at Wedza, Rusape, Mutoko and Karoi for simulating maximum temperature. This model was second in simulating both minimum and maximum temperature. For the MPI_ECHAM5 model, H₀ was accepted only at Mt Darwin for simulating maximum temperature. For the CSIRO_MK3_5 model, H₀ was accepted only at Wedza (Table 4.1(b)). The GFDL_CM2_0 model performed well in simulating maximum temperature at Mt Darwin only and it performed poorly for all other stations. Using the results of statistical analysis, the five models were ranked as shown in Figure 4.12.

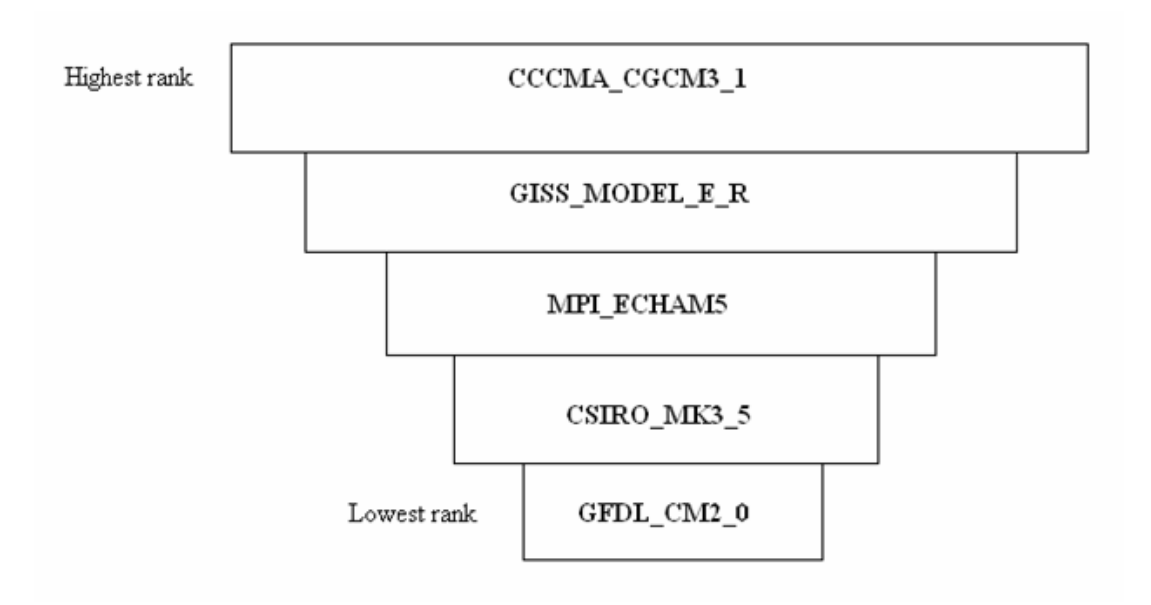


Figure 4.12 Ranking the perfomance of models for simulating temperature

The CCCMA_CGCM3_1 climate model was therefore chosen to construct the baseline temperatures for all the stations based on its control data.

4.4.3 Rainfall

Summary statistics used to assess global climate models' performances in simulating rainfall are shown in Tables 4.3(a) to 4.3(d).

Table 4.3(a) Quantitative measures of the performance of the five global climate models for simulating rainfall at Mt Darwin.

Model	R^2	RMSE	t _{stat}
		(mm)	
CCCMA_CGCM3_1	0.33	55.8	-7.25
CSIRO_MK3_5	0.41	76.8	-11.01
GFDL_CM2_0	0.42	73.2	-10.54
GISS_MODEL_E_R	0.41	66.6	-2.19
MPI ECHAM5	0.35	55.3	-10.98

All models performed poorly in simulating rainfall at Mt Darwin. This is shown by the weak values of R² and high values of RMSE for each model in Table 4.3(a). The null hypothesis was accepted only for the GISS_MODEL_E_R model thus making it the best amongst the five models. The CCCMA_CGCM3_1 model which best simulated temperature at Mt Darwin was found to be the worst for simulating rainfall at the same station. This is shown by the statistics in Table 4.3(a).

Table 4.3(b) Quantitative measures of the performance of the five global climate models for simulating rainfall at Wedza.

Model	R^2	RMSE	t_{stat}
		(mm)	
CCCMA_CGCM3_1	0.33	72.9	3.69
CSIRO_MK3_5	0.22	66.4	2.67
GFDL CM2 0	0.39	89.4	-0.59
GISS MODEL E R	0.18	65.3	1.51
MPI_ECHAM5	0.32	73.2	0.04

The values of R² are very low and RMSE values high for all the models as shown in Table 4.3(b); however the null hypothesis was accepted for the GFDL_CM2_0, GISS_MODEL_E_R and the MPI ECHAM5 models.

Table 4.3(c) Quantitative measures of the performance of the five global climate models for simulating rainfall at Rusape.

Model	R^2	RMSE	t _{stat}
		(mm)	
CCCMA_CGCM3_1	0.33	52.7	6.54
CSIRO_MK3_5	0.37	64.5	3.28
GFDL_CM2_0	0.42	64.6	3.16
GISS MODEL E R	0.21	40.0	6.04
MPI ECHAM5	0.31	51.9	3.94

The statistical indicators in Table 4.3(c) show that the null hypothesis was rejected for all the models thus the models performed poorly in simulating rainfall at Rusape.

Table 4.3(d) Quantitative measures of the performance of the five global climate models for simulating rainfall at Mutoko.

Model	R^2	RMSE	t _{stat}
		(mm)	
CCCMA_CGCM3_1	0.36	53.0	-7.28
CSIRO_MK3_5	0.43	71.4	3.66
GFDL_CM2_0	0.35	72.6	4.82
GISS_MODEL_E_R	0.30	46.0	-10.12
MPI ECHAM5	0.39	53.2	4.61

Table 4.3(d) shows inaccuracy of all climate models in simulating rainfall at Mutoko.

Results of regression analysis and RMSE analysis showed that all the models are poor in predicting rainfall for all the stations. It was difficult to use only these results to select the best model as was done for temperature hence the need for frequency analysis.

4.4.3.1 Frequency analysis

Frequency analysis was done at 50 % probability of exceedance. Figure 4.13(a), 4.13(b) and 4.13(c) show how each model performed to simulate observed rainfall.

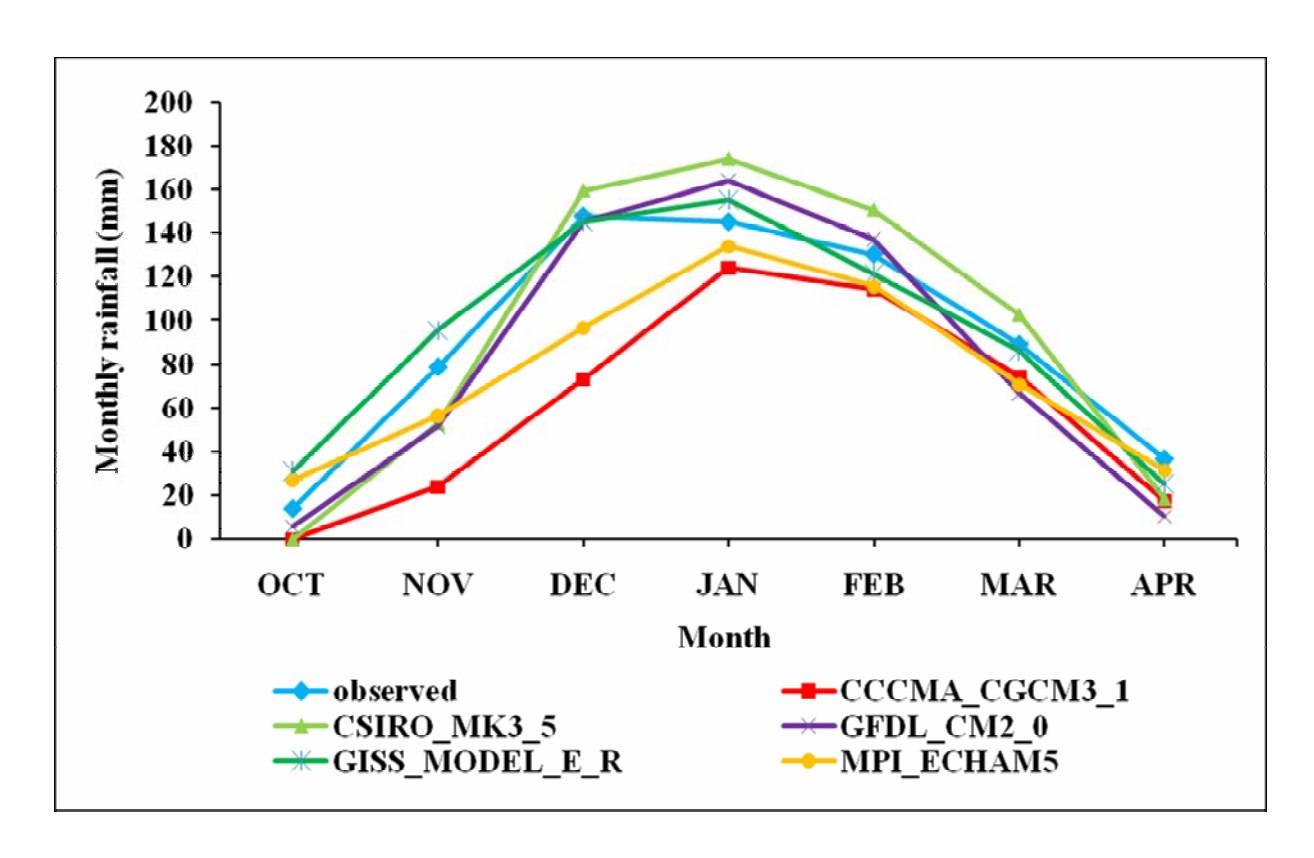


Figure 4.13(a) Model performances at 50% probability of exceedance for Mt Darwin

For Mt Darwin, all the five models simulated rainfall well as shown in Figure 4.13(a). The closest model to observation was the GISS_MODEL_E_R which also agreed with the results of significance test in Table 4.3(a). In terms of rainfall, the baseline climate for Mt Darwin was based on this model.

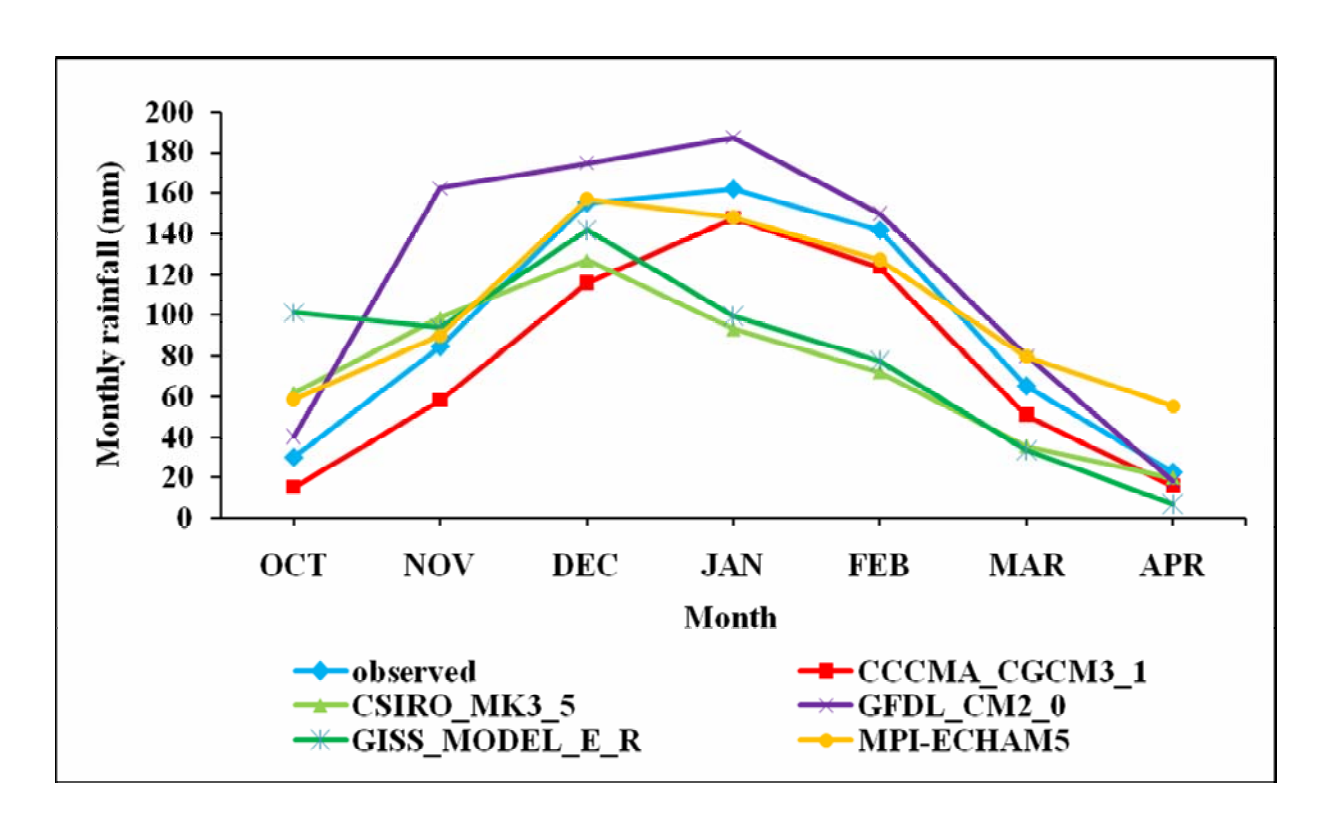


Figure 4.13(b) Model performances at 50% probability of exceedance for Wedza

At Wedza, MPI_ECHAM5 model closely resembled observed data as shown in Figure 4.13(b). This also agreed with the results of significant test in Table 4.3(b). The baseline climate at Wedza was based on this model. The GFDL_CM2_0 model preformed very well towards the end of the season but it had highly overestimated the rainfall amount from October to January.

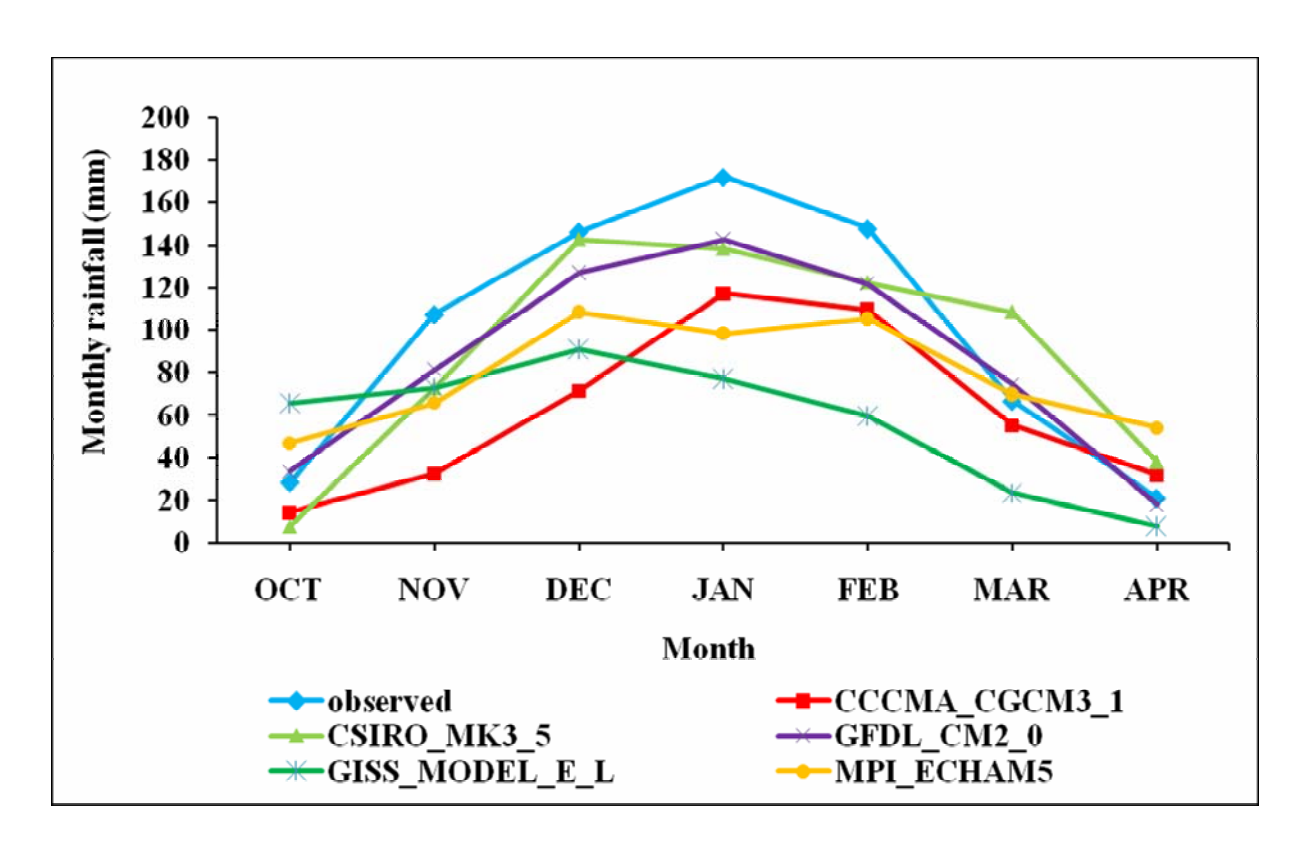


Figure 4.13(c) Model performances at 50% probability of exceedance for Rusape

At Rusape, the GFDL_CM2_0 model preformed fairly well as compared to the other four as shown in Figure 4.13(c) and the baseline climate for Rusape was based on this model. Generally the models followed the trend of rainfall variation in the growing period. The models are good at predicting trends in rainfall variation but not at estimating the actual amount. Inaccuracy of global climate models to predict precipitation was found by many researchers.

Hansen et al. (2007) explain why global climate models are not accurate in predicting precipitation. They say that the space-time correlation between models and observations is small, only about 50 to 60 %. They further point out that the poor correlations originate mainly in the tropics where the spatial variation of precipitation is great. According to Collins et al. (2006), strong horizontal gradients in the field lead to a significant drop in correlations between model output and observations. Another discrepancy between models and observations is that when precipitation is categorised into light, moderate and heavy, models reproduce the observed extent of moderate precipitation (10 to 20 mm/day) but underestimate that of heavy precipitation and overestimate the extent of light precipitation (Dai, 2006). Delworth et al. (2006) point out that

for precipitation, the GFDL model reveals significant widespread errors in the tropics, mostly in the Intertropical convergence zone (ITCZ) where precipitation is underestimated by several millimetres per day.

4.5 Baseline climate for the stations

The baseline climates for Karoi, Wedza, Rusape, Mt Darwin and Mutoko were constructed using the CCE tool based on the most suitable global climate models found in section 4.4. The baseline climates are shown in Figures 4.14(a) to 4.14(e) for temperature and in Figures 4.15(a) to 4.15(e) for rainfall respectively.

4.5.1 Mean monthly temperatures

4.5.1.1 Baseline temperatures for Mt Darwin

Figure 4.14(a) shows the mean minimum and mean maximum temperatures for Mt Darwin for the period 1971 to 2000.

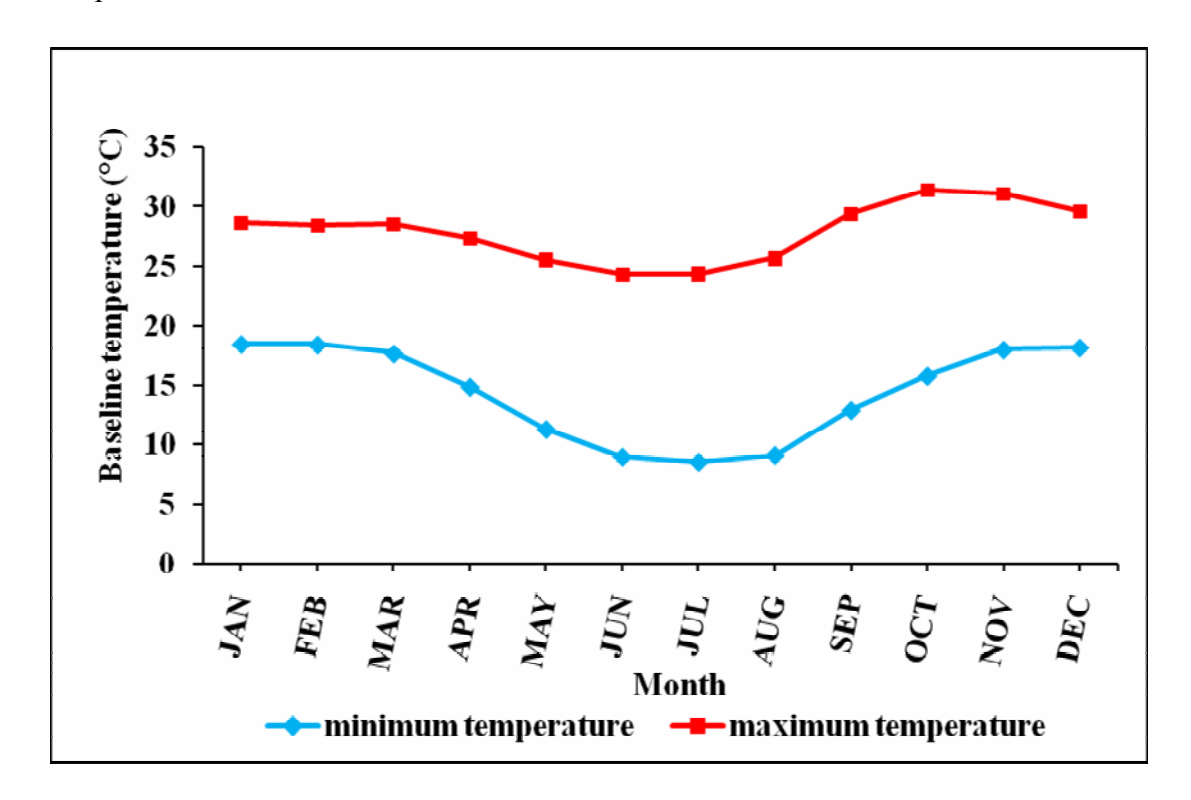


Figure 4.14(a) Baseline temperatures for Mt Darwin for the period 1971 to 2000

Mean minimum temperatures at Mt Darwin range from about 8.5 °C in July to about 18.5 °C in January while mean maximum temperatures range from about 24 °C in June to about 31 °C in October.

4.5.1.2 Baseline temperatures for Karoi

Figure 4.14(b) shows the mean minimum and mean maximum temperatures for Karoi for the period 1971 to 2000.

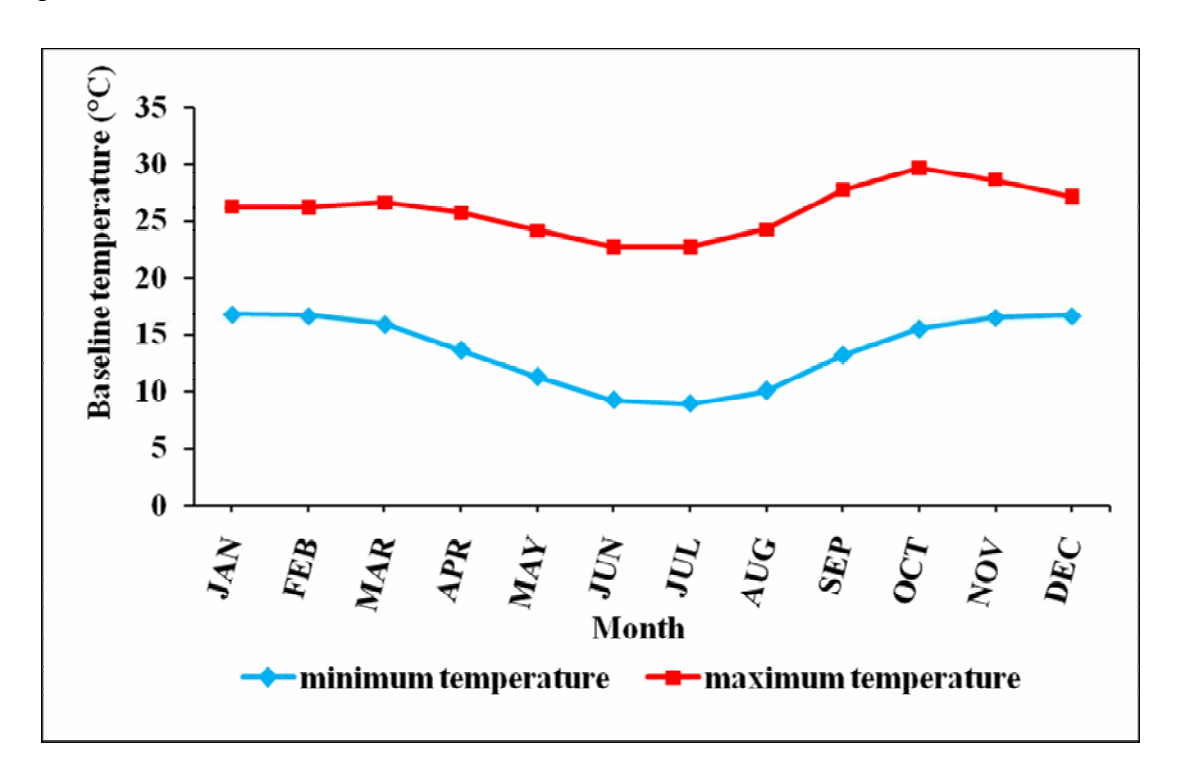


Figure 4.14(b) Baseline temperatures for Karoi for the period 1971 to 2000

Mean minimum temperatures at Karoi range from about 9 °C in July to about 17 °C in January while mean maximum temperatures range from about 23 °C in June to about 30 °C in October.

4.5.1.3 Baseline temperatures for Wedza

Figure 4.14(c) shows the mean minimum and mean maximum temperatures for Wedza for the period 1971 to 2000

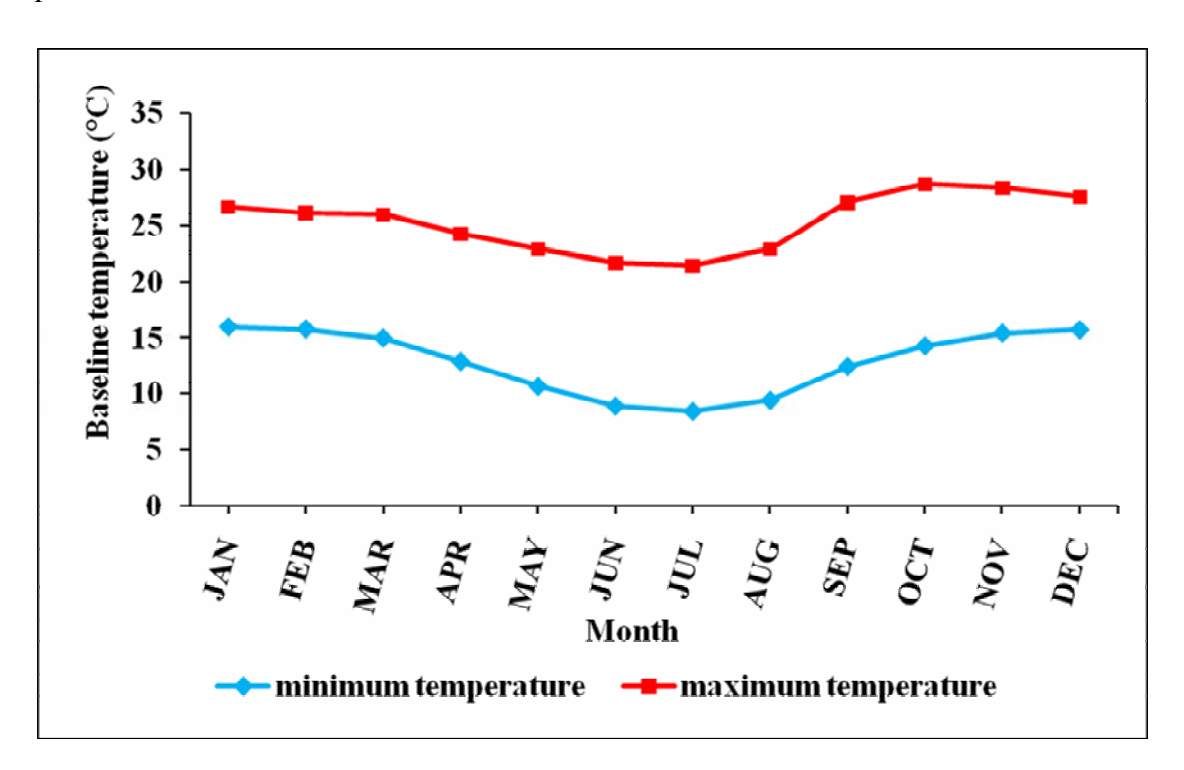


Figure 4.14(c) Baseline temperatures for Wedza for the period 1971 to 2000

Mean minimum temperatures at Wedza range from about 8 °C in July to about 16 °C in December, January and February while mean maximum temperatures range from about 21 °C in June to about 28 °C in October.

4.5.1.4 Baseline temperatures for Rusape

Figure 4.14(d) shows the mean minimum and mean maximum temperatures for Rusape for the period 1971 to 2000.

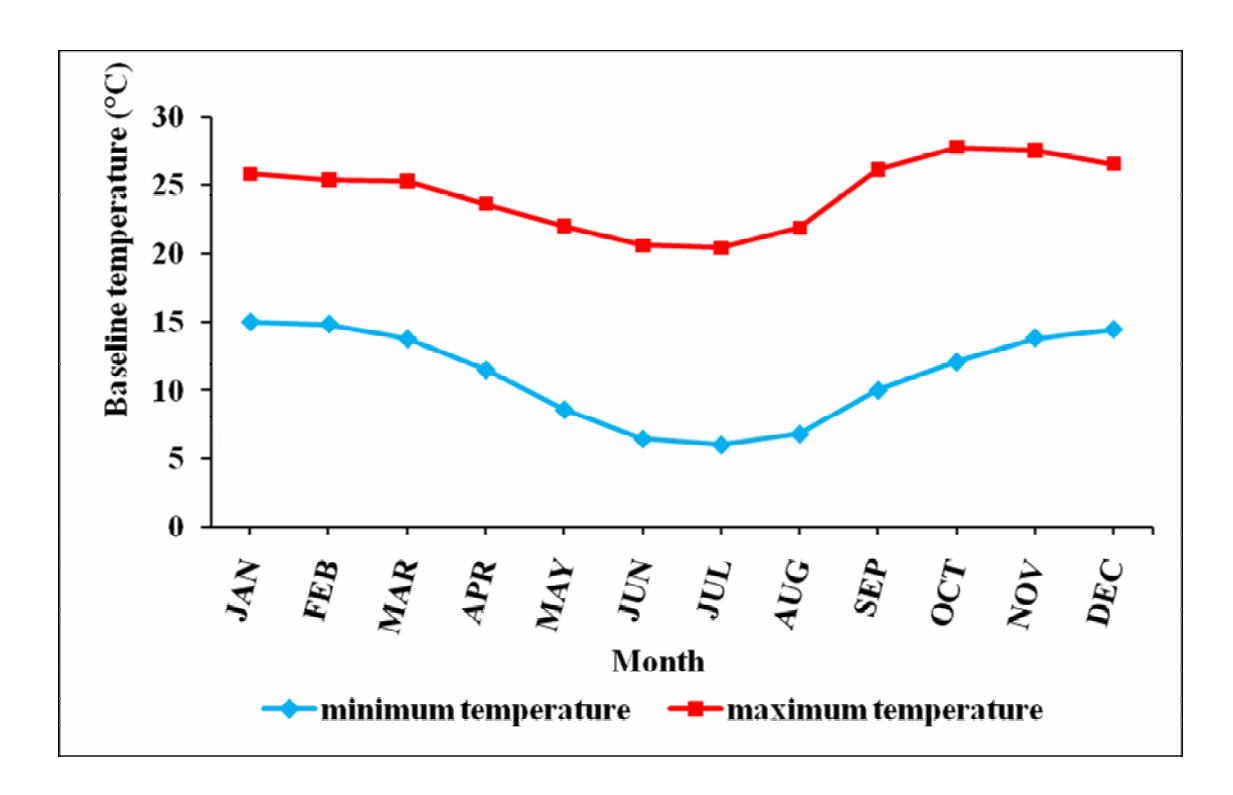


Figure 4.14(d) Baseline temperatures for Rusape for the period 1971 to 2000

Mean minimum temperatures at Rusape range from about 6 °C in July to about 15 °C in January while mean maximum temperatures range from about 20 °C in July to about 28 °C in October, November, December and January.

4.5.1.5 Baseline temperatures for Mutoko

Figure 4.14(e) shows the mean minimum and mean maximum temperatures for Mutoko for the period 1971 to 2000.

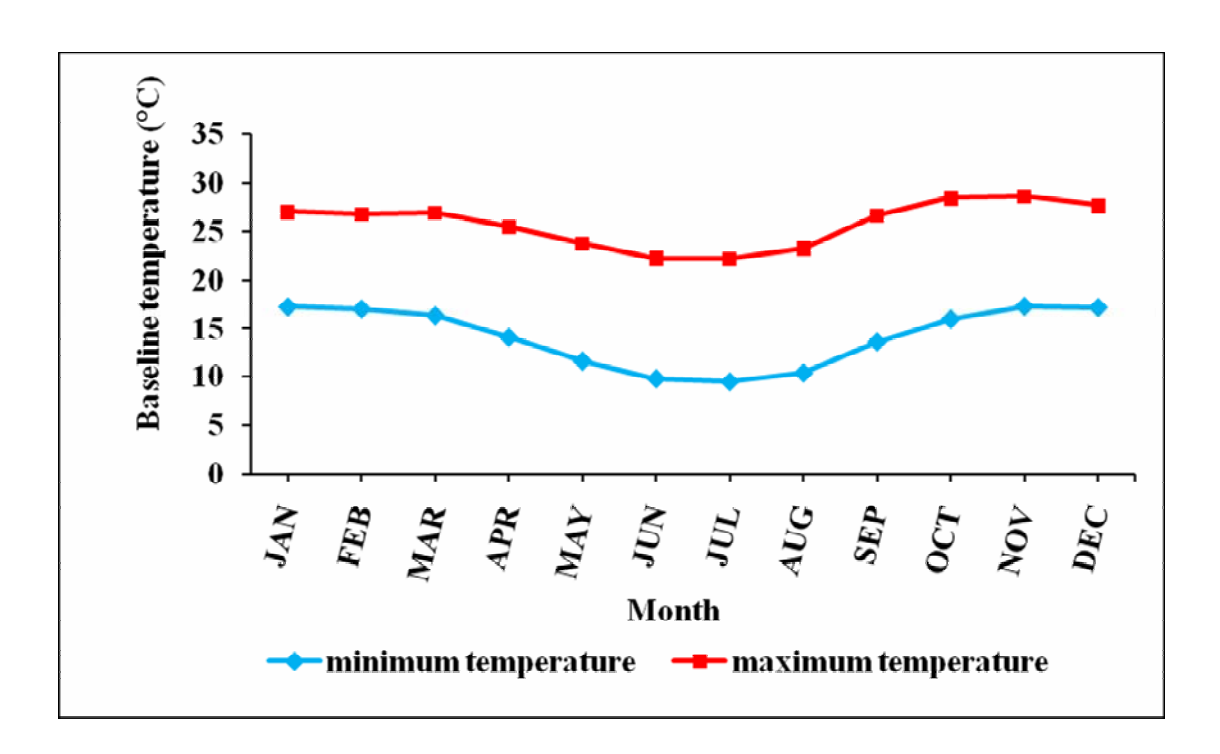


Figure 4.14(e) Baseline temperatures for Mutoko for the period 1971 to 2000

Mean minimum temperatures at Mutoko range from about 10 °C in July to about 17 °C in December and January while mean maximum temperatures range from about 22 °C in July to about 28 °C in October, November and December.

4.5.2 Mean monthly rainfall

Figures 4.15(a) to 4.15 (e) show the mean monthly rainfall for the stations for the period 1971 to 2000

4.5.2.1 Baseline rainfall for Mt Darwin

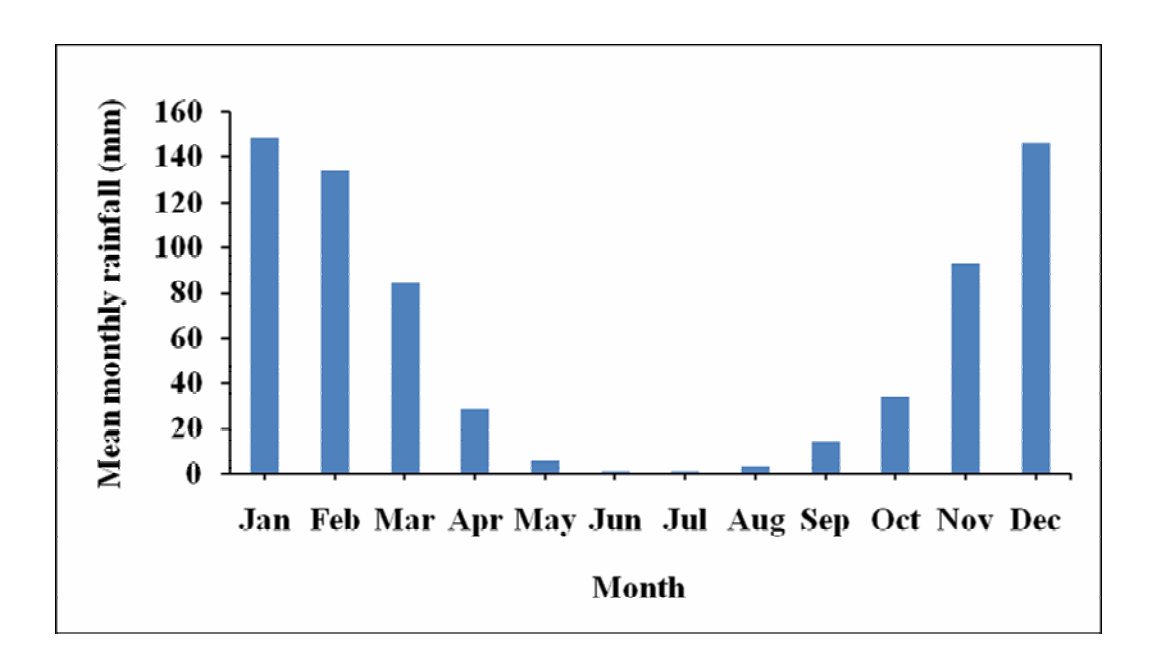


Figure 4.15(a) Baseline monthly rainfall for Mt Darwin for the period 1971 to 2000

The best model for simulating rainfall at Mt Darwin was found to be the GISS_MODEL_E_R model. Based on this model, rainfall increases in the growing period and the months of December and January are the peak rainfall months at Mt Darwin.

4.5.2.2 Baseline rainfall for Karoi

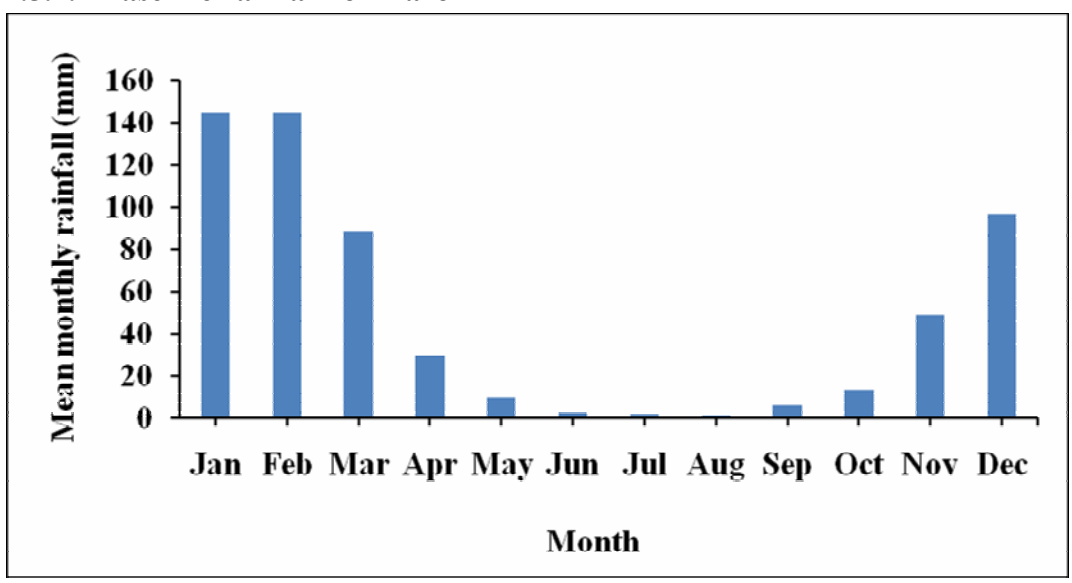


Figure 4.15(b) Baseline monthly rainfall for Karoi for the period 1971 to 2000

Rainfall at Karoi was best simulated by the GISS_MODEL_E_R model. According to this model, the amount of rainfall is low early in the growing season at Karoi. When low rainfall is received in October and November, early planted crops may be adversely affected by shortage of soil moisture. Rainfall peaks in the months of January and February.

4.5.2.3 Baseline rainfall for Mutoko

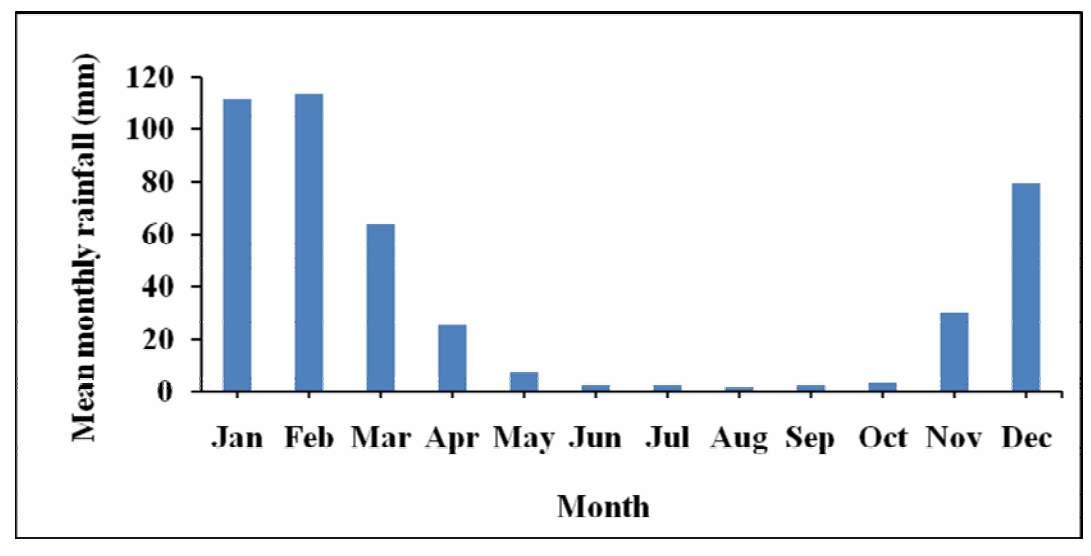


Figure 4.15(c) Baseline monthly rainfall for Mutoko for the period 1971 to 2000

The baseline monthly rainfall at Mutoko was based on simulations by the GISS_MODEL_E_R model. The model shows that the amount of rainfall is very low in October. Crops that are grown in October may not grow well due to inadequacy of soil moisture.

4.5.2.4 Baseline rainfall for Wedza

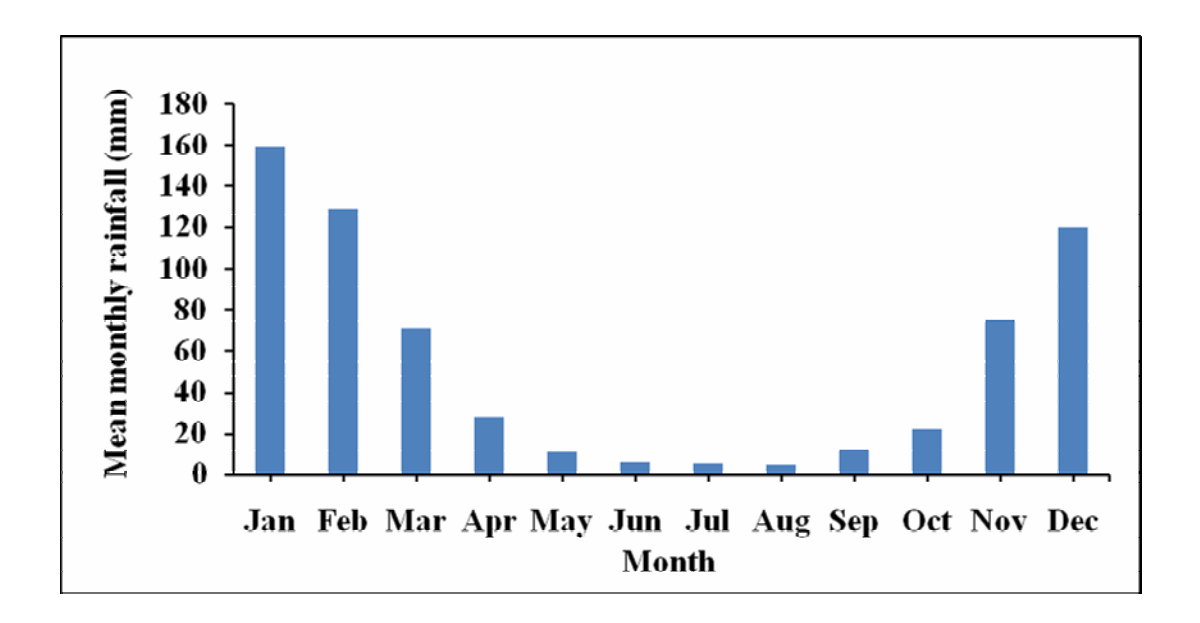


Figure 4.15(d) Baseline monthly rainfall for Wedza for the period 1971 to 2000

The MPI_ECHAM5 model was best suited for simulating rainfall at Wedza and the baseline monthly rainfall at the station was based on it. The growing period is characterised by increasing rainfall amount which peaks in the month of January.

4.5.2.5 Baseline rainfall for Rusape

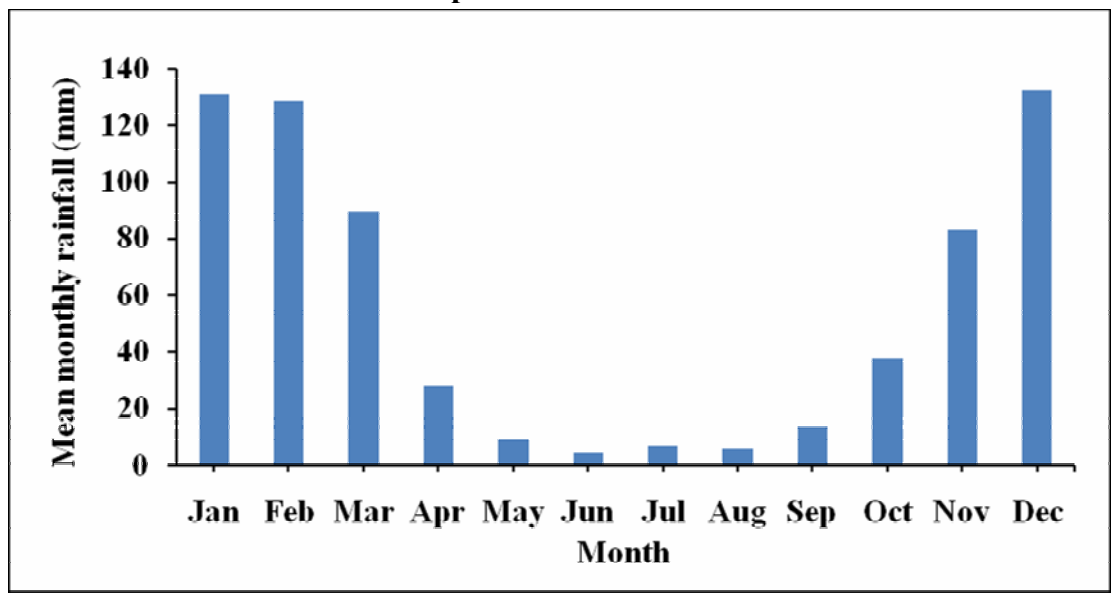


Figure 4.15(e) Baseline monthly rainfall for Rusape for the period 1971 to 2000

The most suitable model for simulating rainfall at Rusape was the GFDL_CM2_0. On average, the highest rainfall is received during the period December to February at Rusape. At all other stations, peak rainfall is observed in the months of January and February with Mutoko receiving the lowest amount.

4.6 Projected changes in temperature and rainfall

4.6.1 Changes in temperature

The best model CCCMA_CGCM3_1 consistently predicted that future temperatures will be higher above the 1971-2000 baseline during the period 2046 – 2065, an indication that the future climate will be warmer than the past.

4.6.1.1 Minimum temperature anomalies

Minimum temperature anomalies predicted by the CCCMA_CGCM3_1 model are shown in Figure 4.16(a).

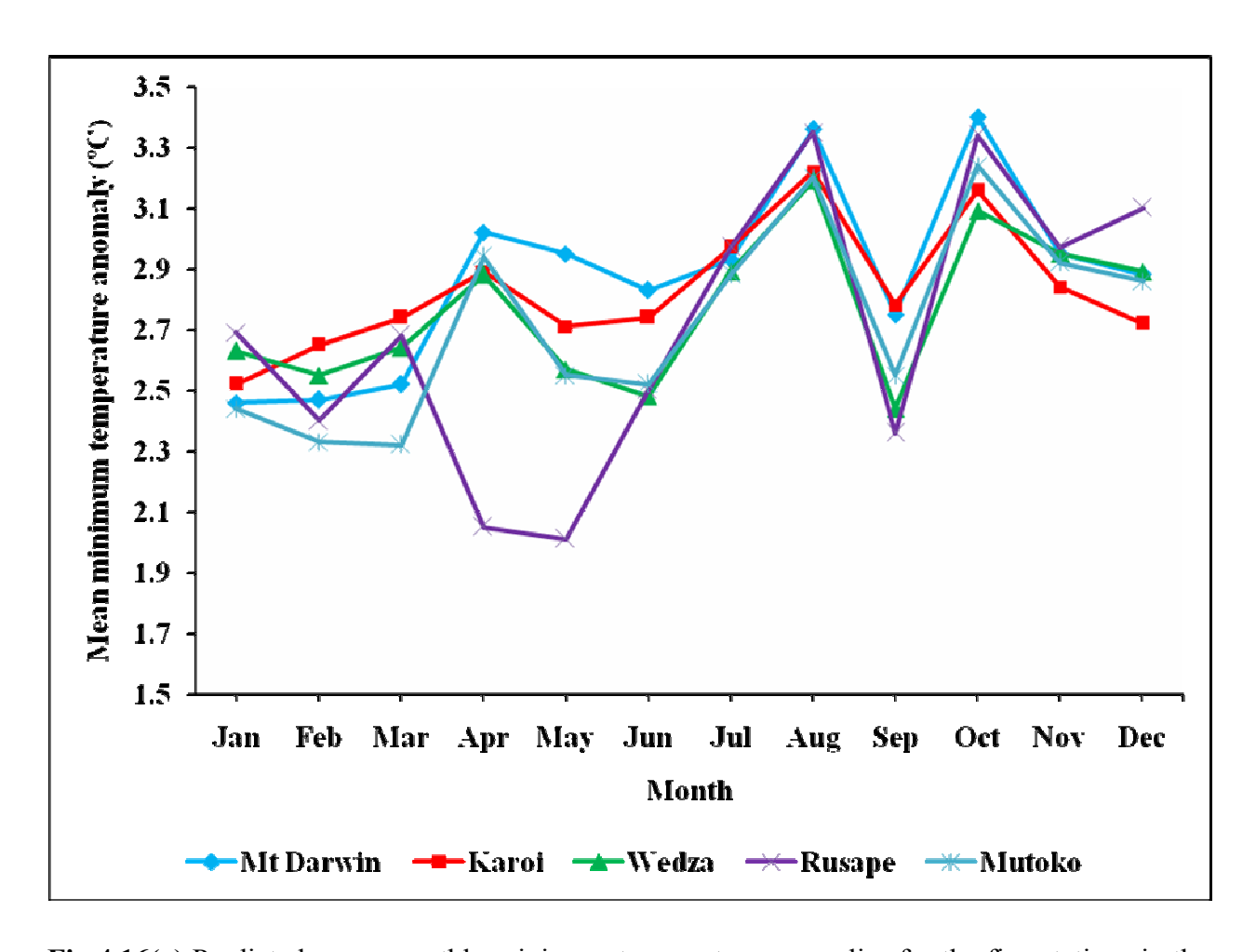


Fig 4.16(a) Predicted mean monthly minimum temperature anomalies for the five stations in the period 2046 - 2065

4.6.1.2 Maximum temperature anomalies

Maximum temperature anomalies predicted by the CCCMA_CGCM3_1 model are shown in Figure 4.16(b).

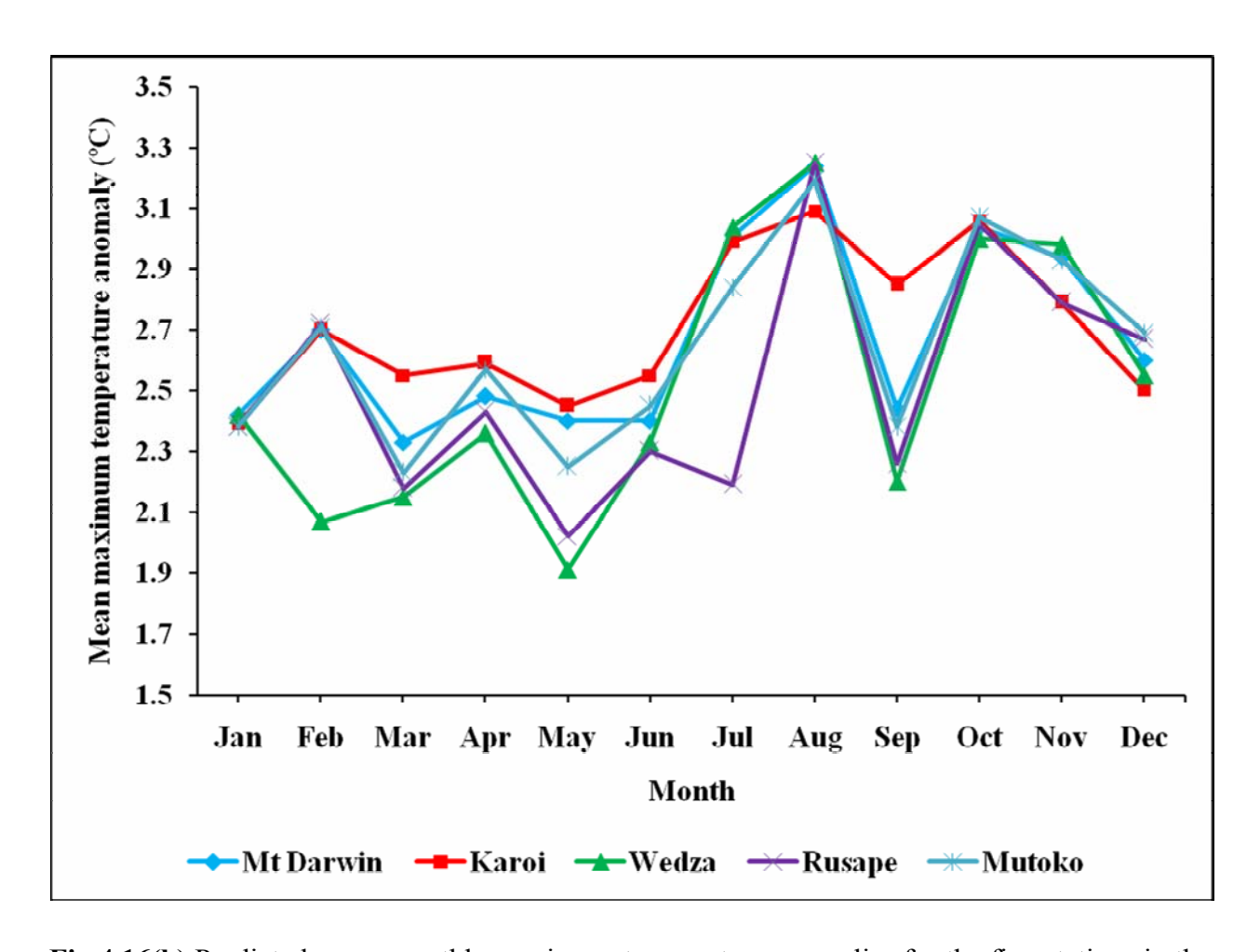


Fig 4.16(b) Predicted mean monthly maximum temperature anomalies for the five stations in the period 2046 - 2065

The CCCMA_CGCM3_1 model predicts temperature increase in the range 2.5 to 3.5 °C at Mt Darwin. Minimum temperatures are expected to increase in the range of about 2.5 to 3.3 °C at Karoi. Maximum temperatures at the same station are predicted to rise by about 0.7 °C. A warming of less than 1 °C is expected at Karoi. Predictions at Rusape and Wedza indicate that day time temperatures will increase within 2 °C to about 3.3 °C, a warming of approximately 1.3 °C. CCCMA_CGCM3_1 also predicts temperature increase in the range of about 2.2 to 3.3 °C at Mutoko. Overally, model predictions show that in the period 2046 – 2065, daytime temperatures are expected to rise by about 1.3 °C at Wedza and Rusape, 1 °C at Mt Darwin and Mutoko and 0.7 °C at Karoi. Day time temperatures are critical for the growth and development of maize.

4.6.2 Changes in rainfall

As explained earlier there was wide variation in rainfall prediction by the five models. The GISS_MODEL_E_R was the most applicable for predicting rainfall at Mt Darwin, Karoi and Mutoko, the MPI_ECHAM5 and the GFDL_CM2_0 models were the most suitable for Wedza and Rusape respectively. These are the models that were used to predict changes in rainfall at the stations.

4.6.2.1 Future rainfall change for Mt Darwin

The predicted rainfall anomalies for Mt Darwin are shown in Figure 4.17 (a)

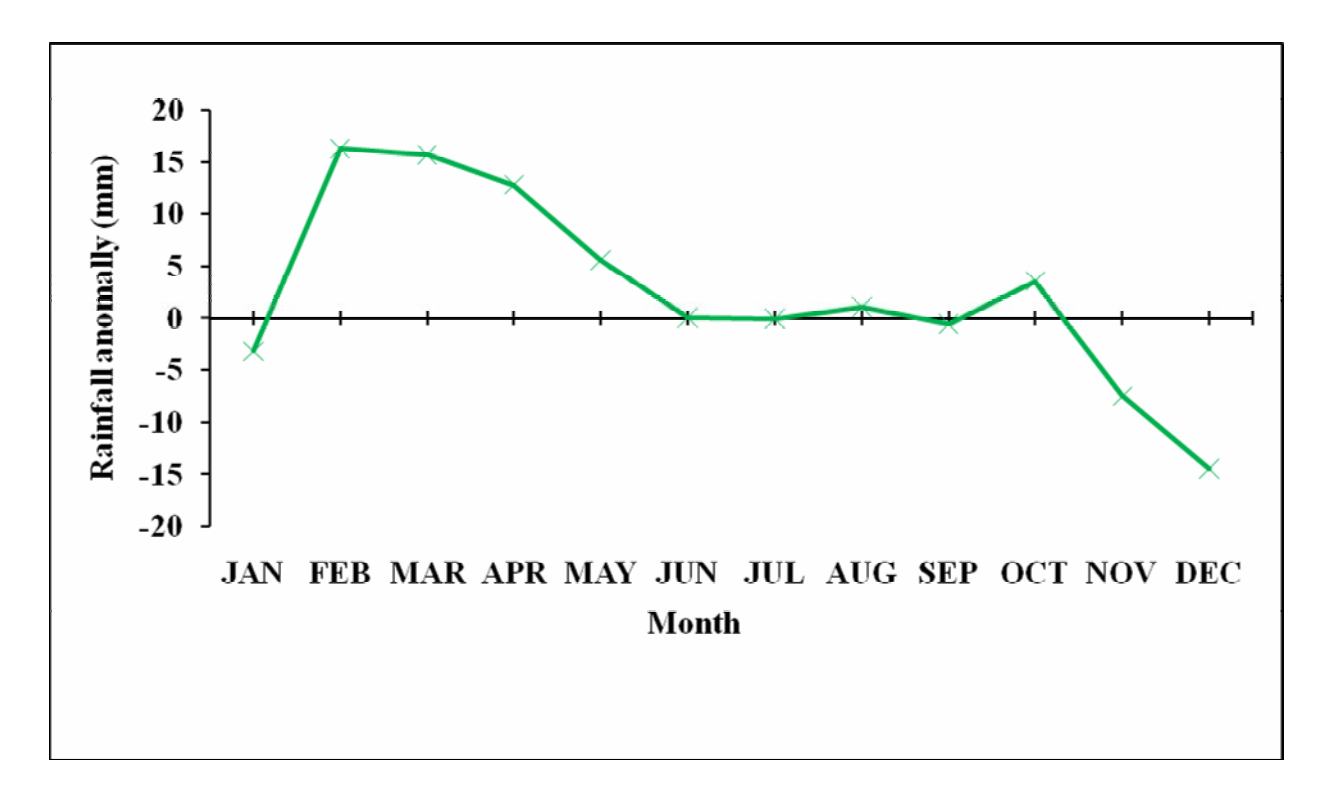


Figure 4.17 (a) Predicted mean monthly rainfall anomalies for Mt Darwin in the period 2046 – 2065

The model predicts wetter conditions in the months of February to May in the period 2046 – 2065, while the months of November, December and January are expected to be drier. If the predicted wetter conditions are realized, the available moisture will be beneficial to crops that are planted late. In Zimbabwe however, this is too late for crops.

If crops are planted between the months of October and December (early in the growing season) under the projected dry conditions, they may be adversely affected by moisture deficit resulting in reduced yields.

4.6.2.2 Future rainfall change for Wedza

The predicted rainfall anomalies for Wedza are shown in Figure 4.17 (b)

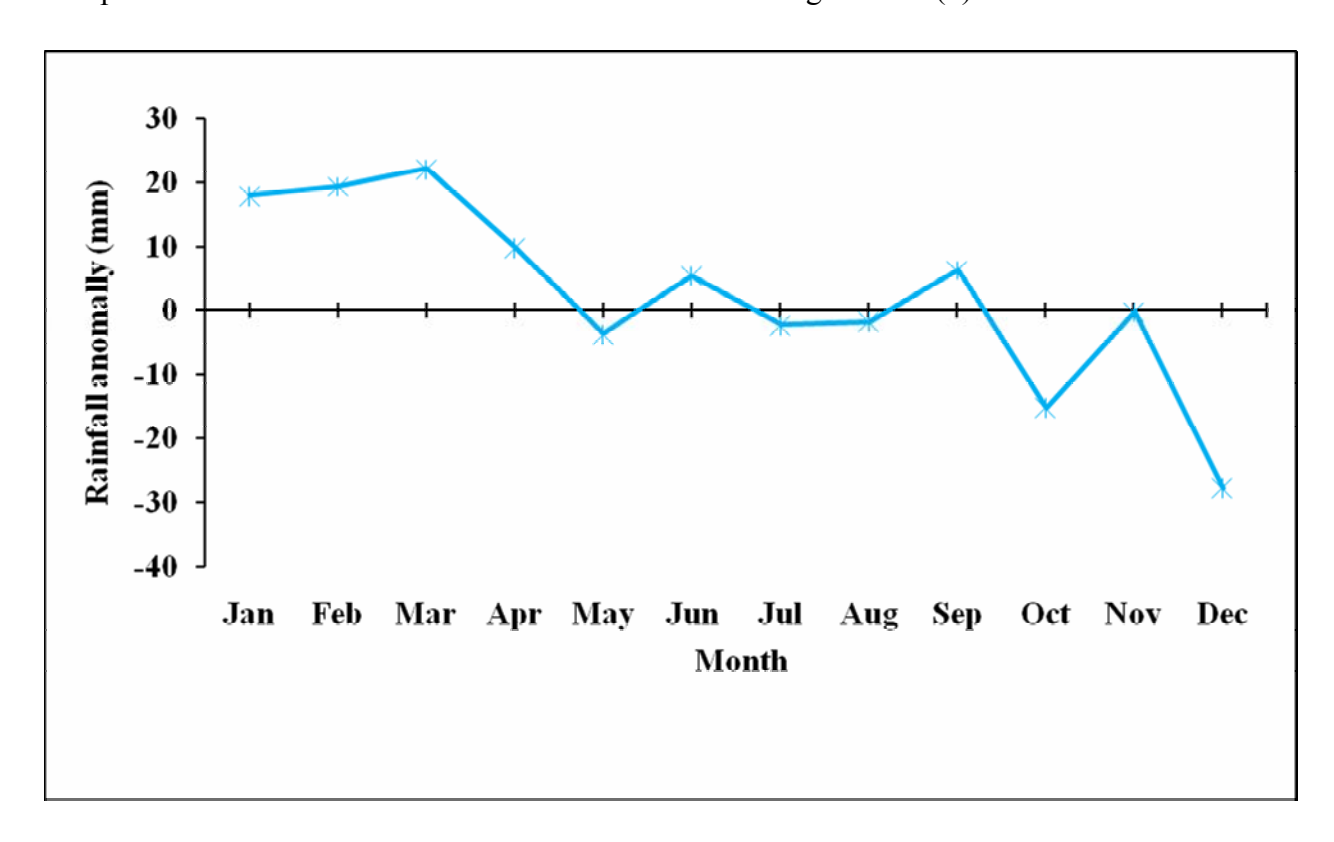


Figure 4.17(b) Predicted mean monthly rainfall anomalies for Wedza in the period 2046 – 2065

At Wedza, the model predicts wetter conditions from January to April and drier conditions from October to December. If the predicted wetter conditions are realized, farmers would be advised to delay planting and also to plant short season varieties.

4.6.2.3 Future rainfall change for Rusape

The predicted rainfall anomalies for Rusape are shown in Figure 4.17 (c)

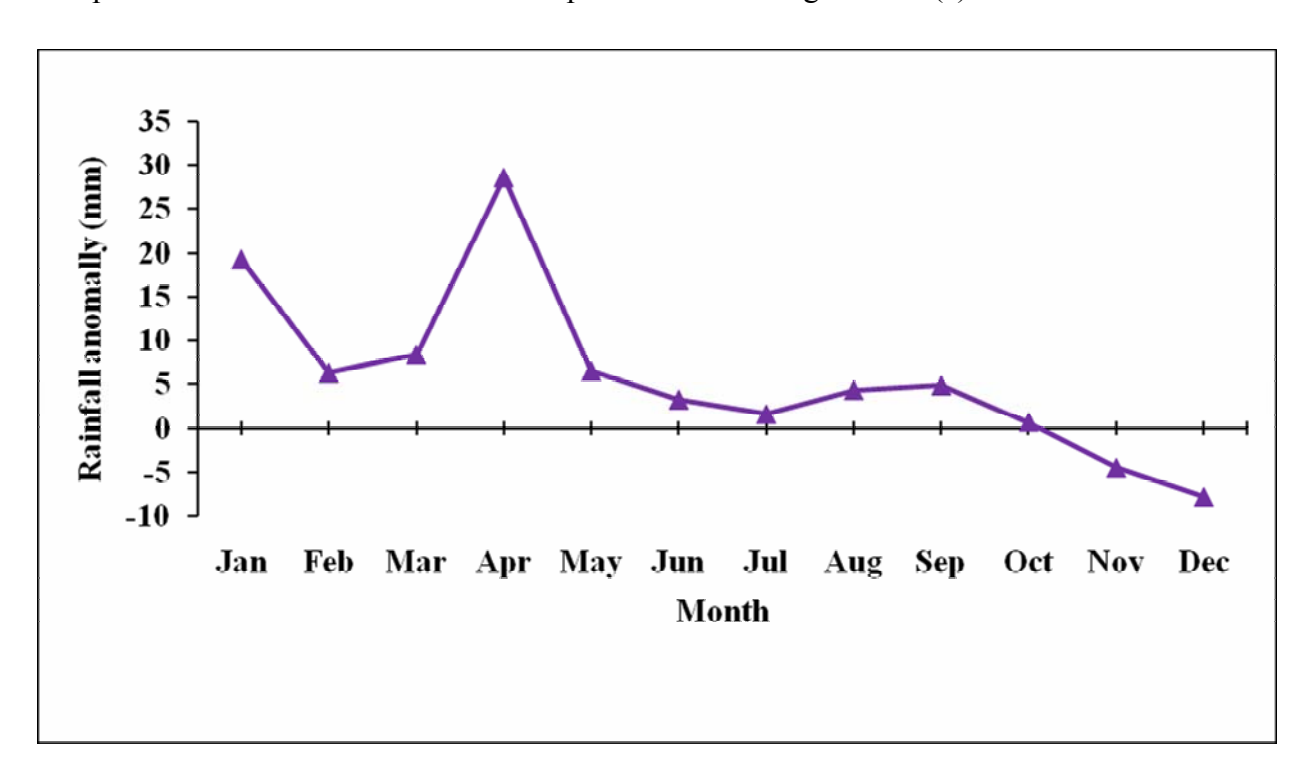


Figure 4.17 (c) Predicted mean monthly rainfall anomalies for Rusape in the period 2046 – 2065

At Rusape, there are chances that rainfall might decrease from November to December thus affecting yields of early planted maize. The late planted maize usually matures in April. According to the model, the month of April is expected to be anomalously wet and this might cause maize rot in the field resulting in reduced yields.

4.6.2.4 Future rainfall change for Karoi

The predicted rainfall anomalies for Karoi are shown in Figure 4.17 (d)

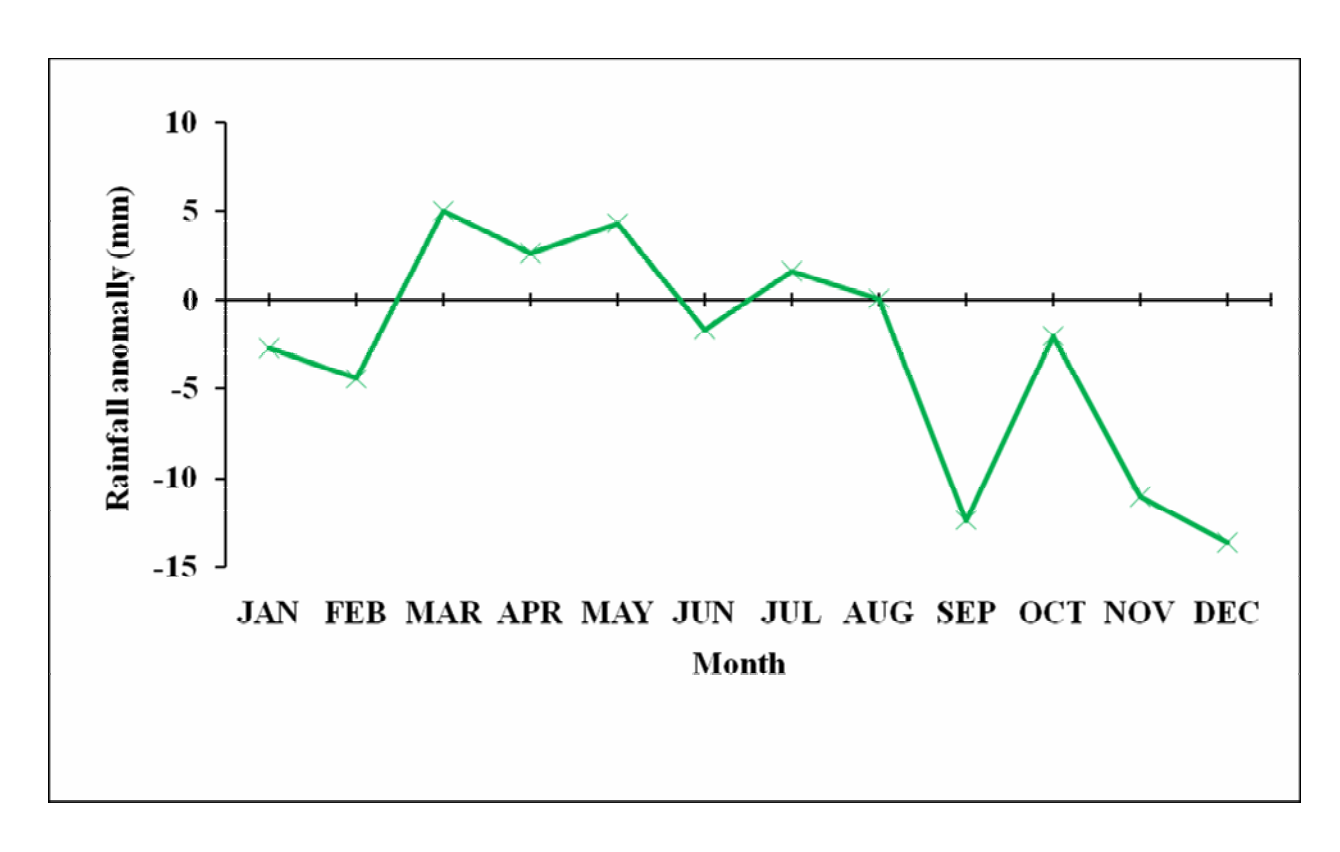


Figure 4.17 (d) Predicted mean monthly rainfall anomalies for Karoi in the period 2046 – 2065

The GISS_MODEL_E_R model predicts dry conditions from October to mid-February at Karoi, and slightly wetter conditions from mid-February to mid-May. If the dry conditions persist, the areas around Karoi may not be suitable for summer crop production. A very short season variety will be most suited to the wetter conditions expected from March to May.

4.6.2.5 Future rainfall change for Mutoko

The predicted rainfall anomalies for Mutoko are shown in Figure 4.17 (e)

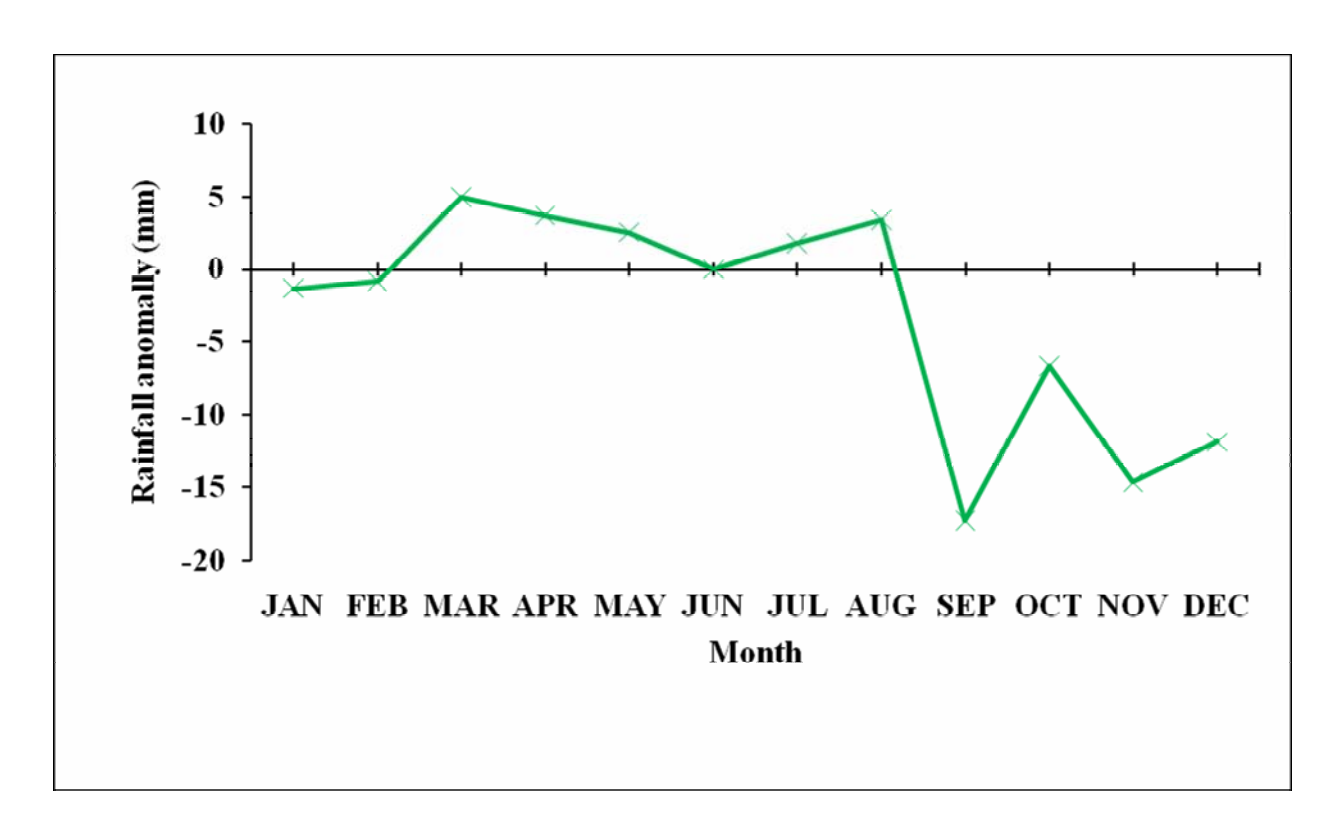


Figure 4.17 (e) Predicted mean monthly rainfall anomalies for Mutoko in the period 2046 – 2065

At Mutoko, the months of October to February are expected to be drier than average in the period 2046 - 2065. The model however predicts that there will be slightly wetter conditions from March to May. Benefits may be realized if farmers consider a very short season variety and plant it in February. In general, the models tested in the study predict that total rainfall will increase between the months of January and May in the period 2046-2065.

4.7 Dry spell analysis

The most suitable model for each station was used in this analysis. The CCE tool was used for the analysis. Data from the tool was exported to EXCEL where the graphics were constructed. The trends obtained were similar for all the stations. Figure 4.18 shows the dry spell analysis for Karoi.

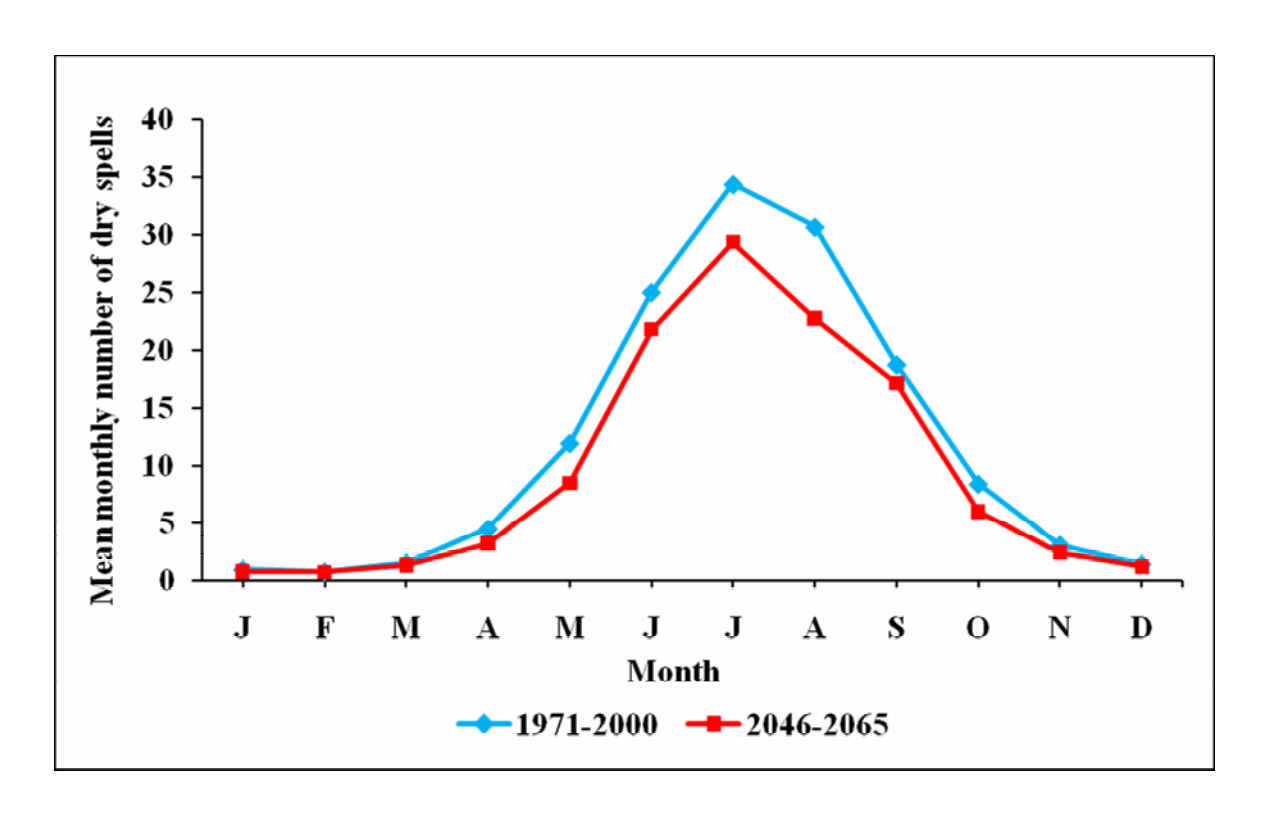


Figure 4.18 Mean monthly dry spells in the periods 1971-2000 and 2046-2065 for Karoi

Both wet and dry spells are necessary in agriculture. Wet spells maintain the soil at adequate moisture content. Dry spells provide time for cultivation, weeding, fertilizer application and spraying. They also provide the heating degree days required during different phenological stages of a crop. However, both wet and dry spells are detrimental to crops if they become excessive. Figure 4.18 shows that dry spells are expected to decrease during the period 2046-2065 compared to the period 1971-2000.

4.8 AquaCrop model validation

The model was validated by considering the performance of each individual maize cultivar. The AquaCrop model was assessed by comparing simulated maize yield with the observed yield. Model performance was judged by the magnitude of R^2 , RMSE and the slope.

4.8.1 Model performance for the SC513 cultivar

Table 4.4(a) Simulated and observed yield for the SC513 maize variety at ART Farm

Season	Planting date	Observed yield (ton/ha)	Simulated yield (ton/ha)
2000-2001	31/10/2000	10.86	9.50
2002-2003	28/10/2002	7.76	6.76
2003-2004	28/10/2003	11.30	11.85
2004-2005	27/10/2004	11.18	11.38
2005-2006	31/10/2005	10.10	8.69

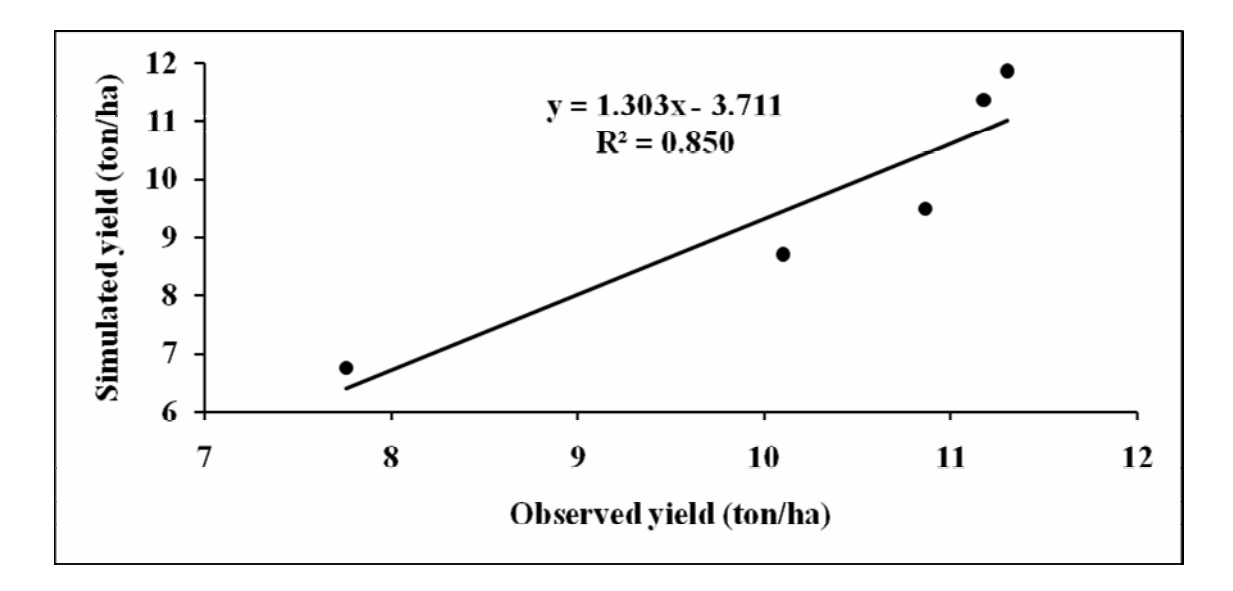


Figure 4.19(a) Comparison of simulated with observed yield at ART Farm for the SC513 maize variety

The simulated and observed yields for the SC513 variety are shown in Table 4.4(a). The simulated yields compare well with the observed yields with $R^2 = 0.850$, RMSE = 2.07 ton/ ha indicating a fairly strong linear relationship. Figure 4.19(a) shows the regression line. In general the model overestimated the yield (slope = 1.3), but in some seasons the model underestimated the yield.

4.8.2 Model performance for the SC715 cultivar

Table 4.4(b) Simulated and observed yield for the SC715 maize variety at ART Farm

Season	Planting date	Observed yield Simulated yield	
		(ton/ha)	(ton/ha)
2000-2001	31/10/2000	9.11	9.62
2002-2003	28/10/2002	7.17	8.36
2003-2004	28/10/2003	11.73	12.17
2004-2005	27/10/2004	10.85	11.79
2005-2006 (SC719)	31/10/2005	14.78	14.45

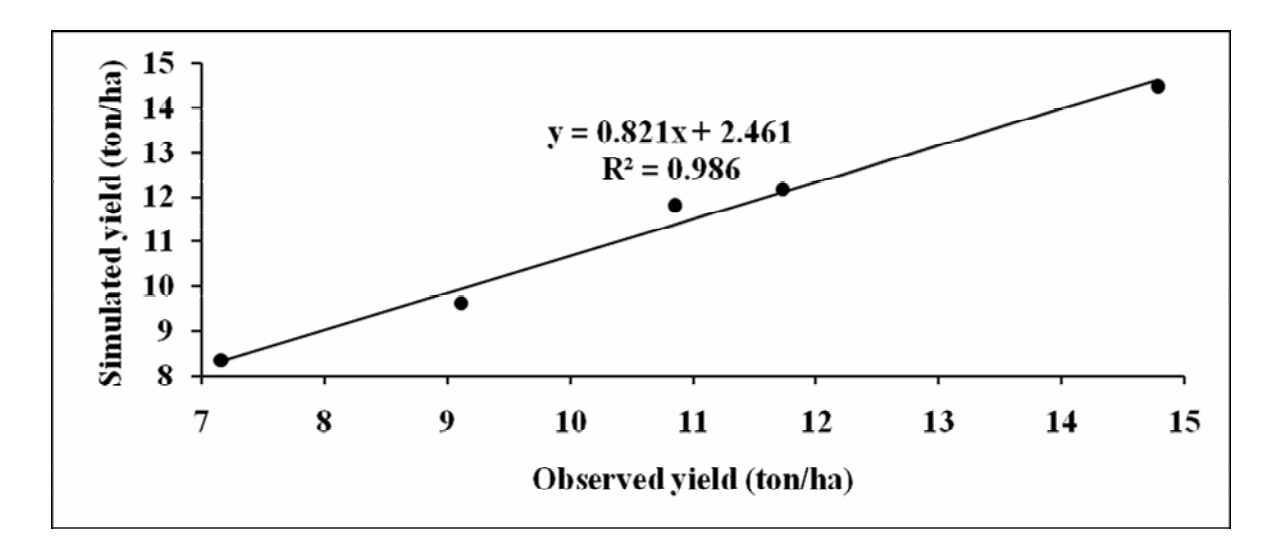


Figure 4.19(b) Comparison of simulated with observed yield at ART Farm for the SC715 maize variety

The results obtained for the SC715 variety are shown in Table 4.4(b). In all seasons except the 2005-2006, the model overestimated the yields. A highly positive R² value of 0.986, RMSE value of 3.32 toh/ha and a slope of 0.82 were however obtained from statistical analysis indicating a very strong linear relationship. The regression line is shown in Figure 4.19(b).

4.8.3 Model performance for the SC633 cultivar

Table 4.4(c) Simulated and observed yield for the SC633 maize variety at ART Farm

Season	Planting date	Observed yield Simulated yield	
		(ton/ha)	(ton/ha)
2000-2001	31/10/2000	10.51	9.32
2002-2003	28/10/2002	10.16	8.37
2003-2004	28/10/2003	14.15	11.72
2004-2005	27/10/2004	11.69	10.22
2005-2006 (SC635)	31/10/2005	13.77	12.34

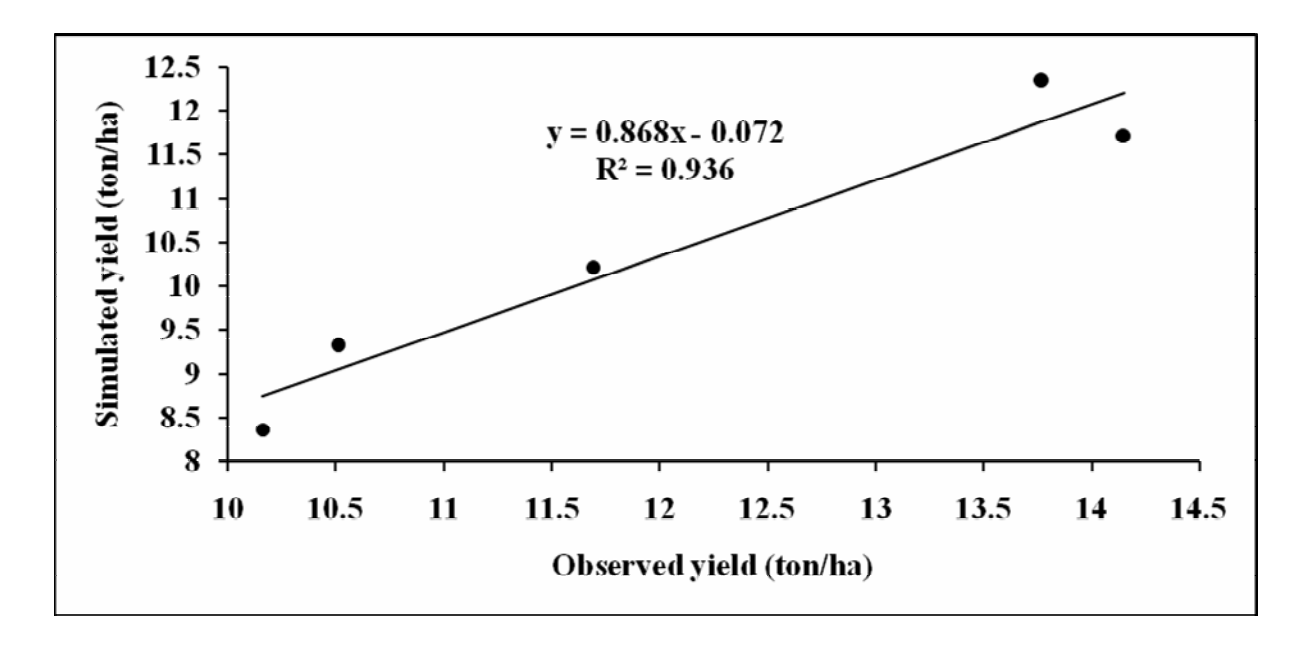


Figure 4.19(c) Comparison of simulated with observed yield at ART Farm for the SC633 maize variety

Results for the SC633 cultivar are shown in Table 4.4(c). The model underestimated the yields in all seasons (slope = 0.87). Statistical analysis showed that $R^2 = 0.936$ and RMSE = 1.64 ton/ha were obtained showing a strong linear relationship. The regression line is shown in Figure 4.21(c).

Values of the statistics used to assess the strength of the correlations for all simulations are shown in Table 4.4(d). The t values obtained in the significance test are also shown in Table 4.4(d).

Table 4.4(d) The statistics used to assess AquaCrop model performance

Cultivar	R^2	RMSE	slope	t_{stat}	t_{α}
		(ton/ha)			
SC513	0.85	2.06	1.3	1.48	3.50
SC633	0.94	1.64	0.87	7.75	3.50
SC715	0.99	3.32	0.82	-2.13	3.50

The null hypothesis that there is no difference between observed and simulated yields was accepted at 5 % level of significance for the SC513 and the SC715 cultivars but it was rejected for the SC633 cultivar. This indicates that the observed and simulated yield for the SC633 were significantly different at the level of significance tested. In general, the model works well and it can be used to make future yield predictions though in some cases it overestimates and in others it underestimates the yield.

4.9 Modelling the impact of climate change on yield

The impact of weather conditions on maize yield was simulated with AquaCrop.

4.9.1 Historical and expected future yields with current planting dates maintained

Figures 4.20 (a) to 4.20(e) show how the yields are expected to change.

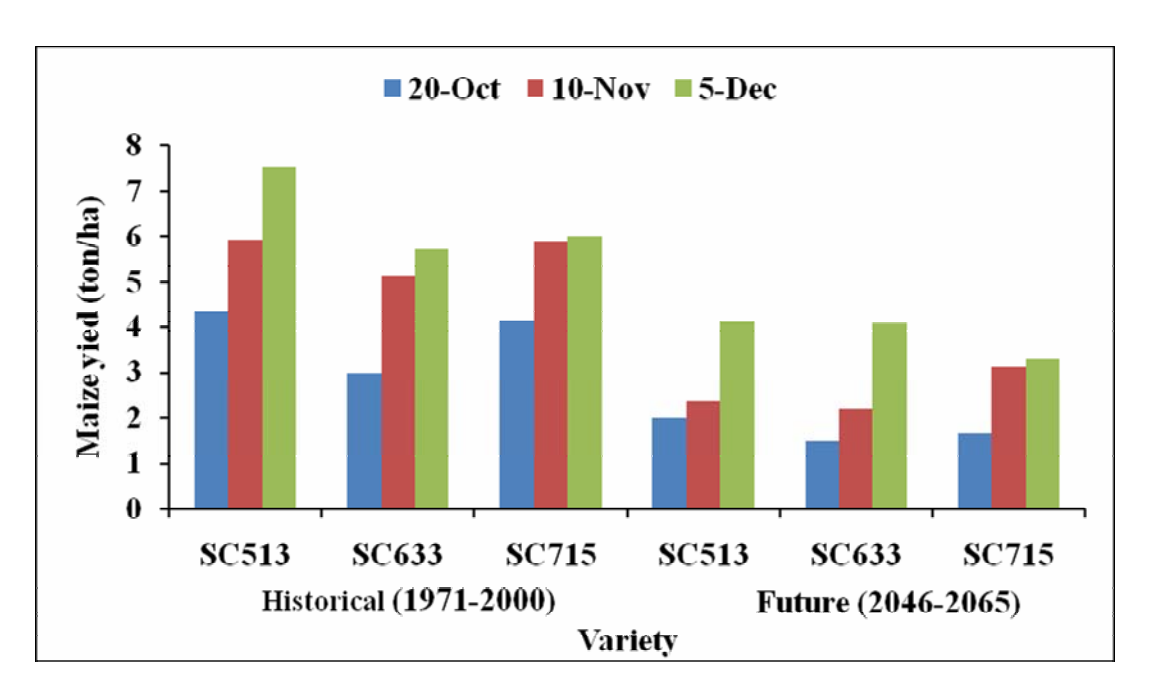


Figure 4.20(a) Changes in yields at Mt Darwin when current planting dates are used

At Mt Darwin, both historical and the expected future yields were found to increase with delayed planting for all cultivars as shown in Figure 4.20(a). When the current planting dates are maintained in the period 2046-2065, Figure 4.20(a) shows that for each cultivar, future yields will be lower than corresponding historical yields. In both regimes, the SC513 cultivar yields more than the SC715 when the two cultivars are planted on 5 December (late planting).

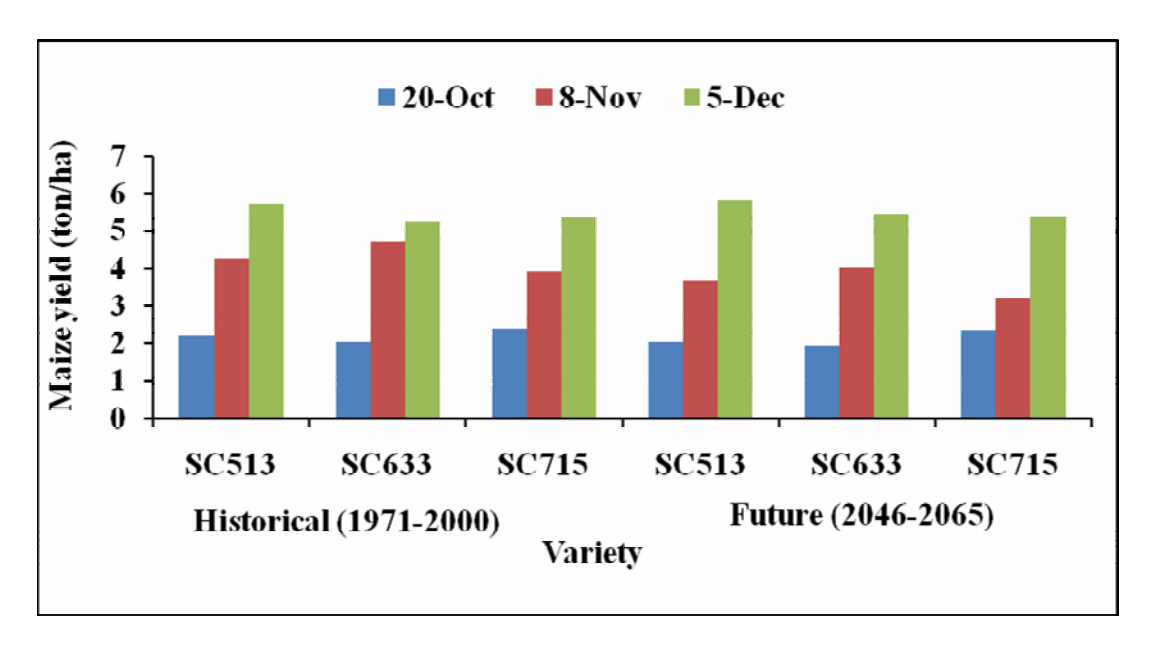


Figure 4.20(b) Changes in yields at Karoi when current planting dates are used

There is not much difference between historical and predicted future yields at Karoi as shown in Figure 4.20(b). However, planting on 5 December (late planting) results in higher yields in future as compared to corresponding historical yields.

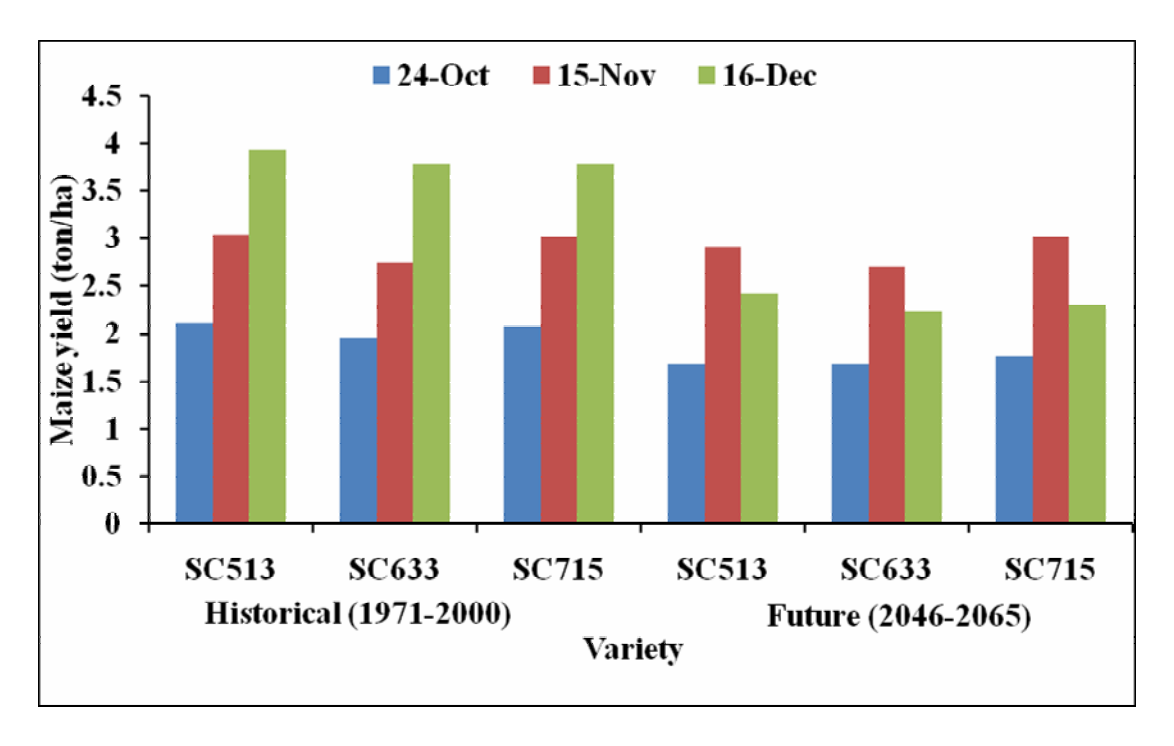


Figure 4.20(c) Changes in yields at Mutoko when current planting dates are used

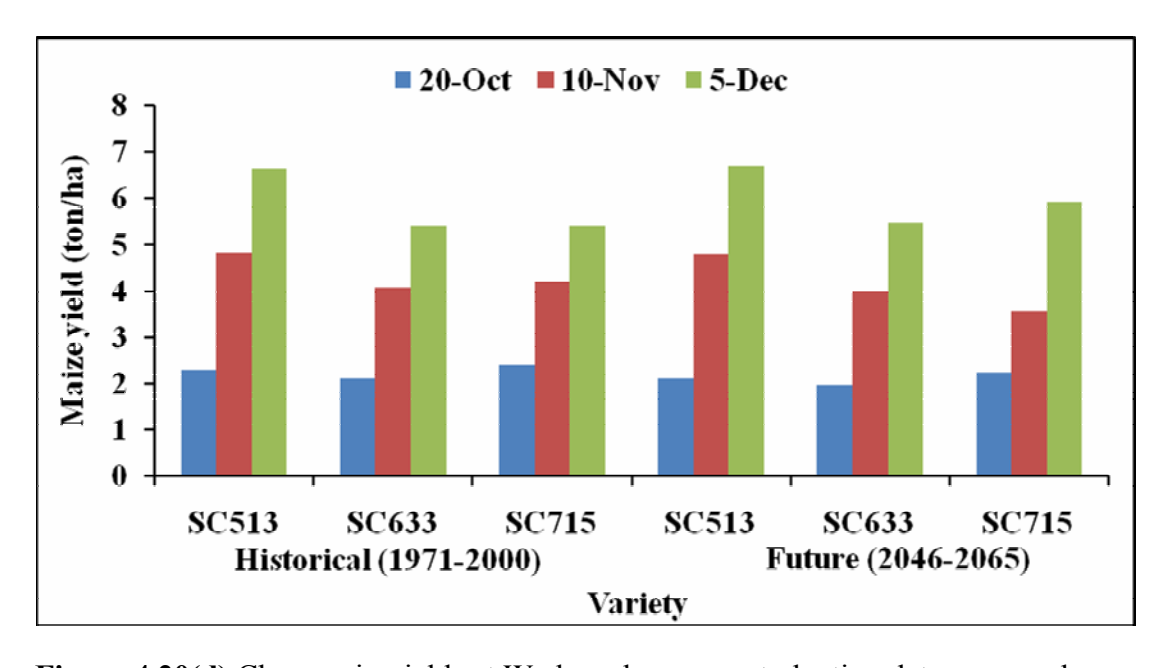


Figure 4.20(d) Changes in yields at Wedza when current planting dates are used

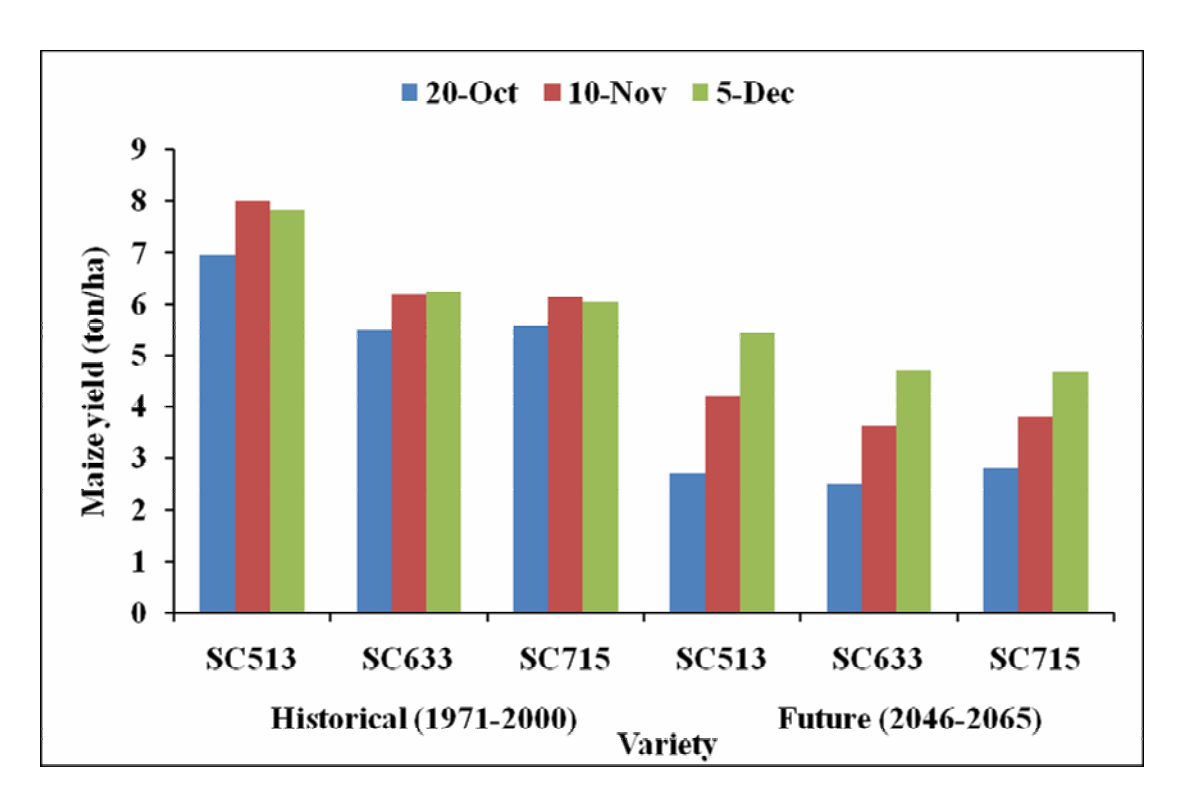


Figure 4.20(e) Changes in yields at Rusape when current planting dates are used

Simulations by the AquaCrop model show that if the current planting dates are maintained in the period 2046-2065, maize yields will decrease at most of the stations. At Karoi (Figure 4.20(b)) and Wedza (Figure 4.20(d)), an increase in yield under these conditions was observed when planting is done on 5 December (late planting). At all stations, both historical and future yields were shown to increase with delayed planting. At most of the stations, delayed planting will result in higher yields for short season varieties and lower yields for medium and long season ones. The AquaCrop model was used to generate new planting dates based on the projected conditions for the period 2046-2065. These projections show that climate change will shift planting dates from 20 October (the current practice) to as late as 17 January by 2046-2065.

4.9.2 Expected future yields with generated planting dates

Figures 4.21(a) to 4.21(e) show how the yields are expected to change when generated planting dates are used.

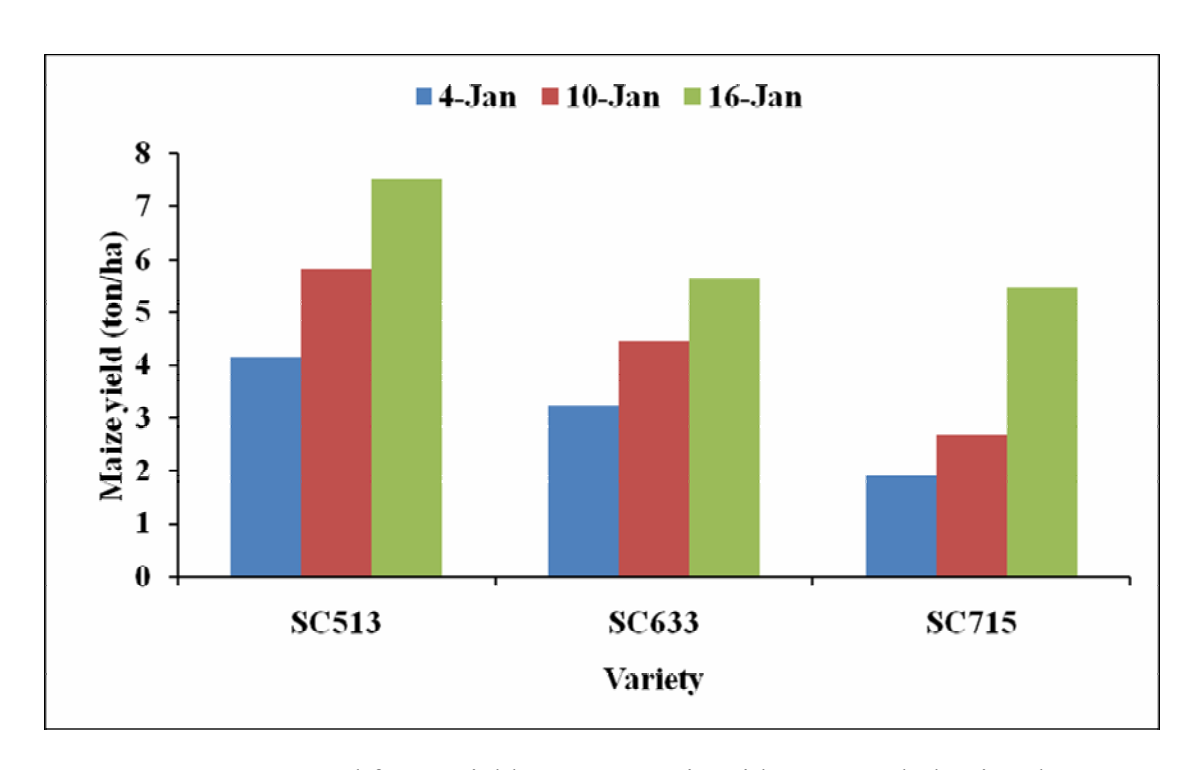


Figure 4.21(a) Expected future yields at Mt Darwin with generated planting dates

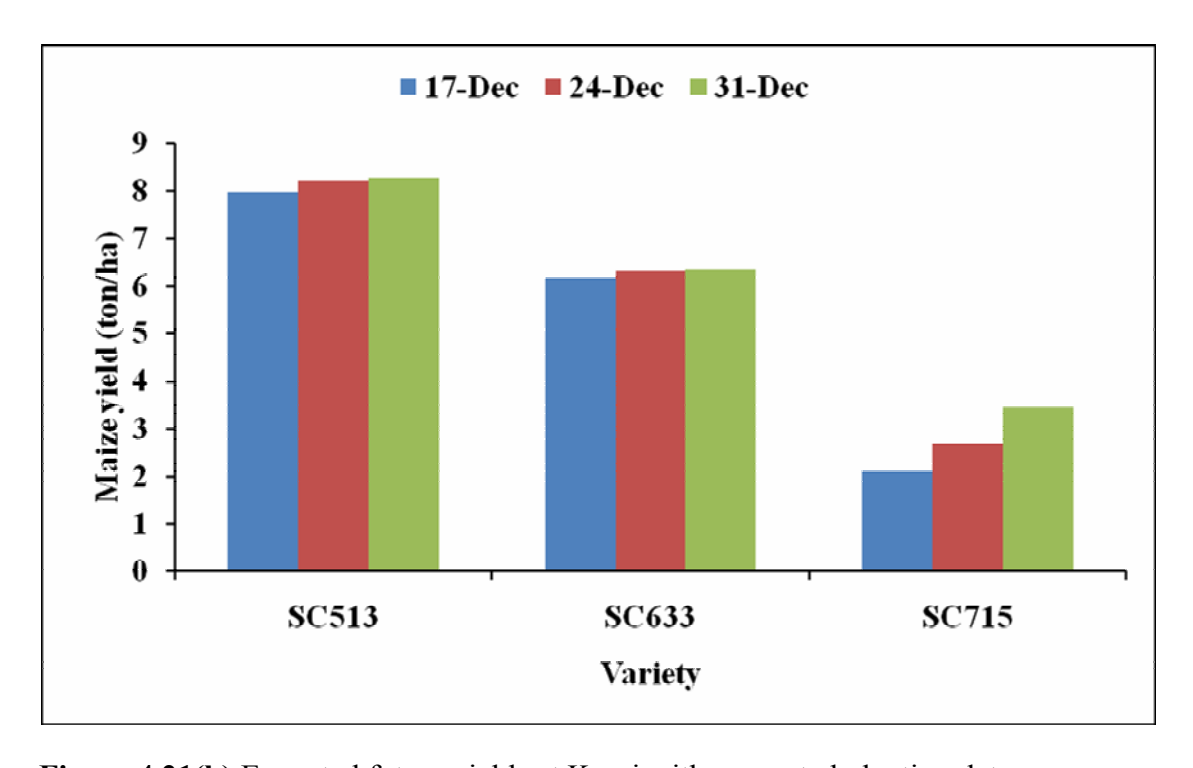


Figure 4.21(b) Expected future yields at Karoi with generated planting dates

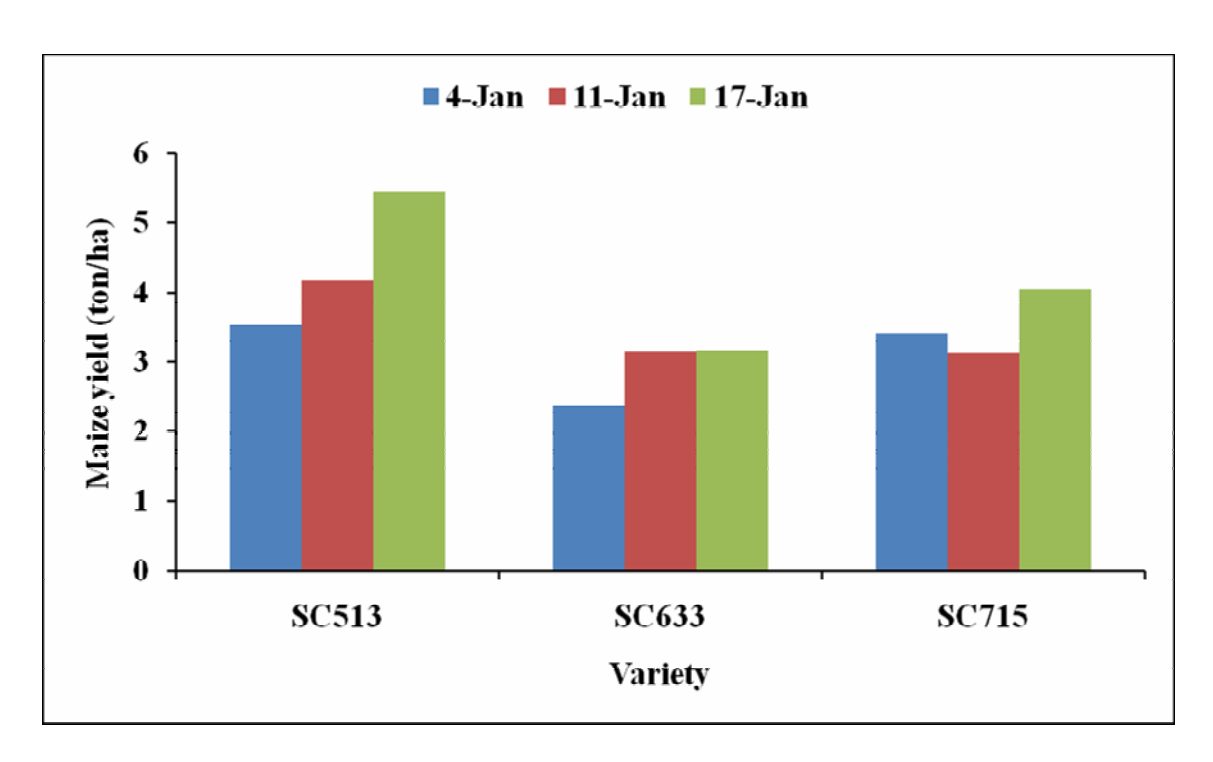


Figure 4.21(c) Expected future yields at Mutoko with generated planting dates

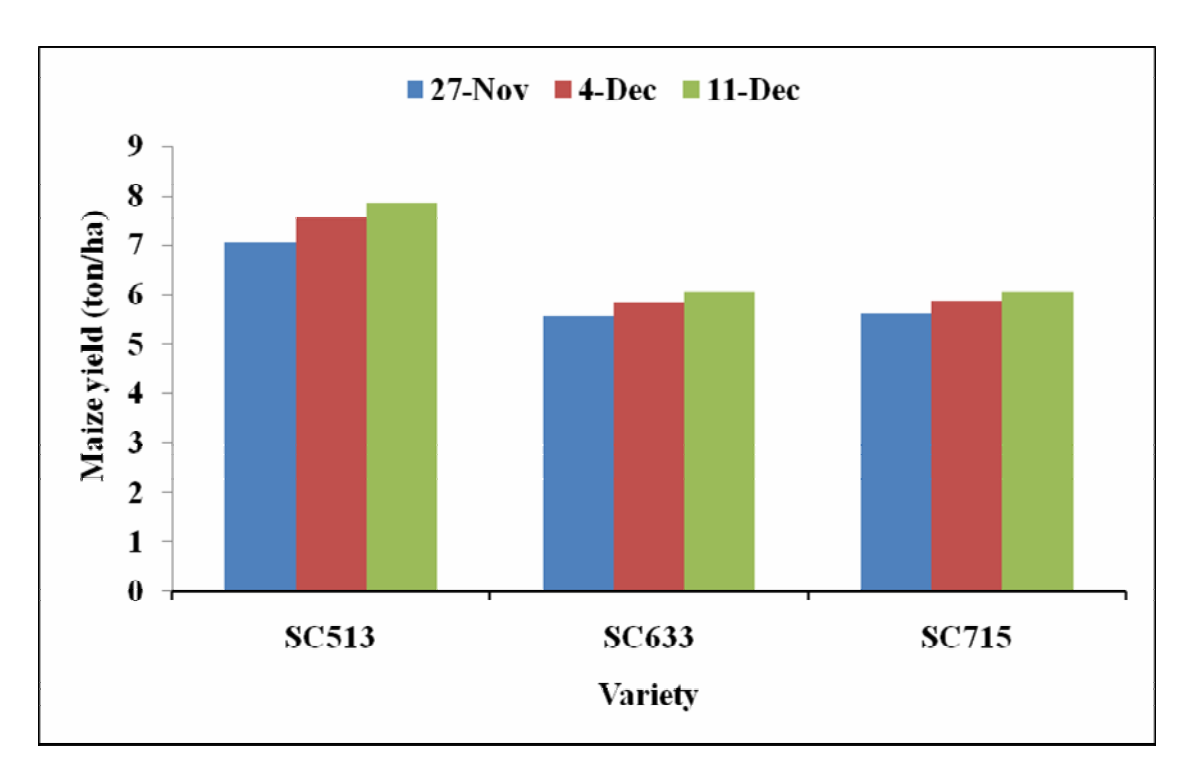


Figure 4.21(d) Expected future yields at Wedza with generated planting dates

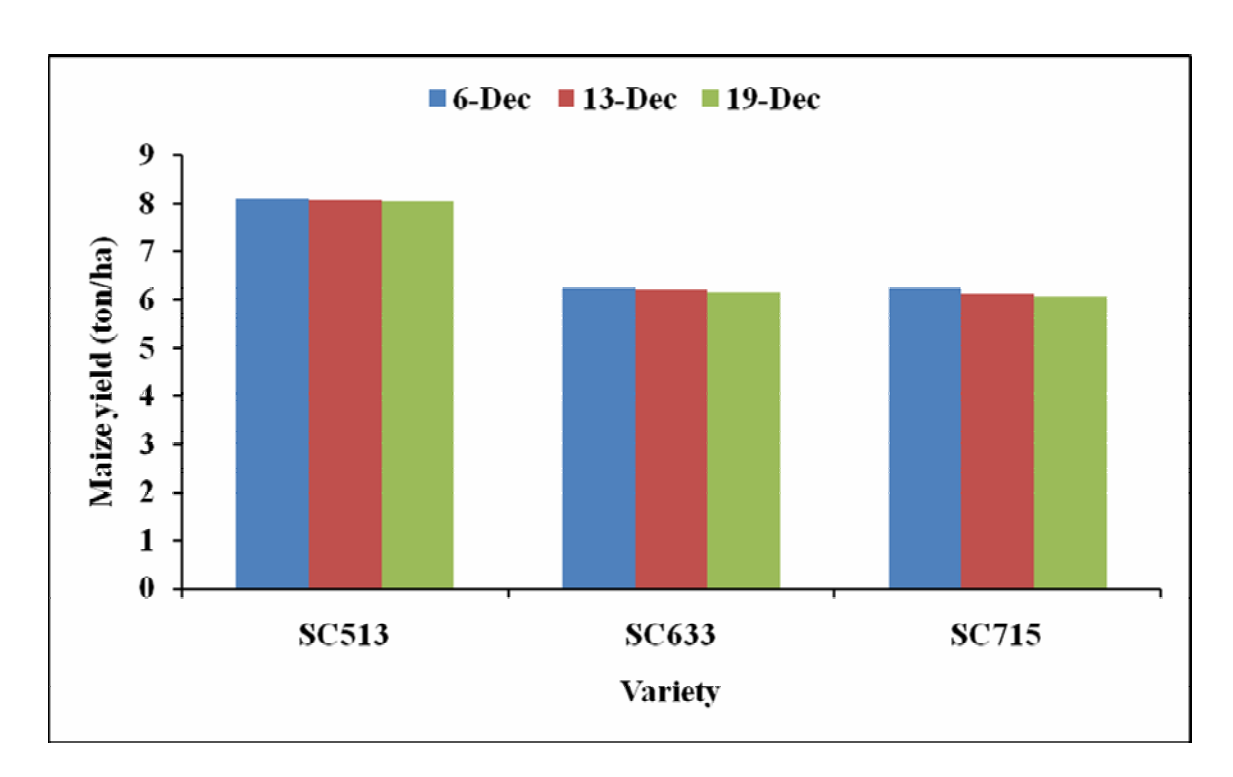


Figure 4.21(e) Expected future yields at Rusape with generated planting dates

AquaCrop predicts increased yields with generated planting dates at all stations. In the 2046-2065 regime, the generated planting dates show that maize yield will increase with delayed planting and that short season varieties will yield more than medium and long season ones under these conditions.

Model rainfall projections for the period 2046-2065 show that at most stations the months of October to December will be drier than normal but the period January to May will be wetter than normal. The earliest and latest planting dates for this period are respectively 27 November at Wedza and 17 January at Mutoko. This explains the observed increase in yield with delayed planting.

The period 2046-2065 is characterised by increased rainfall between January and May. Projected temperatures according to the CCCMA model are still within the suitable range for maize. Many global climate models predict that if there is continued burning of fossil fuels, there will be a further increase in carbon dioxide (CO₂) concentration by 2046-2065 and so the CO₂ fertilization effect will enhance maize growth. This explains why projected future yields are expected to be higher than historical.

The SC513 cultivar (137 days) is a short season variety that will perform well (when late planted) under increased well distributed rainfall and optimal temperatures. The SC715 (152 days) is a long season variety which will not be able to reach maturity under the expected reduced length of growing period. The cultivar will also be under threat from the approaching winter season where temperatures may not be favourable for maize. This may explain why simulation results show that the expected yields in the period 2046-2065 are greatest for the SC513 variety and smallest for the SC715 variety.

Results of the simulations are consistent with findings by Makadho (1996). In his studies at Karoi, Makadho (1996) used the CCCMA and the GFDL climate models and the CERES-Maize model to assess the potential impact of climate change on maize production in Zimbabwe. Makadho (1996) found out that with the current climate, planting on 15 October at Karoi results in 3.7 ton/ ha. If the planting date in maintained, future yield decreases to 2.6 to/ha (CCCMA scenario) and 2.9 ton/ha (GFDL scenario). With climate change and delaying planting to 1 November, the yields increased to 4.6 ton/ha under both climate scenarios (Downing et al., 1996)

It should however be noted that increased yields are realized assuming that the necessary inputs such as fertilizers and seeds are available and that soil conditions do not change. It should also be assumed that by the period 2046-2065, maize remains marketable over other crops so that it will still be widely grown and that the land tenure in Zimbabwe still allows farmers to utilize it.

CHAPTER 5

CONCLUSIONS AND RECOMMENDATIONS

5.1 Introduction

The main objective of the study was to investigate the potential impact of climate variability and change on maize yield in Northeastern Zimbabwe focussing on Natural Region 2. Conclusions and recommendations are presented in this chapter.

5.2 Summary and conclusions

5.2.1 Time series analysis

Time series analysis of rainfall and temperature for the period 1971-2000 was done. It can be concluded from time series plots of temperature that some areas in Zimbabwe have experienced a warming in the 1971-2000 period. Time series plots of rainfall indicate a downward trend in the total annual rainfall at some stations while at other stations, there are no significant changes. An upward trend was observed only at Mutoko. At all stations however, rainfall has been highly variable in the 1971-2000 period.

5.2.2 Evaluation of global climate models and the use of CCE tool

Five global climate models were evaluated and ranked. The CCCMA_CGCM3_1 model obtained the highest ranking for simulating mean minimum and maximum temperatures at all stations. It can be concluded that this model can be applied to simulate future temperature scenarios for Zimbabwe. The research involved comparison of the past and expected future climate at five stations in Natural Region 2. The Climate Change Explorer (CCE) tool was used for climate navigation. For purposes of planning and risk management, knowledge of the future climatic conditions is vital as it helps to reduce the human and economic devastation caused by

extreme weather conditions. The Climate Change Explorer tool was found to be a useful software package in climate science studies in Natural Region 2 of Zimbabwe.

In the case of temperature, it was found that a warming of between 1 and 2 °C is expected in Northeastern Zimbabwe by 2046-2065. The tool also demonstrated inaccuracy of global climate models to predict precipitation. This is in agreement with findings by Collins et al. (2006), Hansen et al. (2007), Dai (2006) and Delworth et al. (2006). It can therefore be concluded that the Climate Change Explorer can be applied in studying climates of other Natural Regions in Zimbabwe.

5.2.3 Validation and use of the AquaCrop model

The AquaCrop model was validated and used to predict expected future maize yields. The goodness of fit tested for AquaCrop for simulating maize yields in the validation process shows that the model is a usable tool. The following are the ranges of the statistical parameters used to assess its performance: R² (0.8-0.99), RMSE (1.6-3.3 ton/ha) and slope (0.8-1.3). It can be concluded that AquaCrop is reliable and it can be used as a maize yield forecasting tool. AquaCrop demonstrated that if the present planting dates are maintained in the period 2046-2065, maize yields will decrease but delayed planting in the same period will result in increased yield. Similar studies were carried out at Karoi by Makadho (1996) who obtained the same trend but using a different crop-growth model, the CERES-maize model. This shows that the newly developed AquaCrop model is a competent model that can be used with confidence for maize yield forecasting in Zimbabwe. AquaCrop however has got some associated shortcomings. The model overestimated yields in some instances while in other cases it underestimated the yield. The model simulated maize yields as high as 3 ton/ha in rural areas, a situation highly unlikely under the current farming practices.

5.3 Adaptation strategies

Predictions of downscaled model simulations indicate that the 2046-2065 period will be warmer than the past in Northeastern Zimbabwe. These simulations also indicate that in the case of rainfall, climate will create times of both excess and deficit rainfall. Maize growers in

Northeastern Zimbabwe need to focus more on the adverse impacts that are associated with higher temperatures.

In the case of rainfall, the distribution is highly unpredictable so there is need for expansion of irrigation as a source of supplementary water for agriculture in the country. However, the projected temperature rise may increase evapotranspiration leading to rapid depletion of the available water from reservoirs and from the soil. Farmers are advised to seek advice from climatologists and agrometeorologists on the onset and cessation of the rains together with seasonal dry spells so that they can manage the negative impacts.

Predictions of downscaled model simulations also indicate that there will be increased rainfall for the months January to May in the 2046-2065 regime and AquaCrop predicted increased yields during the period 2046-2065. Crop production is however influenced by various factors, some of which are uncertain in future. The future geographic distribution of vectors and pests for example is unknown and these can be a menace to crops. Farmers therefore need to consider such factors. Downscaled model simulations predict that climate change will shift planting dates towards delayed planting in the period 2046-2065. Generated planting dates are spread over the months of November to January. As an adaptation strategy, maize growers in Zimbabwe are advised to observe proper timing of planting dates and stagger their planting over say three months. Farmers can do their first planting in November, second in December and then lastly in January. In the same period, AquaCrop demonstrated that expected yields then will be highest for the SC513 cultivar as compared to the SC633 and SC715 cultivars. Farmers can therefore adapt by growing short season varieties in order to maximize production. A 90- to 100- day maize would be most suited to the new climate regime.

Research institutes such as the Centro Internacional de Mejoramiento de Maiz y Trigo (CIMMYT) are encouraged to embark on breeding programs that anticipate warming environments. The projected conditions call for heat tolerant varieties. Breeding and biotechnology coupled with improved agronomy will help moderate the impacts of climate change in Zimbabwe.

At present, science-based technology for adaptation is still inadequate in rural areas. The challenge that agrometeorological advisories may face is resistance by farmers. It is not known

whether farmers will accept to embrace new knowledge and information or they will stick to tradition.

For farmers who are ignorant of the phenomenon of climate change, it might be very difficult to convince them. If this ignorance persists, it might take time for communities to accept the reality of climate change and adopt appropriate measures to mitigate its devastating impacts.

5.4 Recommendations for further studies

It is recommended for further research that a longer time period (say 60 - 100 years) be considered in similar studies so that the present state of Zimbabwe's climate is clear. The use of only five global climate models in this study was due to limited time. More than five models are required to provide broader coverage of the uncertainties in greenhouse gas emissions. The six stations considered in this study did not fully represent the study area. It is recommended for further research that more stations be considered. More statistical approaches are required to assess how well global climate models simulate real observations. Inaccuracy of climate models to predict precipitation needs further investigation.

REFERENCES

- Arntzen, J., Downing, T., Leemans, R., Malcolm, J., Reynard, N., Ringrose, S. and Rogers, D. 1996: Climate change and Southern Africa: An exploration of some potential impacts and implications in the SADC region. Climatic research unit. Norwich. UK, pp 45-46.
- Ausubel, J. and Biswas, A.K. 1980: Climate constraints and human activities. Pergamon Press, New York, pp 59-61.
- Barry, D.C. 1997: Southern Africa beyond the millennium: Environmental trends and scenarios to 2015. Environmental Planning Issues No. 13. (Accessed 13/10/2009) (http://www.oneworld.org/iied).
- Batchelor, W.D.1999: Crop growth models and yield variability. (Accessed 24/10/2009) (http://www.ipm.iastate.edu/ipm/icm/indices/announcements.html).
- Boote, J.K., Jones, W.J., Nigel, B. Pickering, N.B. 1995: Potential Uses and Limitations of Crop Models. Journal Series no. R-05079. Florida.
- Buishand, T.A. 1982: Some methods for testing the homogeneity of rainfall records. In *RAINBOW software package for hydrometeorological frequency analysis and testing the homogeneity of historical data sets.* Raes, D., Willems, P. and GBaguidi, F. Islamabad, Pakistan.
- Burroughs, W. J. 2001: Climate change. A multidisciplinary approach. Cambridge University Press. United Kingdom.
- CARA, 2006: Global emissions scenarios. (Accessed 27/09/2009) (www.cara.psu.edu).
- Cavero, J., Farre, I., Debaeke, P. and Faci, J.M. 2000: Simulation of maize yield under water stress with the EPIC phase and CROPWAT models. In *Validating the FAO AquaCrop Model for Irrigated and Water Deficient Field Maize*. Heng, L.K, Hsiao, T., Evett, S, Howell, T. and Steduto, P. Agronomy Journal **101**:488-498. American Society of Agronomy, Madison. USA.
- Clayton, B.D. 1997: Southern Africa Beyond the Millennium: Environmental Trends and Scenarios to 2015. Environmental Planning Issues Number 13. (Accessed 13/09/2009) (www.oneworld.org/iied).
- Climate Handbook of Zimbabwe. 1981: Zimbabwe Meteorological Services Department, Salisbury. 11pp.
- Collins, W., Roel, T., Nigan, H. 2006: The Community Climate System Model version 3 (CCSM3). J. Climate. **19:** 2122-2143.

- Costa, L. C., Justino, F., Oliveira, L. J. C., Sediyama, G. C., Ferreira, W.P.M. and Lemos, C. F. 2009: Potential forcing of CO2, technology and climate changes in maize (Zea mays) and bean (Phaseolus vulgaris) yield in southeast Brazil. Environ. Res. Lett. **4.** 10pp. IOP Publishing Ltd UK. (Accessed 10/10 2009). (http://www.iop.org).
- CSO, 1989: Zimbabwe in maps. A Census Atlas. Central statistical office. Harare. Zimbabwe.
- CSO, 2004: Census 2002. National report. Central statistical office. Harare. Zimbabwe.
- Dai, A. 2006: Precipitation characteristics in eighteen coupled climate models. J. Climate 19: 4605-4611 (Accessed 3/04/2010) (http://www.cgd.ucr.edu/cas/adai/papers/Dai-cmeppaper.pdf).
- Decker, W.L., Jones, V.K. and Achutuni, R. 1985: The impact of CO2 induced climate change on US agriculture. In *Characterization of Information Requirements for Studies of CO2 Effects: Water Resources Agriculture Fisheries Forests and Human Health.* White, M.R. US Dept. of Energy, DOE/ER-0236, Washington, D.C.
- Delworth, D., Boyle, C., Li, R. 2006: GFDL's CM2 global coupled climate models. Part 1: Formulation and simulation characteristics. J. Climate **19:** 643-674.
- Doorenbos, J. and Kassam, A.H. 1979: Yield response to water. Irrigation and Drainage Paper no. 33. In *AquaCrop-The FAO crop model for predicting yield response to water: II. Main algorithms and software description.* Raes, D., Steduto, P., Hsiao, T. C. and Fereres, E. 2009. Ag. Journal (in press).
- Easterling, W. E., Weiss, A. Hays, C. J. and Mearn, L. O. 1998: Response of maize to climate change in north east China *Agric. Forest Meteorol.* **90:** 51–63.
- Easterling, W. E., Hays, C. J., Mearn, L. O. and Marx, D. 2001: Clim Change. 51: 173–197.
- FAO, 1999: Fertilizer use by crop in Zimbabwe. (Accessed 17/09/2009) (www.fao.org)
- FAO, 2009: Software: AquaCrop.(Accessed 17/10/2009) (http://www.fao.org/nr/water/index.html).
- FAQ, 2008: Impact of Climate Change on Crop Production. (Accessed 20/10/2009) (http://www.articlesbase.com/environment-articles/impact-of-climate-change-on-crop-production-199651.html).
- France, J. and Thorney, J.H.M. 1984: Mathematical models in Agriculture. Butterworth and Company publishers (Limited). England.
- Goldsworthy, P.R. and Fisher, N.M. 1984: The physiology of tropical field crops. Pitman press LTD, Bath, Avon.

- Grant, 1967a, 1967b, 1970; Nyamapfene, 1981: Fertilizer use by crop in Zimbabwe (Accessed 16/09/2009) (www.fao.org).
- Gullett & Skinner, 1992: SOE Report No. 92-2, Environment Canada (Accessed 25/09/2009) (www.ec.gc.ca).
- Hansen, F., Arkin, J., Kitoh, H. 2007: Climate simulations for 1880-2003 with GISS Model E. Climate dynamics **29**: 661-696.
- Hejnak, V. 2009: The Response of Maize to Water Stress: The Effect of Abscisic Acid and Benzylaminopurine. Department of Botany and Plant Physiology, Czech Republic. (Accessed 25/10/2009) (http://www.acs.confex.com).
- Hoogenboom, G. 2000: Contribution of agrometeorology to the simulation of crop production and its applications. *Agric. For. Meteorol.* **103**:137–157. (Accessed 13/10/2009) (http://www.aiaccproject.org/working_papers/Working%20Papers/AIACC_WP28_Trava sso.pdf).
- Houghton, J. 1999: Global warming: The complete briefing. Cambridge University Press, United Kingdom, pp 22-23.
- Houghton, J.T., Jenkins, G.J. and Ephraums, J.J. 1990: Climate Change: The IPCC Scientific Assessment. World Meteorological Organization and United Nations Environmental Program. Cambridge University Press. 365 pp.
- Hosier, R. 1985: Energy use in Kenya; Household Demand and rural transformation. Stockholm, Beijer Institute. 140 pp.
- Ikisan, 2000: Climate suitable for maize. (Accessed 23/09/2009) (http://www.ikisan.com).
- IPCC, 2007: Climate change 2007: Impacts, Adaptation and Vulnerability. (Accessed 07/10/2009) (http://www.epa.gov/climatechange/effects/agriculture.html).
- IPCC, 2007: Climate Change 2007: The Physical Science Basis. Contribution of Working Group I to the Fourth Assessment Report of the Intergovernmental Panel on Climate Change [Solomon, S., Qin, D., Manning, M., Chen, Z., Marquis, M., Averyt, K.B., Tignor, M and Miller, H.L. (eds.)]. Cambridge University Press, Cambridge, United Kingdom and New York, NY, USA.
- IPCC, 2009: Special Report on Emissions Scenarios (Accessed 03/10/2009) (http://en.wikipedia.org/wiki/Special_Report_on_Emmissions_Scenario#column-one).
- Jame, Y. W. Cutforth, H. W. 1996: Crop growth models for decision support systems. Canadian Journal of Plant Science **76**: 9–19. (Accessed 22/09/2009) (http://www.aiaccproject.org/working_papers/Working%20Papers/AIACC_WP28_Trava sso.pdf).

- John, M., Bardzik, H. V., Marsh, Jr. and Havis, J. R. 1970: Plant Physiology. Vol. 47, No. 6, American society of plant biologists. pp. 828-831 (Accessed 06/11/2009) (http://www.jstor.org/stable/4262463).
- Jones, C.A., and Kiniry, J.R. 1986: CERES-Maize: A simulation model of maize growth and development. In *Validating the FAO AquaCrop Model for Irrigated and Water Deficient Field Maize*. Heng, L.K, Hsiao, T., Evett, S, Howell, T. and Steduto, P. Agronomy Journal **101**:488-498 American Society of Agronomy, Madison. USA.
- Kinball, B. A., Pinter, P. J., Garcia, R. L., Mort, R. L. L., Wall, G. W., Hunsaker, D. J., Wechsung, G., Wechsung, F. and Kartschall, T. 1995: *Glob. Change Biol.* 1: 429-42.
- Lal, R. 1979: Modification of soil fertility characteristics by management of soil physical properties. In *The ecology of tropical food crops*. Norman, M.J.T., Pearson, C. J. and Searle, P. G. E., Cambridge university press, London.
- Lobell, D. and Asner, G. 2003: Science. In *Potential forcing of CO2, technology and climate changes in maize (Zea mays) and bean (Phaseolus vulgaris) yield in southeast Brazil*. Costa, L. C., Justino, F., Oliveira, L. J. C., Sediyama, G. C., Ferreira, W.P.M. and Lemos, C. F. Environ. Res. Lett. **4.** 10pp.
- Lobell, D. B., Burke, M. B., Tebaldi, C., Mastrandrea, M. D., Falcon, W. P. and Naylor, R. L. 2008: Science. In *Potential forcing of CO2, technology and climate changes in maize (Zea mays) and bean (Phaseolus vulgaris) yield in southeast Brazil.* Costa, L. C., Justino, F., Oliveira, L. J. C., Sediyama, G. C., Ferreira, W.P.M. and Lemos, C. F. Environ. Res. Lett. **4.** 10pp.
- Long, S.P., Ainsworth, E.A., Leaky, A.D.B. and Morgan, P.B. 2005: Global Insecurity. Treatment of major crops with elevated carbon dioxide or ozone under large-scale fully open air conditions suggest recent models may have overestimated future yields. *Philosophical Transactions of the Royal Society* **360**: 2011-2020.
- Loomis, R. S. and Williams, W. A. 1963: Maximum crop productivity: An estimate, Crop science volume 3, pp. 67-72. Washington, D.C.
- Luo, Q., Bellottib, W., Williamsa, M. and Bryan, B. 2005: Predictions in models for studying ecological and agronomic systems. *Agric. Forest. Meteorol.* **132:** 273-85.
- Makadho, J.M. 1996: Potential effects of climate change on corn production in Zimbabwe. Clim Res **6**: 147-151, Department of Agricultural, Technical and Extension Services (AGRITEX), Harare, Zimbabwe.
- Matarira, C.H., Makadho, J. M., Mukahanana-Sangware, M. 2004: Vulnerability and adaptation of maize production to climate change in Zimbabwe. Government of the Republic of Zimbabwe, Ministry of Environment and Tourism, Harare, Zimbabwe.

- Muchow, R.C., Sinclair, T.R. and Bennett, J.M. 1990: Temperature and solar radiation effects on potential maize yield across locations. In *Validating the FAO AquaCrop Model for Irrigated and Water Deficient Field Maize*. Heng, L.K, Hsiao, T., Evett, S, Howell, T. and Steduto, P. Agronomy Journal **101**:488-498 American Society of Agronomy, Madison. USA.
- Nash, J.E. and Sutcliffe, J.V. 1970: River flow forecasting through conceptual models. A discussion of principles. J. Hydrol. **10:** 282-290
- Nishiyama, I. 1976: Effects of temperature on the vegetative growth of rice plants. In *The ecology of tropical food crops*. Norman, M.J.T., Pearson, C. J. and Searle, P. G. E., Cambridge university press, London.
- Nurmohamed, R. and Naipal, S. 2006: Development of scenarios for future climate change in Suriname. Journal of Geophysical Research, Vol. 108, no. D16, 4519.
- Parry, 1990: Climate Change and World Agriculture. (Accessed 17/10/09) (http://www.ciesin.columbia.edu/docs/004-036/004-036.html).
- Raes, D., Steduto, P., Hsiao, T.C. and Fereres, E. 2009: AquaCrop-The FAO crop model to simulate yield response to water: II. Main algorithms and soft ware description. In *Validating the FAO AquaCrop Model for Irrigated and Water Deficient Field Maize*. Heng, L.K, Hsiao, T., Evett, S. Howell, T. and Steduto, P. Agronomy Journal 101:488-498 American Society of Agronomy, Madison. USA.
- Raes, D., Willems, P. and GBaguidi, F. 2006: RAINBOW a software package for hydrometeorological frequency analysis and testing the homogeneity of historical data sets. Islamabad, Pakistan.
- Richter, G. M. and Semenov, M. A. 2005: Fertilizers to sustain the production of 100 million tonnes of grain in Argentina (Accessed 25/05/2010) (http://www.INPOFOS.org)
- Ruddiman, W.F. 2003: The anthropogenic era began thousands of years ago. Climate change 61:261-293 (Accessed 13/05/2010). http://en.wikipedia.org/wiki/climate variability
- Rukuni and Eicher, 1994: Fertilizer use by crop in Zimbabwe. (Accessed 16/09/2009)(www.fao.org).
- SeedCo, 2008: SeedCo Agronomy Manual, SeedCo Limited, Harare. (Accessed 14/02/2010) (http://www.seedco.zw). pp 1-8.
- Shaw, R.H.1983: Estimates of yield reductions in corn caused by water and temperature stress. In *Crop reactions to water and temperature stresses in humid temperate climates* Raper, C.D. and Kramer, P.J. Westview Press. pp. 35-48.
- Sithole, A. 2003: Optimal planting dates for rainfed maize (*Zea mays* L) and sorghum (*Sorghum bicolor* L) in agro-ecological zones of Zimbabwe. Unpublished MSc thesis.

- Sithole, A. and Murewi, C.T.F. 2009: Climate variability and change over Southern Africa: Impacts and challenges. Afr. J. Ecol., **47** (Suppl. 1), 17–20.
- Slater, L.E. 1981: Three approaches to reducing climate's impact on food supplies. In *Climate and Food Security*. IRRI, Washington, D.C., USA.
- Steduto, P., Hsiao, T.C., Raes, D. and Fereres, E. 2009: AquaCrop-The FAO crop model to simulate yield response to water: Concepts and underlying principles. In *Validating the FAO AquaCrop Model for Irrigated and Water Deficient Field Maize*. Heng, L.K, Hsiao, T., Evett, S. Howell, T. and Steduto, P. Agronomy Journal **101**:488-498 American Society of Agronomy, Madison. USA.
- Stöckle, C.O., Donatelli, M. and Nelson, R. 2003: CropSyst, a cropping systems simulation model. In *Validating the FAO AquaCrop Model for Irrigated and Water Deficient Field Maize*. Heng, L.K, Hsiao, T., Evett, S, Howell, T. and Steduto, P. Agronomy Journal **101**:488-498 American Society of Agronomy, Madison. USA.
- Travasso, M. I., Magrin, G. O., Baethgen, W. E., Castaño, J. P., Rodriguez, G. R., Pires, J.L., Gimenez, A., Cunha, G. and Fernandes, M. 2006: Adaptation Measures for Maize and Soybean in Southeastern South America. AIACC Working Paper No. 28. AIACC publishing. Washington, DC 20009 USA. (Accessed 16/10/2009) (www.aiaccproject.org).
- Tsiko, S. 2008: Country at Risk of Climate Change Effects. (Accessed 07/09/2009). (http://allafrica.com).
- Unganai, L. 2008: Climate change. Scenarios for the Save catchment of Zimbabwe with special reference to Chiredzi. Environmental management agency. Harare. Zimbabwe, pp 1-10.
- Unganai, L. 2010: Climate change spawns conflict, The Zimbabwe Herald, 11 February 2010, p C2.
- Wales, J. and Snow, M. 2009: Special Report on Emissions Scenarios. (Accessed 16/09/2009) (www.wikipedia.org).
- Wang, J., and Lin, E., 1992: The impacts of climate change and climate variability on simulated maize production in China. In. *modelling the impacts of weather and climate variability on crop productivity over a large area.* Tao, F., Zhang, Z., Liu, J., Yokozawa, M. *Agric For. Meteorol.* **149**:1266-1278.
- Williams, J. R., Jones, C. A., Kiniry, J. R., and Spanel, D.A. 1989: The EPIC crop growth model. Transactions of American Society of Agricultural Engineers **32**: 497-511.
- Woodward, F.I. 1993: Global climate change: The ecological consequences. Academic Press, New York, pp 34-35.
- Xiong, W., Matthews, R. Holman, I., Li, E., Xu, Y., 2007: Modelling China's potential maize production at regional scale under climate change. In. *Modelling the impacts of weather*

- and climate variability on crop productivity over a large area. Tao, F., Zhang, Z., Liu, J., Yokozawa, M. Agric. For. Meteorol. **149**:1266-1278.
- Yang, H.S., Dobermann, A., Lindquist, J.L., Walters, D.T., Arkebauer, T.J. and Cassman, K.G. 2004: Hybrid-maize-a maize simulation model that combines two crop modelling approaches. In *Validating the FAO AquaCrop Model for Irrigated and Water Deficient Field Maize*. Heng, L.K, Hsiao, T., Evett, S., Howell, T. and Steduto, P. Agronomy Journal **101**:488-498 American Society of Agronomy, Madison. USA.
- Zermoglio, 2007: The Climate Change Explorer, An Introduction. (Accessed 14/03/2010) (http://www.wikiadapt.org). pp 1- 42.
- Zhang, X. C. and Liu, W. Z. 2005: Modelling the impact of climate change on maize production over a large area *Agric. Forest Meteorol.* **131:** 127–142.

APPENDICES

APPENDIX A: Regression lines for simulating minimum temperature **Karoi minimum temperatures**

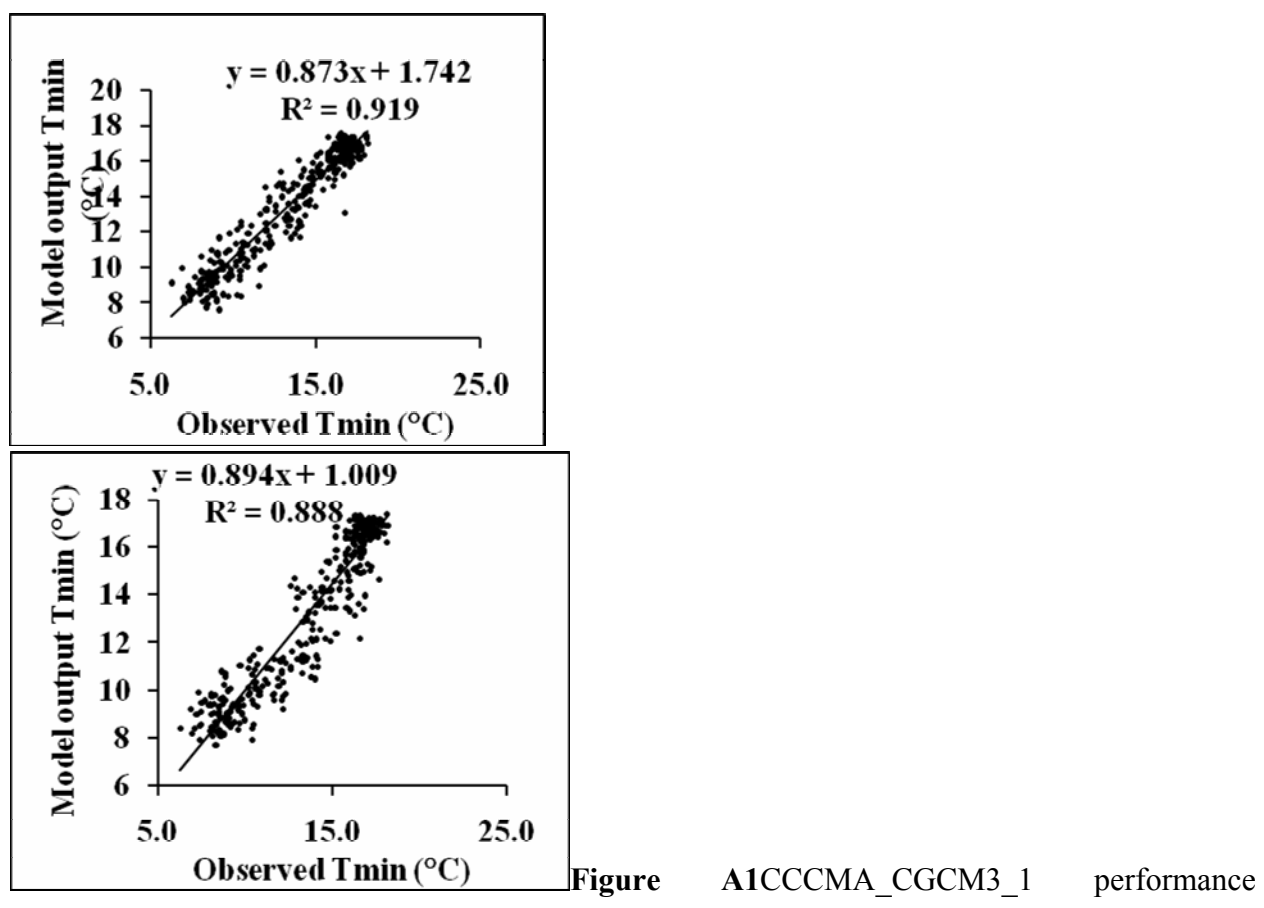


Figure A2 CSIRO_MK3_5 performance

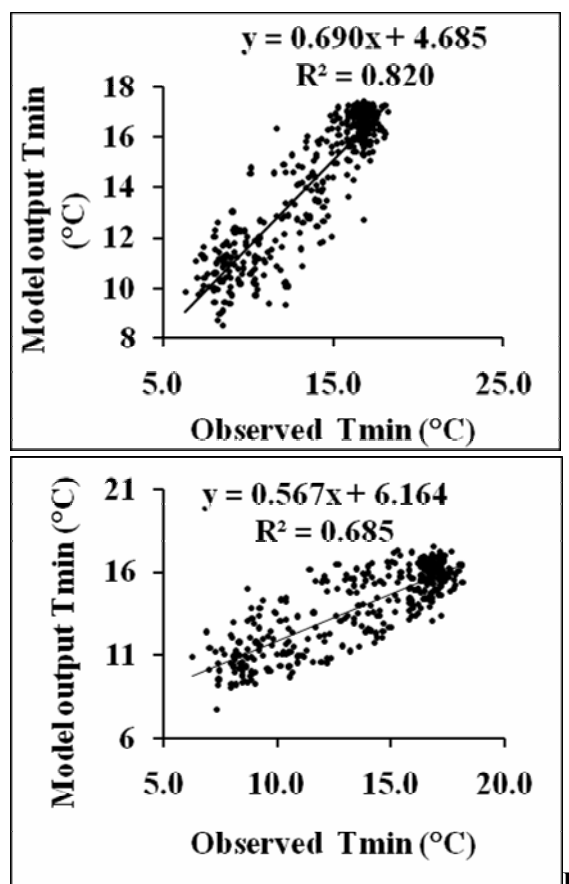


Figure A3 GFDL CM2 0 performance

Figure A4 GISS MODEL E R performance

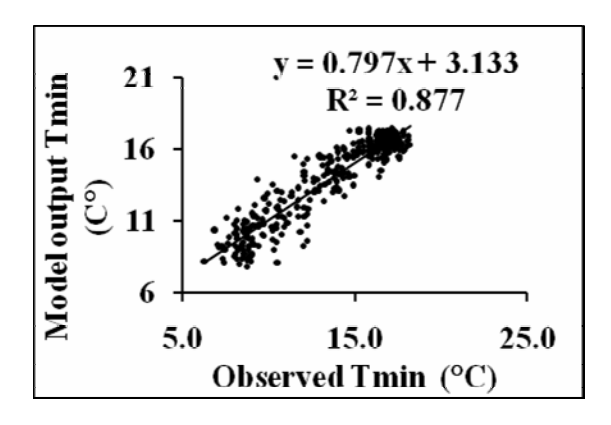


Figure A5 MPI_ECHAM5 performance

Wedza minimum temperatures

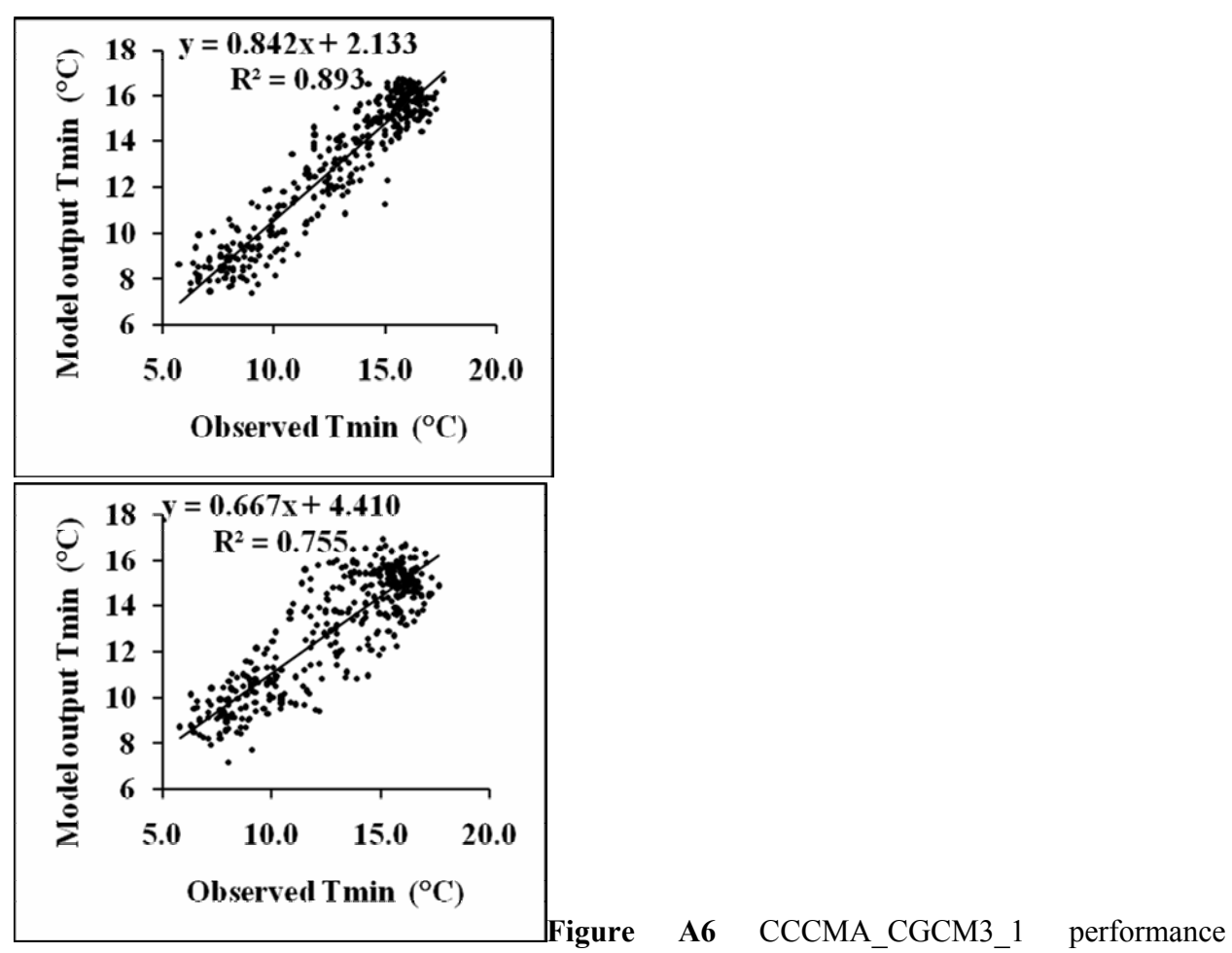
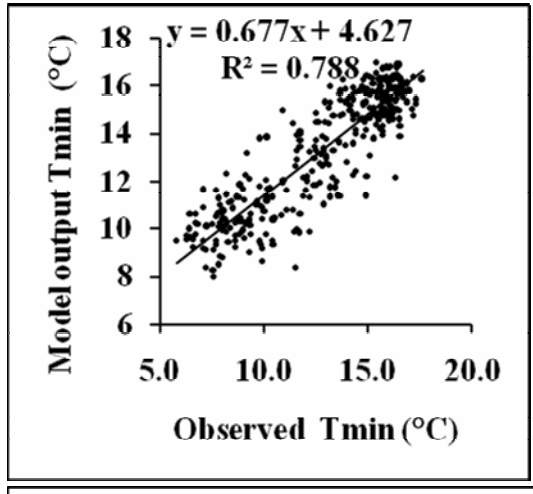


Figure A7 CSIRO_MK3_5 performance



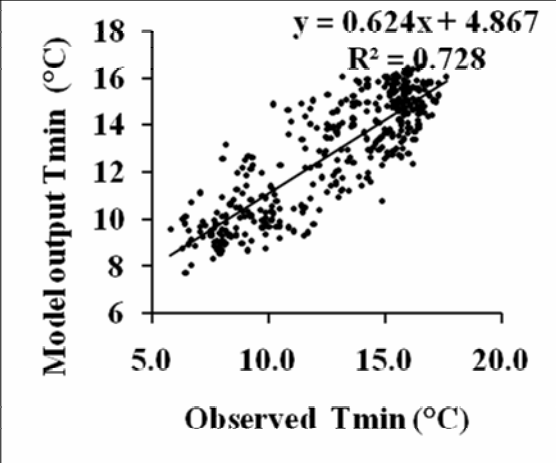


Figure A8 GFDL_CM2_0 performance

Figure

A9 GISS_MODEL_E_R performance

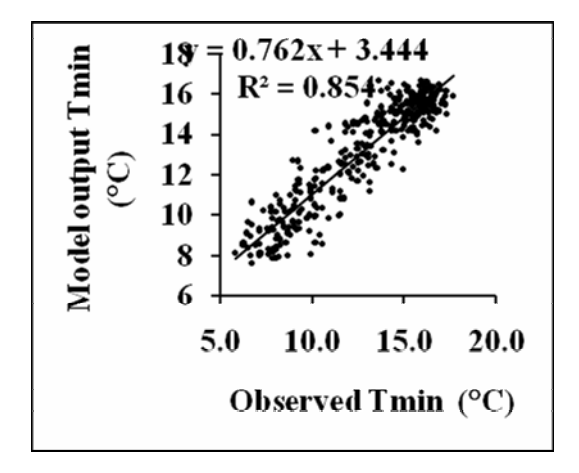


Figure A10 MPI_ECHAM5 performance

Rusape minimum temperatures

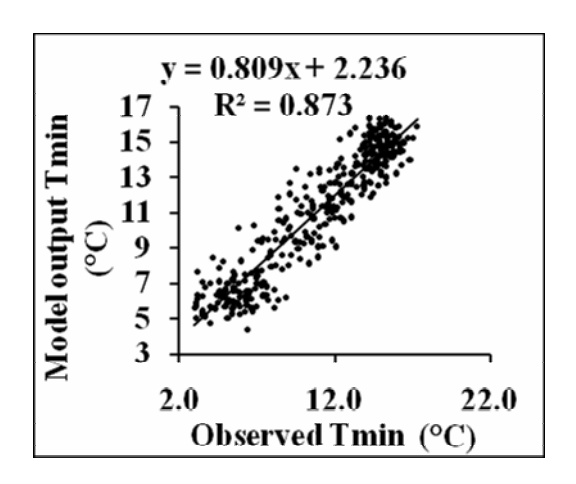


Figure A11 CCCMA_CGCM3_1 performance

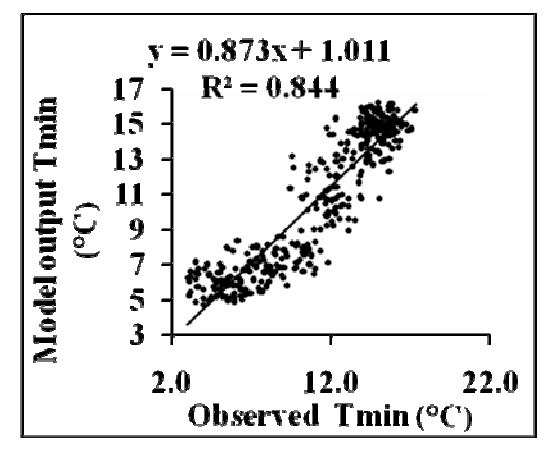


Figure A12 CSIRO MK3 5 performance

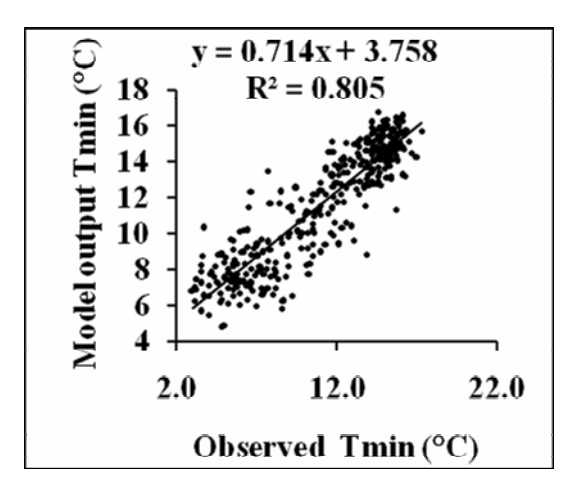
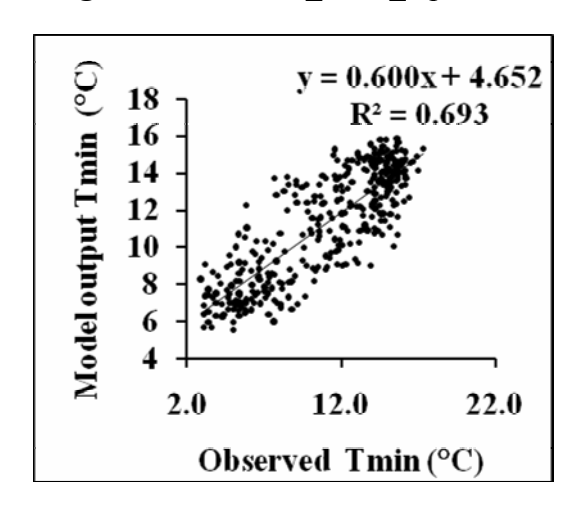


Figure A13 GFDL CM2 0 performance



FigureA14GISS MODEL E R performance

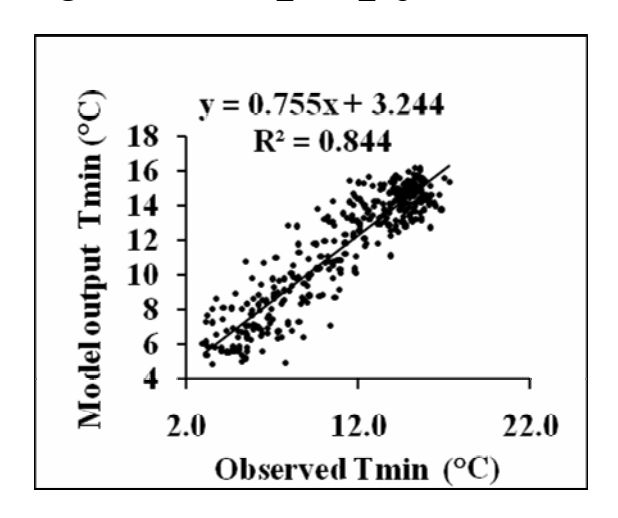


Figure A15 MPI ECHAM5 performance

APPENDIX B: Regression lines for simulating maximum temperature **Mt Darwin maximum temperatures**

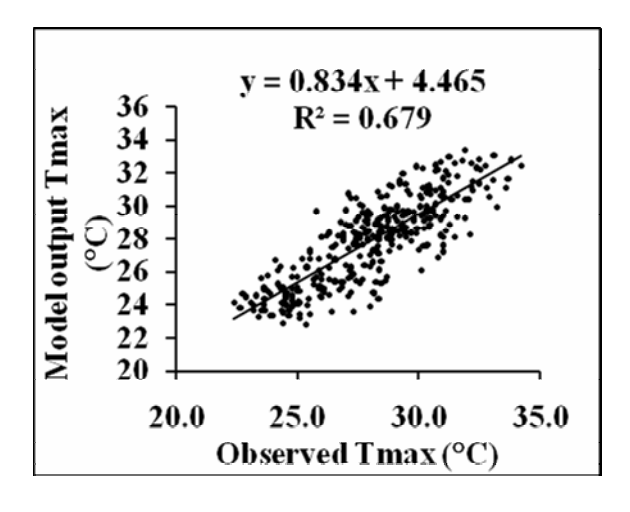


Figure B1 CCCMA_CGCM3_1performance

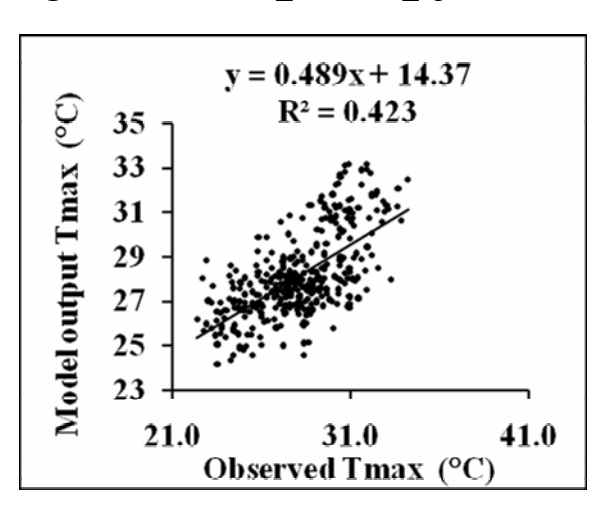


Figure B3 GFDL CM2 0 performance

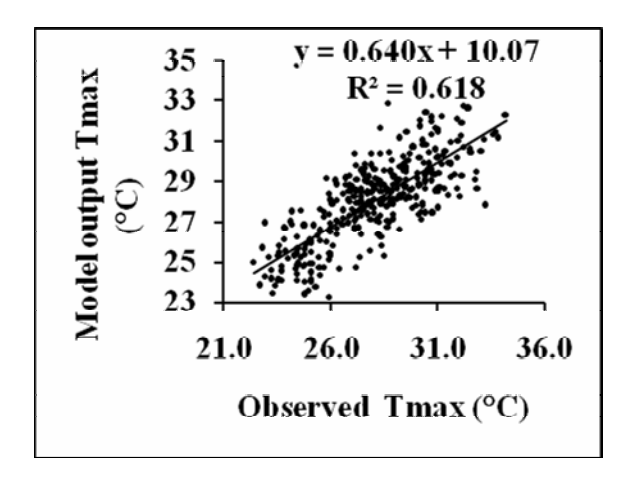


Figure B5 MPI ECHAM5 performance

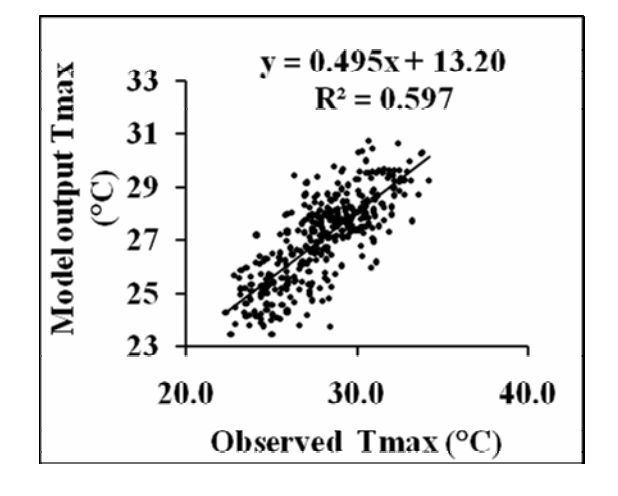


Figure B2 CSIRO MK3 5 performance

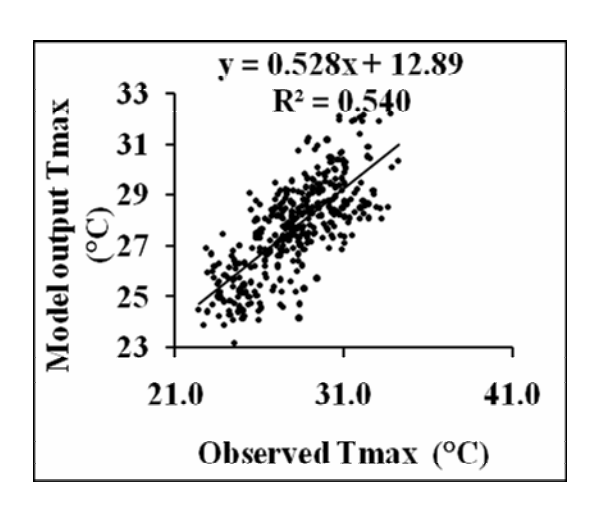


Figure B4 GISS MODEL E R performance

Karoi maximum temperatures

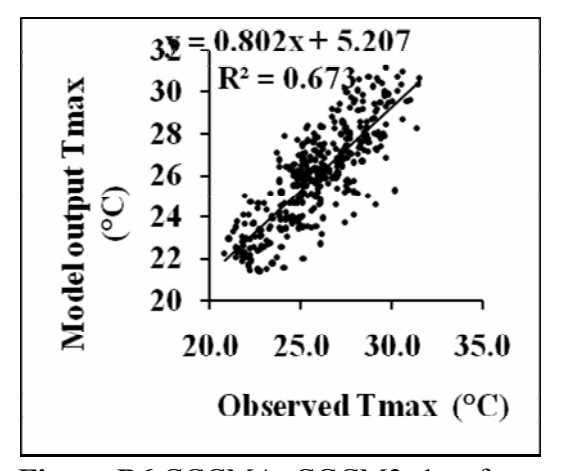


Figure B6 CCCMA_CGCM3_1performance

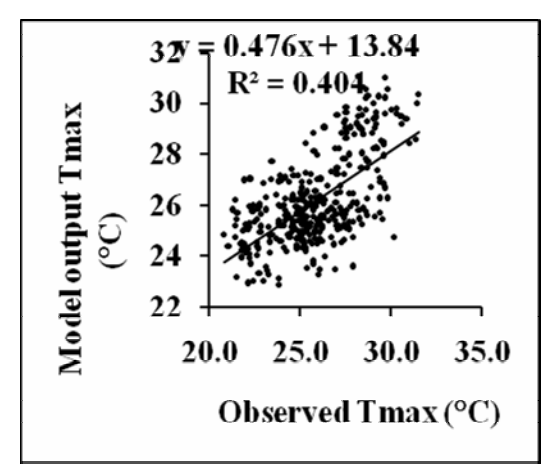
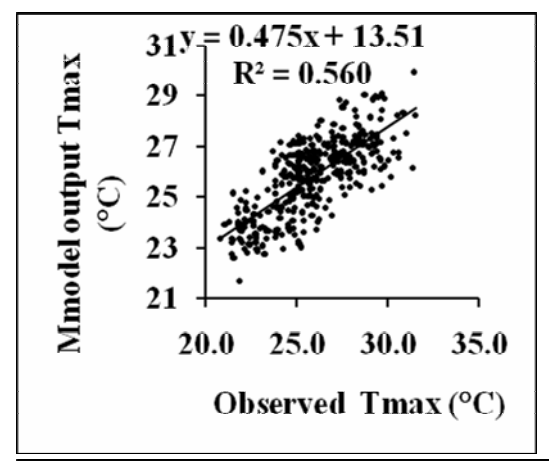


Figure B7 GFDL_CM2_0 performance



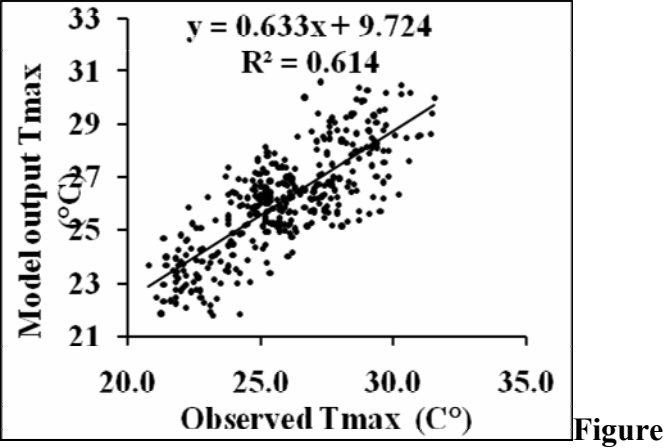


Figure B9 MPI_ECHAM5 performance

B8 GISS MODEL E R performance

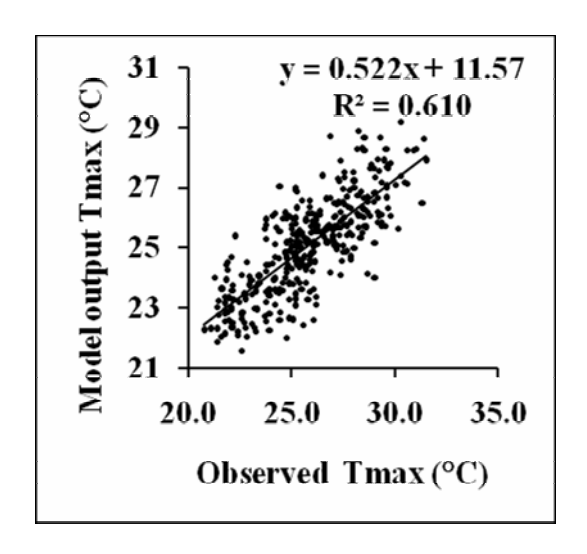


Figure B10 CSIRO_MK3_5 performance

Wedza maximum temperatures

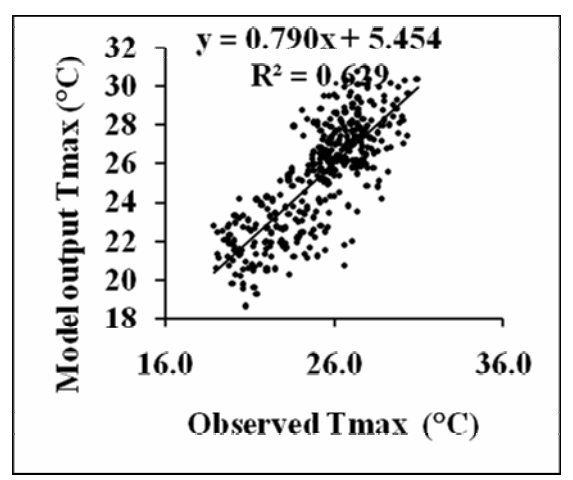


Figure B11 CCCMA CGCM3 1 performance

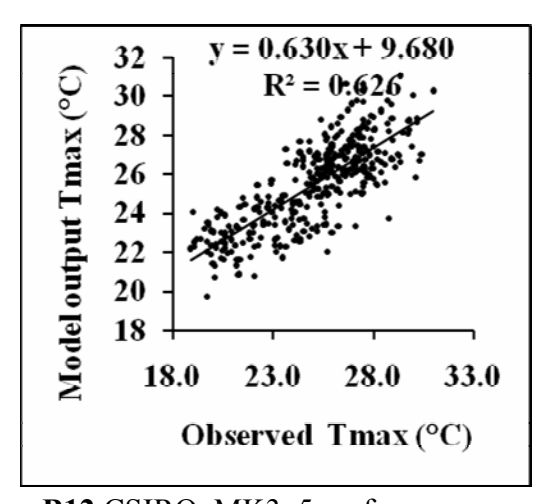


Figure B12 CSIRO_MK3_5 performance

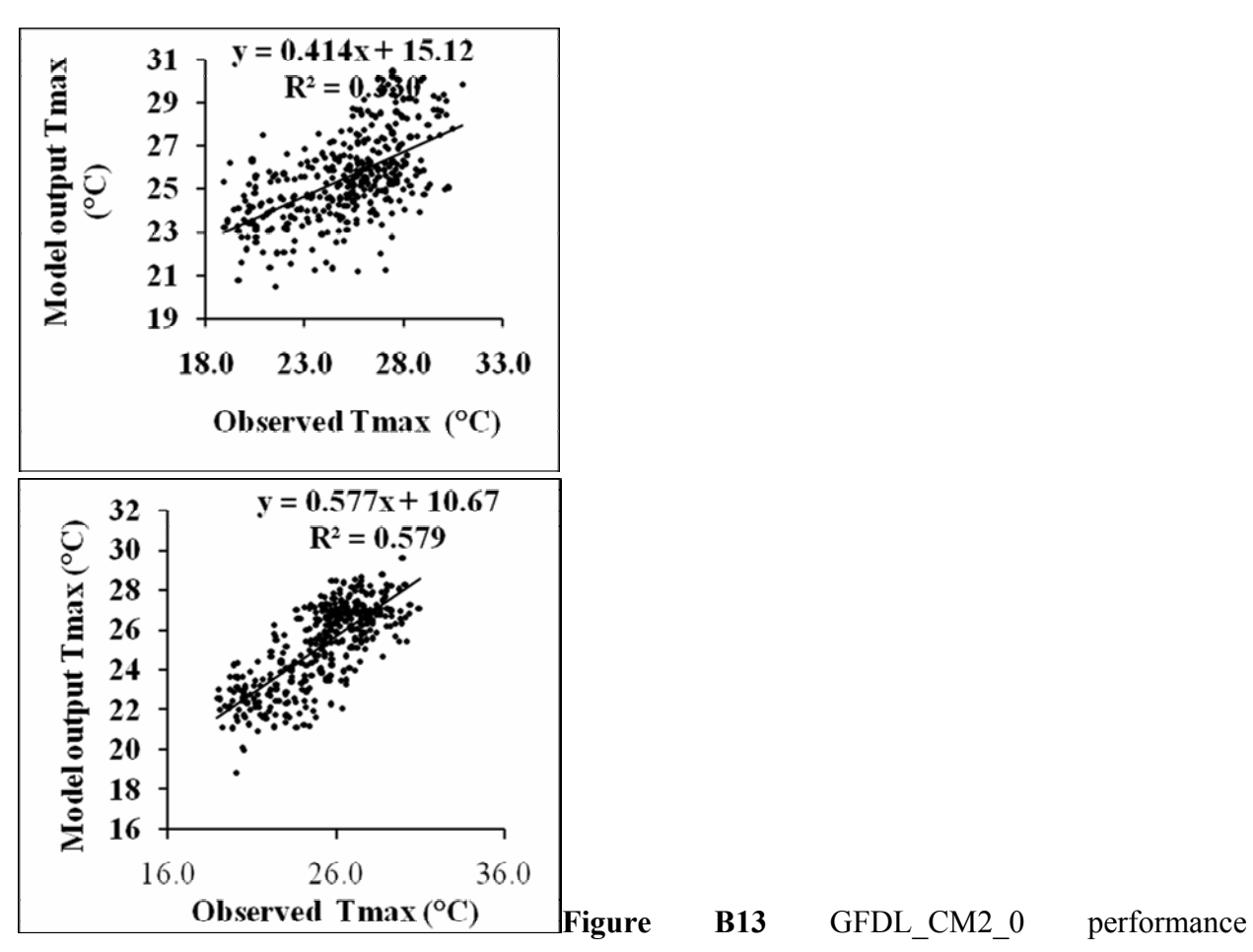


Figure B14 GISS_MODEL_E_R performance

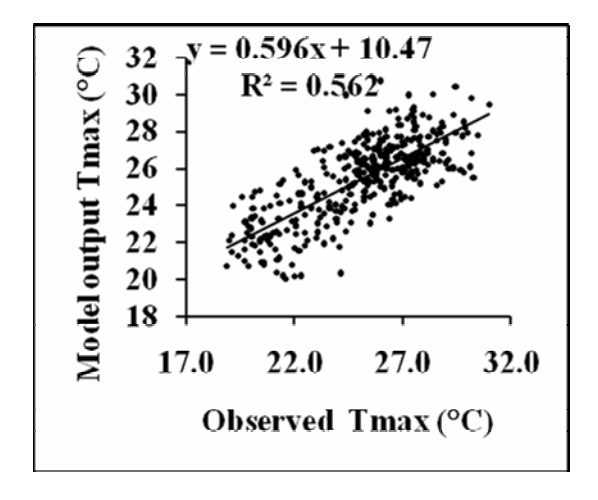


Figure B15 MPI ECHAM5 performance

Rusape maximum temperatures

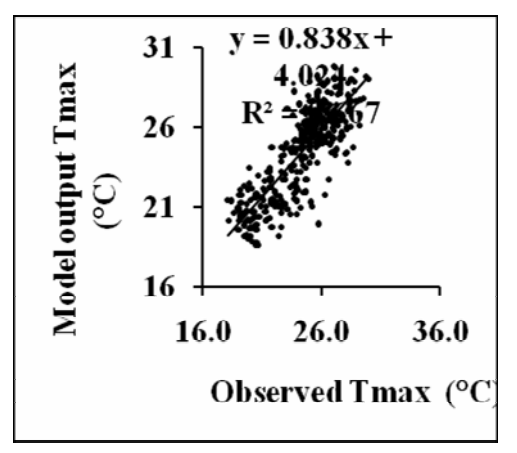


Figure B16 CCCMA_CGCM3_1 performance

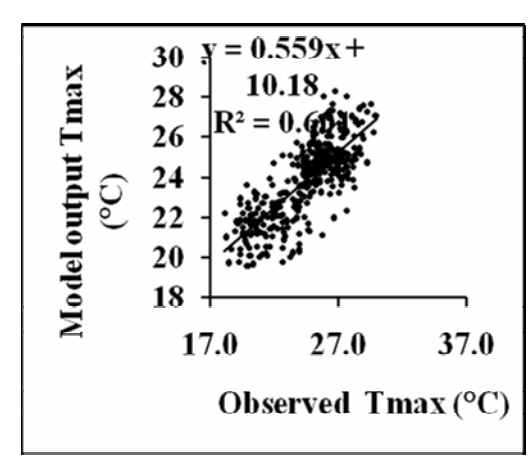


Figure B17 CSIRO_MK3_5 performance

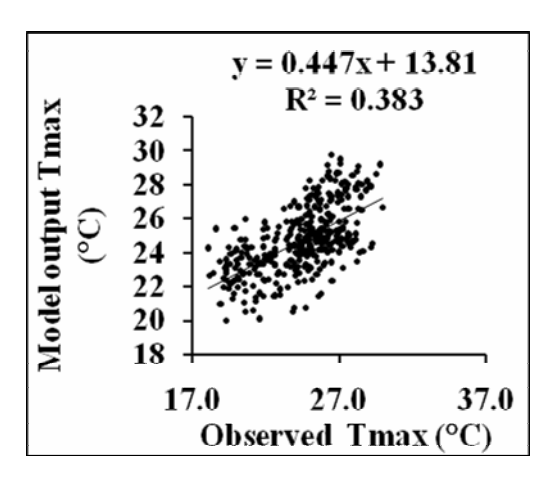


Figure B18 GFDL_CM2_0 performance

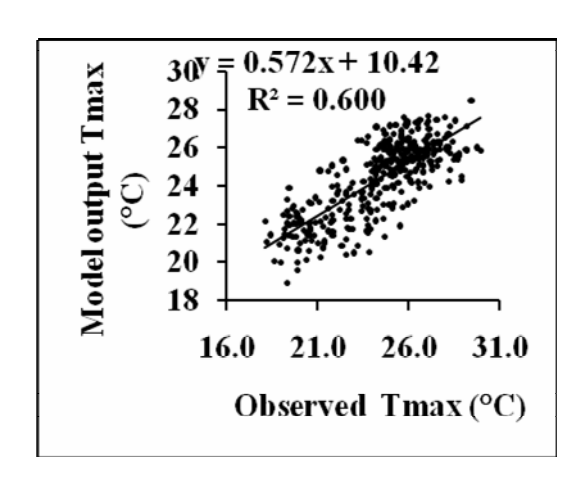


Figure B19 GISS MODEL E R performance

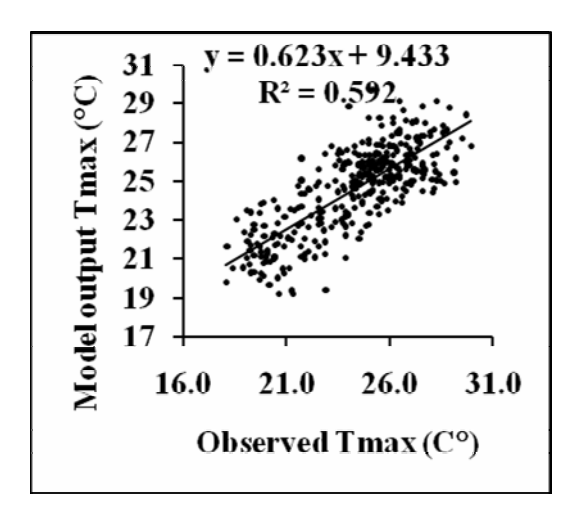


Figure B20 MPI ECHAM5 performance

Mutoko maximum temperatures

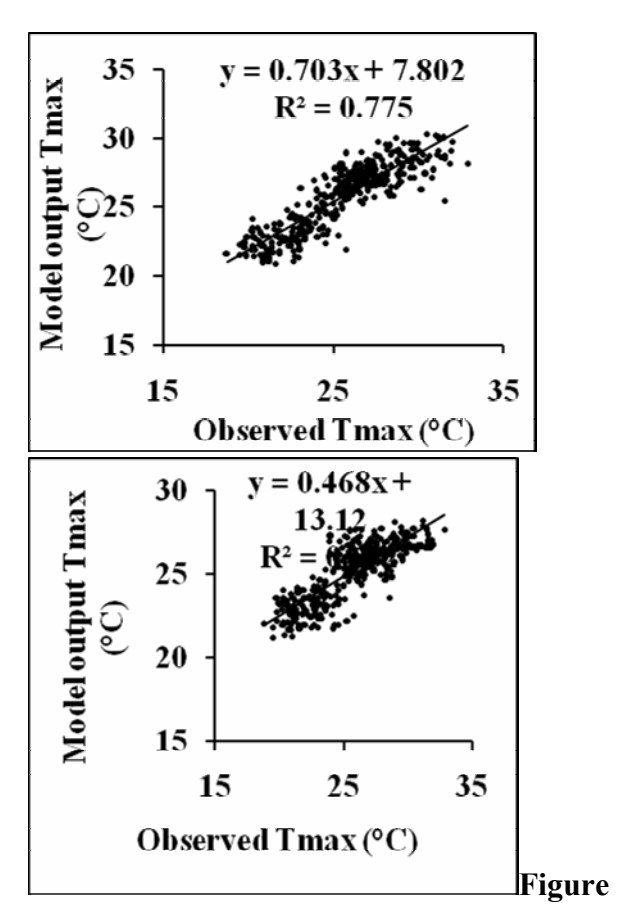


Figure B22 CSIRO_MK3_5 performance

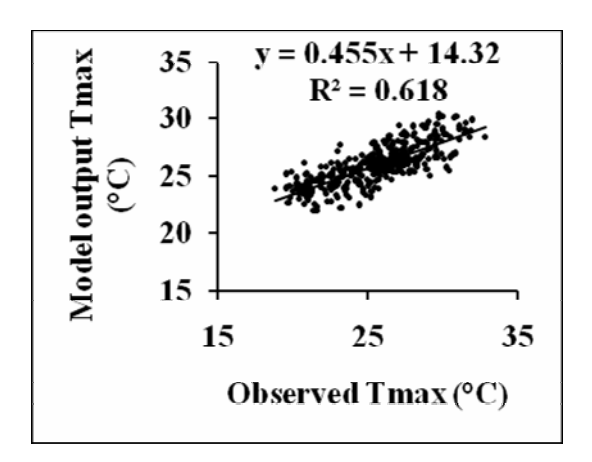


Figure B23 GFDL_CM2_0 performance



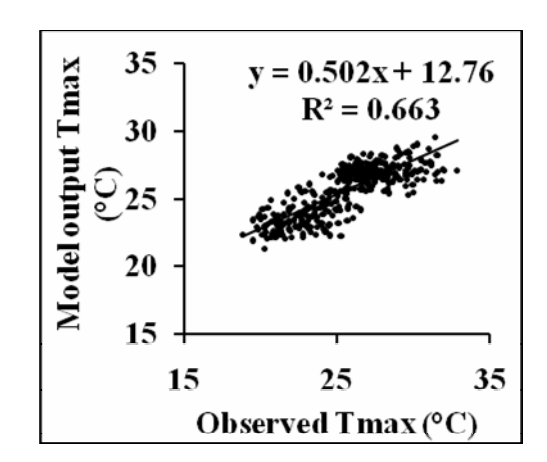


Figure 24 GISS_MODEL_E_R performance

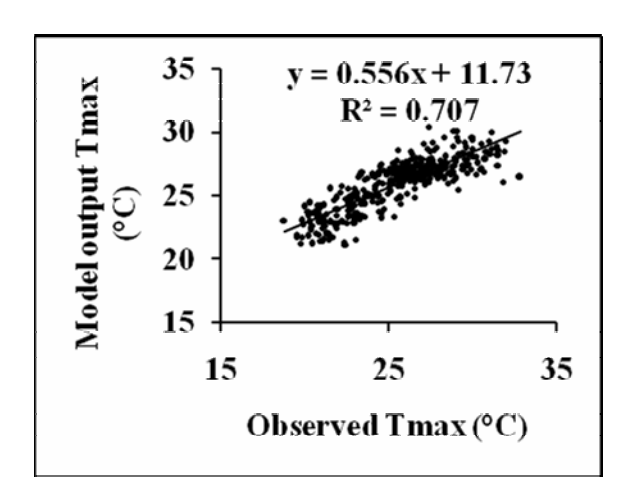


Figure B25 MPI ECHAM5 performance

APPENDIX C: Regression lines for simulating rainfall **Mt Darwin rainfall**

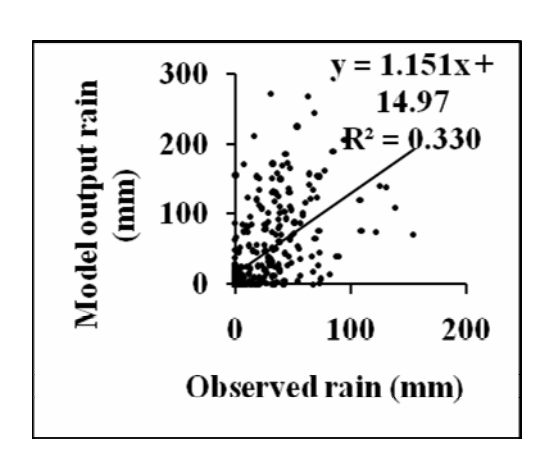
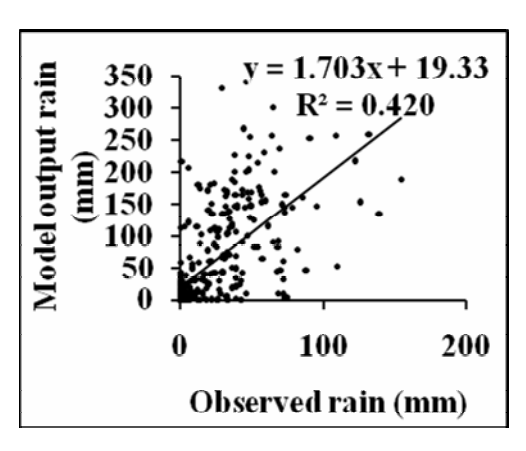


Figure C1 CCCMA_CGCM3_1 performance



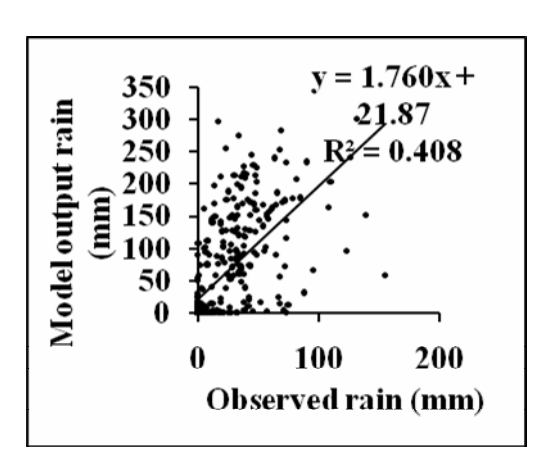
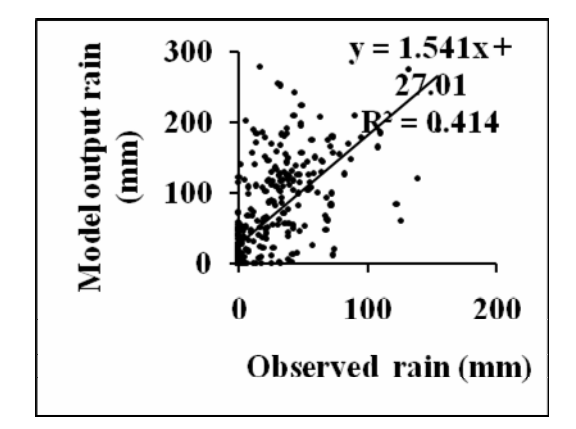


Figure C2 CSIRO_MK3_5 performance



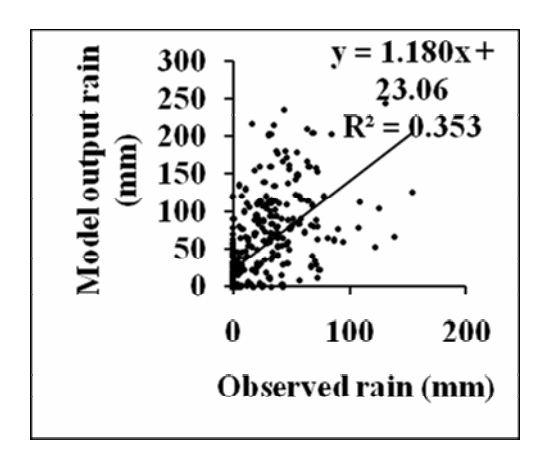
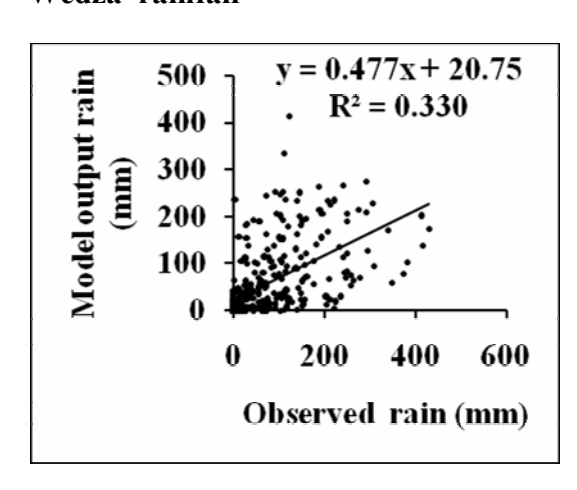


Figure C5 MPI_ECHAM5 performance

Wedza rainfall



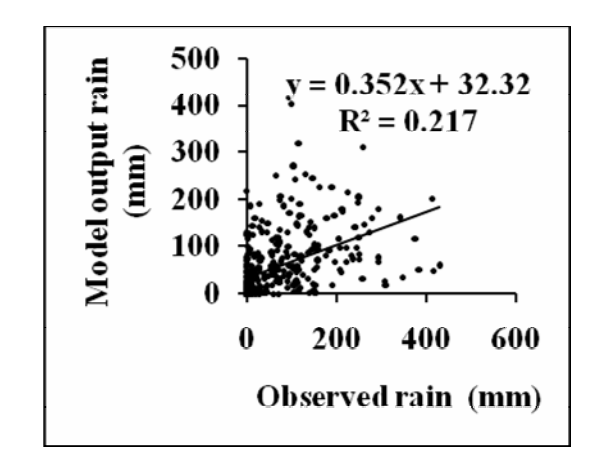
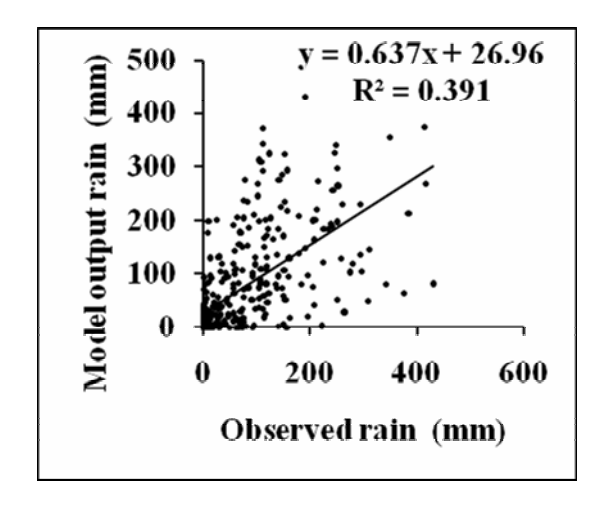


Figure C6 CCCMA CGCM3 1 performance Figure C7 CSIRO MK3 5 performance



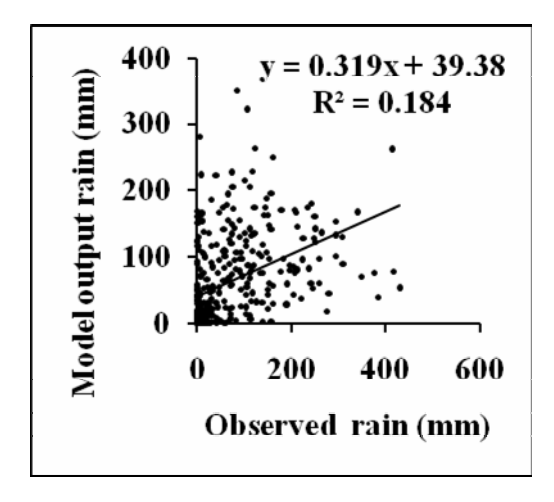


Figure C8 GFDL CM2 0 performance

Figure C9 GISS_MODEL_E_R performance

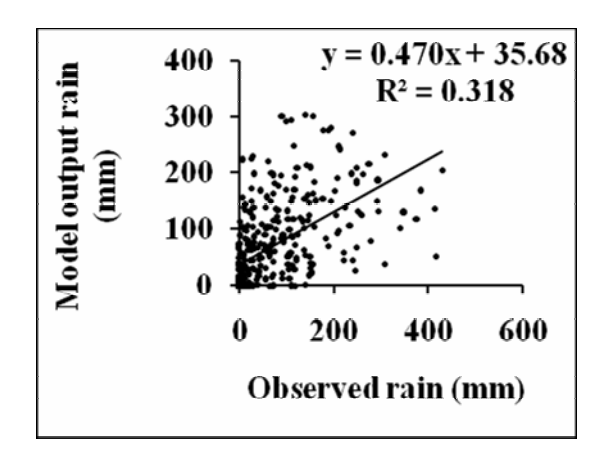
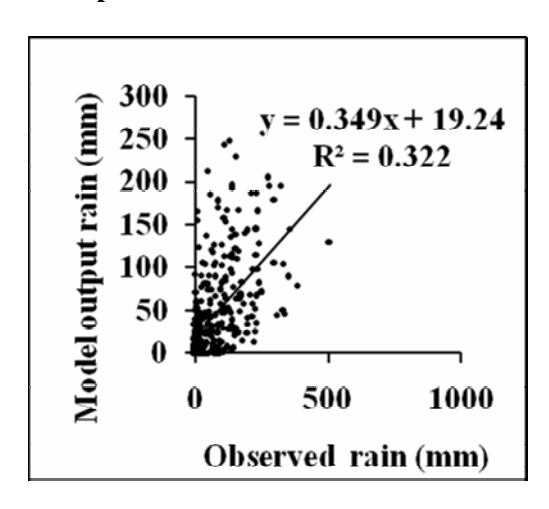


Figure C10 MPI ECHAM5 performance

Rusape rainfall



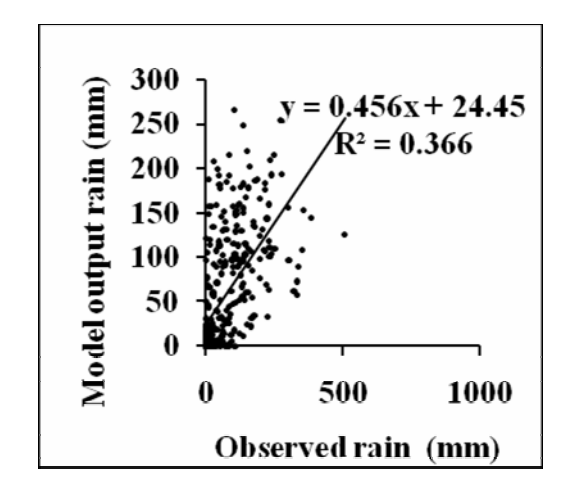
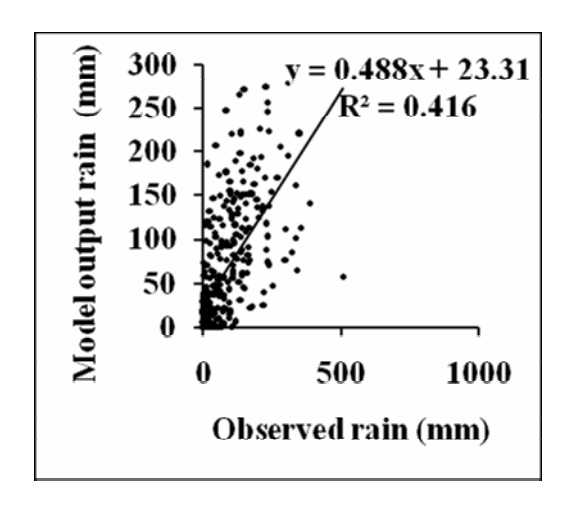


Figure C11 CCCMA CGCM3 1 performance Figure C12 CSIRO MK3 5 performance



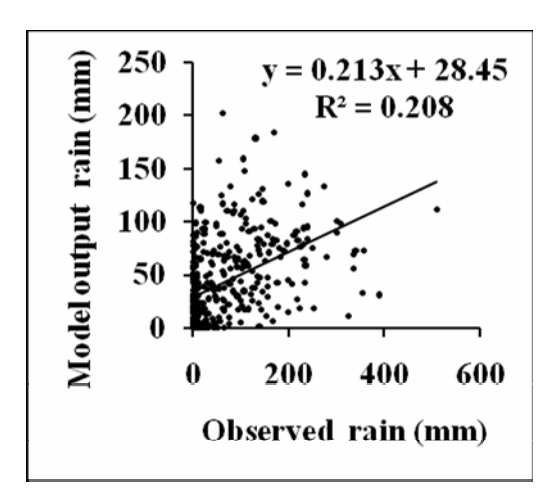


Figure C13 GFDL_CM2_0 performance

Figure C14 GISS MODEL E R performance

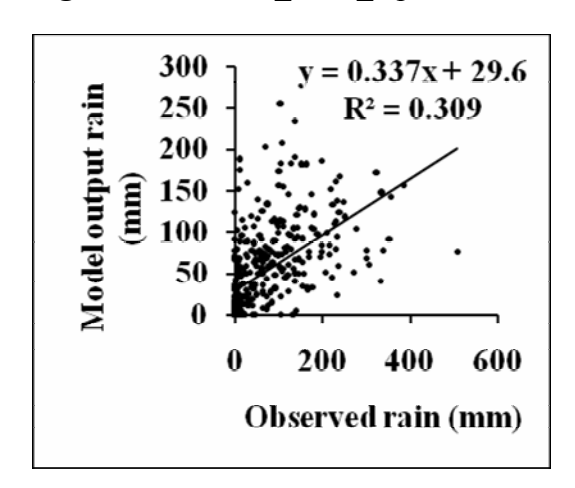


Figure C15 MPI_ECHAM5 performance

Mutoko rainfall

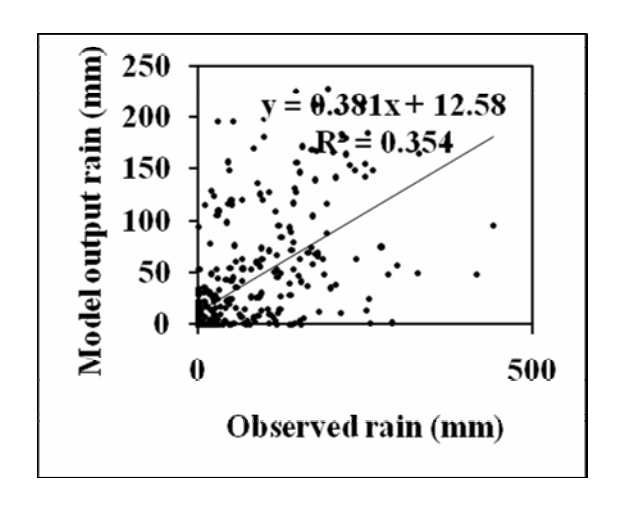
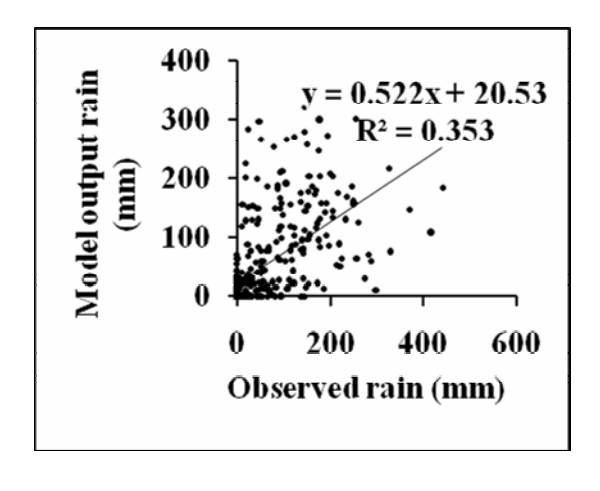


Figure C16 CCCMA_CGCM3_1 performance



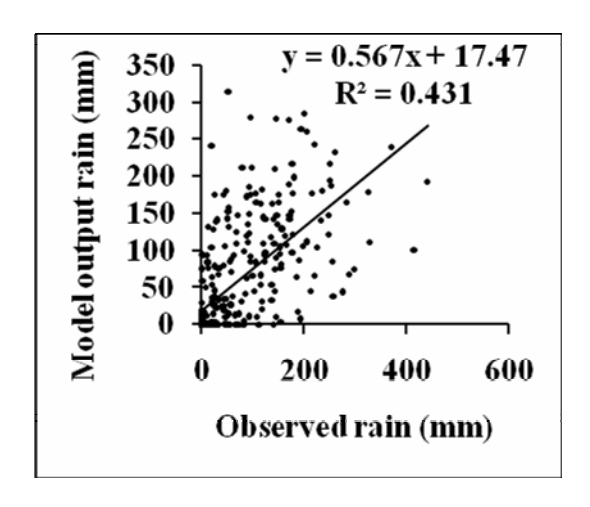
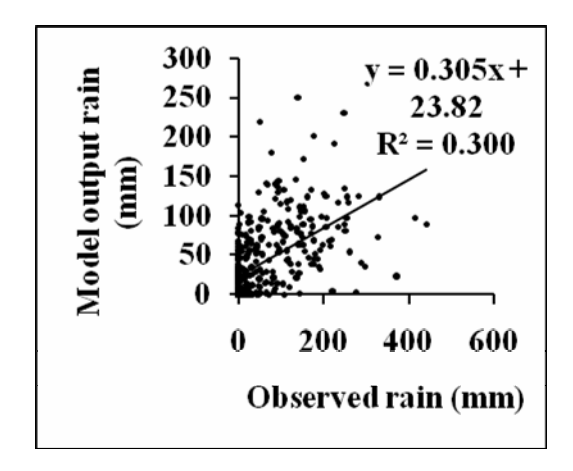


Figure C17 CSIRO_MK3_5 performance



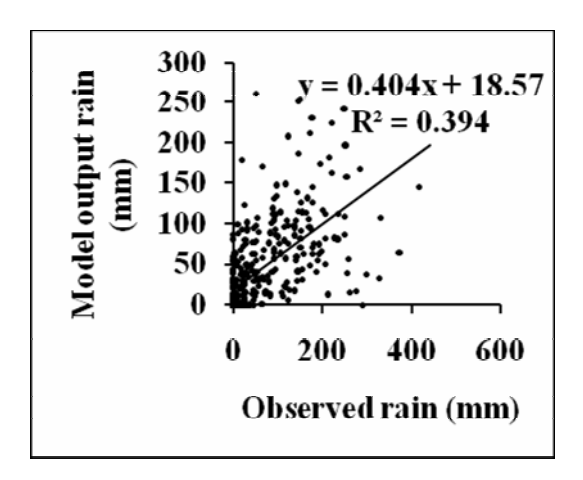


Figure C20 MPI_ECHAM5 performance